Integrated Design Process for the Development of Semi-Active Landing Gears for Transport Aircraft

Bei der Fakultät für Luft- und Raumfahrttechnik der Universität Stuttgart
zur Erlangung der Würde eines Doktors der
Ingenieurwissenschaften (Dr.-Ing.) genehmigte Abhandlung

vorgelegt von

Wolf Krüger

aus Hannover

Hauptberichter:	Prof. K. Well, Ph.D.
Mitberichter:	Prof. Dr.-Ing. habil. D. Bestle
Tag der mündlichen Prüfung:	18.12.2000

Institut für Flugmechanik und Flugregelung der Universität Stuttgart

2000

Aircraft Landing Gears, Active Landing Gears, Semi-active Control, Multibody Simulation, Roll Comfort, Multi-objective Optimization, Rough Runways

Abstract

Aircraft landing gears are currently optimized to have optimal performance in the rare case of a hard landing. The resulting suspension layout may lead to unsatisfactory oscillations when the aircraft is taxiing on a rough runway; runway unevenness can excite elastic structural modes, leading to passenger and crew discomfort.

Although there are existing modifications of aircraft shock absorbers to reduce the problem, the basic design conflict between the requirements for landing and for rolling cannot be fully overcome by a passive suspension layout. Semi-active suspension techniques promise a solution to this problem. A semi-active suspension, i.e. a damper with a variable, controlled orifice cross-section, is capable of reducing fuselage vibrations effectively while being relatively light-weight and of low system complexity.

In the thesis, three control laws, a skyhook-type controller, a fuzzy-logic controller, and a state feedback controller are designed for the application to a semi-active suspension for an aircraft nose landing gear. Regarding the aircraft flexibility, the landing gears can no longer be designed independently from the aircraft. The layout of the controllers is therefore undertaken using an integrated design approach. Airframe and landing gear properties are determined taking into consideration models from different engineering disciplines involved in the aircraft development process, making the oleo design part of the concurrent engineering loop.

The aircraft model is set up in a multibody simulation environment. The control laws are developed in a control design tool; special consideration is given to the requirements of semi-active actuators. The controllers are exported into the simulation environment and their parameters are optimized by means of multi-objective optimization. In a further step, the performance of the three control strategies are compared with each other and additionally with passive and fully active approaches. The dependence of the control performance on operational parameters (aircraft weight and speed, runway roughness) is assessed, and limitations due to realistic actuator restrictions are discussed. Finally, the benefits and disadvantages of semi-active nose landing gear control are summarized and open problems are addressed.

Flugzeug-Fahrwerke, Aktive Fahrwerke, Semiaktive Regelung, Mehrkörpersimulation, Rollkomfort, mehrzielige Optimierung, schlechte Rollbahnen

Zusammenfassung

Flugzeugfahrwerke werden zur Zeit für den seltenen Fall einer harten Landung optimiert. Die sich daraus ergebende Stoßdämpferauslegung kann zu unerwünschten Schwingungen beim Rollen über unebene Start- und Landebahnen führen. Durch Strukturschwingungen kann es zu erheblichen Komforteinbußen bei Passagieren und Crew kommen.
Obwohl der Einsatz modifizierter Stoßdämpfer das Verhalten des Flugzeugs am Boden verbessert, kann der zugrunde liegende Zielkonflikt zwischen der Auslegung für die Landung und derjenigen für das Rollen durch passive Systeme nicht vollständig gelöst werden. Semi-aktive Stoßdämpfer, die mit einem variablen, regelbaren Drosselquerschnitt arbeiten, sind dagegen in der Lage, die Rumpfschwingungen effektiv zu verringern. Gleichzeitig stellen sie eine relativ leichte und mechanisch unkomplizierte Alternative zu herkömmlichen Systemen dar.
In dieser Dissertation werden drei Regelgesetze, ein Skyhook-Regler, ein Fuzzy-Regler und ein Zustandsregler, für die Anwendung auf ein semi-aktives Bugfahrwerk entworfen. Der Entwurf der Fahrwerke kann heute nicht mehr unabhängig vom Entwurf des Rumpfes geschehen, da die Strukturelastizitäten eine wichtige Rolle spielen. Daher werden die Regelgesetze mit Methoden des Integrierten Entwurfs ausgelegt, wobei die Eigenschaften von Rumpf, Flügeln und Fahrwerk durch die Einbindung von Modellen aus verschiedenen Fachdisziplinen berücksichtigt werden. Durch dieses Verfahren findet die Auslegung der Stoßdämpfer Eingang in den „Concurrent Engineering“ - Prozess.
Das Flugzeugmodell wird als elastisches Mehrkörpermodell aufgebaut. Die Regelgesetze werden in einem Programm für den Reglerentwurf ausgelegt. Beim Entwurf werden die Besonderheiten der semi-aktiven Regelung berücksichtigt. Die Regler werden in die Simulationsumgebung exportiert und die endgültigen Reglerparameter durch die Strategie der mehrzieligen Optimierung gefunden. In einem weiteren Schritt wird die Effizienz der Regler untereinander verglichen und dem Verhalten eines passiven sowie eines voll aktiven Systems gegenübergestellt. Des Weiteren wird die Abhängigkeit der Regelqualität von den Einsatzbedingungen (Flugzeuggewicht, Geschwindigkeit), sowie die Beschränkungen, die sich durch den Einsatz realistischer Stellglieder ergeben, untersucht. Schließlich werden die Vor- und Nachteile der semi-aktiven Regelung diskutiert und offene Punkte angesprochen.

Acknowledgments

The work was performed in the Department for Vehicle System Dynamics of the Institute for Aeroelasticity at the German Aerospace Center in Oberpfaffenhofen, partly under a grant of EADS Aerospace Airbus, Hamburg.
First of all I would like to express my thanks to Prof. W. Kortüm of the German Aerospace Center in Oberpfaffenhofen who, as a principal advisor, has strongly supported this work and has been ready to give educational and technical advice at any time.
I would further like to thank Prof. K. Well of the University of Stuttgart who has shown a lot of interest in this work which has much benefited from his inputs, and who has made it possible for me to conduct the thesis at the Institute for Flight Mechanics and Flight Control in Stuttgart.
Equally, I am indebted to Prof. D. Bestle who not only agreed to join as second reviewer on short notice but also did a very thorough revision of the work.
The Department for Vehicle Systems Dynamics in Oberpfaffenhofen has provided a unique working environment. My thanks go to all my colleagues who have always been open to provide assistance and information without which the work in this form would not have been possible. Knowing I will not be able here to give everybody the justice he deserves I would nevertheless like to thank especially K. Deutrich, A. Veitl, M. Spieck, and W. Rulka.
From the industrial partners I want to thank especially Mr. R. Sonder and Mr. G. Roloff from EADS Airbus Hamburg, as well as Mr. U. Grabherr from Liebherr Aerospace Lindenberg, for providing realistic data and discussing the results.
Finally my thanks go to my wife and my parents for the continuous support they gave while the thesis was taking shape.

List of Symbols

symbol	unit	meaning
A,B,C,D	[-]	linear system matrices
A_g	$[m^2]$	gas room cross section
a_{com}	$[m^2]$	commanded orifice cross section
a_z	$[m/s^2]$	vertical (cockpit) acceleration
D	[-]	skyhook gain for vertical (cockpit) acceleration
d	$[N/(m/s)^2]$	damping coefficient of oil damping
d_{com}	$[N/(m/s)^2]$	commanded damping factor
$d_{comp,}$ d_1, d_2	$[N/(m/s)^2]$	damping coefficients for compression of oleo
d_{exp}	$[N/(m/s)^2]$	damping coefficient for expansion of oleo
d_{min}, d_{max}	$[N/(m/s)^2]$	minimum and maximum damping coefficients
d_z	[m]	tire deflection
F_0	[N]	oleo pre-stress force
F_d	[N]	oleo damping force
F_{DR}	[N]	seal friction force
F_{DB}	[N]	bending friction force
F_f	[N]	oleo spring force
F_N	[N]	normal force in oleo
F_x	[N]	longitudinal tire force
F_z	[N]	vertical tire force
K_c	[-]	constant factor on P and D for skyhook controller
M_s	[kg]	sprung mass (mass of vehicle and those parts of the suspension “above” the spring/damper element)
m_{us}	[kg]	unsprung mass (mass of wheel, tire, brakes, and those parts of the suspension “below” the spring/damper element)
n	[-]	polytropic coefficient ($1 \leq n \leq \kappa$)
P	[-]	skyhook gain for vertical (cockpit) velocity
pa	$[m/s^2]$	points describing input fuzzy sets for vert. cockpit acceleration

pd	$[N/(m/s)^2]$	points describing output fuzzy sets for damping
ps	[m/s]	points describing input fuzzy sets for stroke velocity
pv	[m/s]	points describing input fuzzy sets for vert. cockpit velocity
Q_w	[-]	spectral density matrix representing system noise (Kalman filter)
q	[-]	weighting vector for measurements (LQR controller design)
r_{nom}	[m]	nominal radius of tire
r_r	[m]	rolling radius of tire
$r_{r,eff}$	[m]	effective rolling radius of tire
R	[-]	scalar for weighting of control effort (LQR controller design)
R_v	[-]	spectral density matrix representing measurement noise (Kalman filter)
s	[m]	stroke of landing gear
s_m	[m]	oleo gas length
sp *or* $\dot{s}$	[m/s]	stroke velocity = compression velocity
T_y	[N/m]	torque on wheel by tire force
v_z	[m/s]	vertical (cockpit) velocity
α_D	[-]	discharge coefficient
κ	[-]	adiabatic coefficient
ρ	$[kg/m^3]$	oil density
μ	[-]	degree of membership in fuzzy set
μ_{RW}	[-]	friction coefficient between runway and tire

1 Semi-Active Landing Gears for the Reduction of Ground Induced Vibrations

1.1 Problems of Large Transport Aircraft - Ground Induced Vibrations and their Effects

The landing gear is one of the basic aircraft systems which has a significant effect on aircraft performance and economy. The tasks of aircraft landing gears are complex and lead to a number of sometimes contradictory requirements. At landing, the landing gear has to perform its “name-giving” task of absorbing the aircraft vertical energy via the shock absorber and the horizontal energy by means of the brakes. At taxiing, the landing gear has to carry the aircraft over taxiways and runways of varying quality, a requirement that is mirrored by its British name “undercarriage” [37]. The requirements for the absorption of a hard touch-down and for comfortable rolling lead to a design conflict which is responsible for the problems discussed in this work.

Landing gears are optimized to perform well at a landing with a vertical speed of 3.05 m/s = 10 fps. This requirement is imposed by the certification rules of FAR 25 and JAR 25 [112]. One of the main problems is that the requirements for a landing with high vertical aircraft velocity and for comfort and oscillation-free taxiing are conflicting: while a low damping factor is required for the touch-down to make use of the full oleo stroke, this setting is too soft for rolling. This leads to an increase in rigid body motion, namely pitch and heave, as well as to the excitation of elastic fuselage modes. An early example for problems of this kind was the Concorde where some take-offs on rough runways like New York and San Francisco led to oscillations that were so extreme that they almost prevented the aircraft from entering into service [37]. Military and potential future civil supersonic aircraft are especially prone to this phenomenon, see Figure 1, [89].

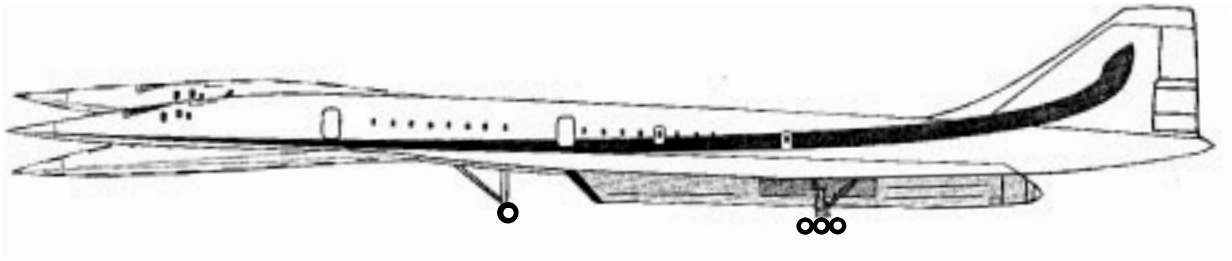

Figure 1: Expected oscillations of the SSCT (Super Sonic Civil Transport)

For conventional current and future civil aircraft, ground induced vibrations become more and more of a problem, too. Structures of modern aircraft become increasingly flexible. The main reasons are slender fuselages that frequently arise from the stretching of existing aircraft, see [101], and the use of new, light-weight structures and materials that influence the vibrational properties of fuselage and wings.

Typical modifications for stretching, as used e.g. at the DC 9-90 and the A321, include the

insertion of additional fuselage segments [42]. Most of the other important systems of the aircraft remain unchanged, though, including very often the landing gear layout. However, a landing gear that worked well for one aircraft configuration does not necessarily perform satisfactory for a stretched aircraft version. Thus, a landing gear might satisfy the certification requirements, but might not fit well with respect to the overall dynamics of aircraft plus landing gears. Unexpected vibrations can be the consequence.
Critical natural frequencies of a suspension can be changed within certain limits. In the case of the Concorde, for example, the shock absorber was changed to include a dual-stage air spring [37]. Main landing gears of large aircraft often are equipped with valves that open at touchdown, where the shock absorber stroke velocity is high, thus allowing a different damping coefficient for landing and taxiing (a so-called “taxi valve”). All modifications at conventional suspensions have in common that they can only be optimized for one design point and are therefore in principle not able to overcome the basic design conflict mentioned above. This, however, is possible with the application of semi-active landing gears and their respective control laws as they are described in this work. Landing gears of that kind are able to adapt their properties to the motion of the aircraft at any instant.

1.2 Aircraft Suspension Control - The Solution?

There are a number of books and articles of landing gear design which must be mentioned here. The books of Conway [11], Currey [14], Pazmany [73], and Roskam [82] are standard textbooks which cover the whole standard landing gear design process from questions of landing gear location, suspension layout and the selection of tires. An important - German language - reference about problems of the aircraft on the ground and landing loads is still the article by König [50]. The “SAE Committee A-5 for Aerospace Landing Gear Systems” is an association of aerospace engineers who are engaged in landing gear design which was formed in the frame of the Society of Automotive Engineers (SAE). Thirty publications by members of this committee concerning questions of landing gear design have been selected by Tanner and published in [90]. A second volume of papers [91] has been published by the same editor. Ohly describes in [70] the current state and trends for future developments in landing gear design. Further collections of articles have been published by the AGARD (Advisory Group for Aerospace Research and Development) in their conference proceedings CP-484 [108], “Landing Gear Design Loads”.
While all these publications are concerned with landing gear design in general, some specific publications exist with respect to the simulation of aircraft ground dynamics. An early overview of computer simulation of aircraft and landing gear is given by Doyle [17]. Further papers are published in another AGARD volume [109], which, however, has its main emphasis on the simulation of shimmy. Shepherd, Catt, and Cowling describe a program funded by British Aerospace for the analysis of aircraft-landing gear interaction with a high level of detail,

including brakes and anti-skid, steering control, to simulate standard hardware rig test (dynamometer and drop tests) as well as flight tests involving ground contact [86]. Two publications of the IAVSD (International Association for Vehicle System Dynamics), Hitch in 1981 [37] and Krüger et al. in 1997 [57] are state-of-the-art overviews of aircraft ground simulation, the latter article also discussing different modeling approaches and tools.

The suspension design conflict mentioned above has long been known to aircraft designers, and a number of studies have been undertaken to assess the potential of adaptive landing gears to resolve the problem of aircraft-runway-interaction. As far back as in 1972, Corsetti and Dillow have conducted a study of the potentials of landing gear control to improve ground ride [12]. In 1977, Somm, Straub, and Kilner [88] have published the results of a study of simulations of three military transport aircraft equipped with simple landing gear modifications, such as dual stage air chambers - values for the pressure have been set to a fixed value prior to landing according to the aircraft weight - and passive by-pass orifices. The authors predict a reduction of CG acceleration (RMS) by as much as 47% on semi-prepared and repaired bomb damaged runways. Fatigue investigations indicate improvements on austere airfields, while no improvement can be shown for missions on prepared runways. With the advent of microelectronics at the beginning of the eighties suspensions with computerized closed loop control have been subject of investigations because they promise greater improvements than the open loop approaches like those of [12] and [88]. Karnopp has published the so-called skyhook control concept (see chapter 4.2.1) for automotive applications [48]. This concept has found wide application in automotive, truck, and railway suspensions, both for research purposes as well as for production vehicles, and has been used for fully active and semi-active suspensions. In 1984 an AGARD conference has been dedicated to the state-of-the-art of active suspensions [108]. Among the work presented there are the studies of Freymann, who proposes a fully active nose landing gear for the reduction of ground loads [26]. He obtaines reductions of vertical acceleration of approximately 42% for a rough runway excitation on a test rig representing aircraft pitch, with considerable technical effort because an external high pressure oil reservoir is needed for fully active oleo control. Most investigations presented at the AGARD meeting, however, have been dedicated to the reduction of peak loads at landing impact. One example is the study of active landing gears for an F-106 fighter aircraft, aimed at operation on an aircraft carrier [39]. Here, also on a test rig with a high pressure oil source, modest improvements in the reduction of landing loads can be shown.

Only recently semi-active concepts for landing gear control have been introduced. Studies by Karnopp [46] for automotive applications suggest that the efficiency of semi-active dampers is only marginally lower than of a fully active system, provided that a suitable control concept is used. Goodall [63] investigates semi-active suspensions for the lateral damping of railway cars and makes some studies on filtering methods for the use of a skyhook control in curves. Quite a similar situation arises when a vehicle with vertical skyhook damping drives on a road, track, or - in the case of an aircraft - on a runway with a slope. Catt, Cowling, and Sheppard [8] perform simulation studies on active and semi-active aircraft suspensions. They investigate differ-

ent feedback strategies, including feedback of pitch rate, pitch acceleration, and normal (vertical) acceleration, the last choice showing the most potential. They also conclude, as Karnopp has done, that the improvement of ride comfort for a fully active system is only marginally better than for a semi-active system and agree not to pursue the investigation of a fully active scheme any further because of its high system complexity. Wentscher [101] investigates the use of a semi-active skyhook-controller for an A300 to improve ride comfort. He predicts considerable improvements; however, he works with a relatively simple model of the airframe structure and uses harmonic excitations, at a fixed speed and a single aircraft configuration, investigating only slight aircraft weight changes. Duffek [19] develops a semi-active control concept for the landing impact which could be combined with a control concept for ground ride. Wang studies a main landing gear model of an A320 with a fuzzy-controller for landing and rolling, but restricts himself in [98] to a two-mass landing gear model and in [99] to a rigid aircraft model.

There have also been practical applications of the technology in road vehicles. Mercedes builds its new S-Class with semi-active skyhook damping [80]. In the European COPERNICUS project, a truck has been equipped and tested with semi-active shock absorbers [94]. In that project the main aim has been to show that semi-active shock absorber control can be used to reduce dynamic tire forces which are a main cause of road damage.

In the course of another European project, ELGAR (European Advanced Landing Gear Research, [107]), Liebherr Aerospace Lindenberg has built a test-rig demonstrator with a modified helicopter nose landing gear on a vertical shaker to prove the technical feasibility of the semi-active damping concept for aircraft.

1.3 An Integrated Design Process for Semi-Active Landing Gears

Even though a considerable amount of research has been performed on the topic of semi-active suspensions in general, discussions with airframers and landing gear manufacturers as well as experience gained in the course of ELGAR and the German national Flexible Aircraft Project [59] led to the identification of a number of open problems which have to be addressed before the implementation of semi-active landing gears on production aircraft can be considered.

It is the intention of this thesis to give answers to some of the most important open questions, most notably concerning the choice of a suitable controller, the influence of the semi-active control on aircraft flexible modes and the behavior of the controlled aircraft at different speeds and different weight configurations.

To be able to examine these topics not only for a “generic“ but also for a technical relevant aircraft, it is vital that it is possible to combine submodels of different partners and engineering disciplines which are involved in the design of the aircraft concerned to be able to analyze the complete model. For the evaluation of aircraft-landing gear dynamics, this thesis therefore makes use of concurrent engineering methods for the development of the simulation model.

Multibody simulation has been chosen as the method for model set-up, simulation and analysis because it allows a good mean between the requirements of high model accuracy at a moderate model complexity as well as low computation times. It also offers a large number of analysis methods in both the frequency and the time domain. Furthermore, the used multibody code can be connected to other tools from the concurrent engineering area by a number of intelligent, bi-directional interfaces.

The following analysis strategy is employed in the thesis: the airframe and landing gear properties are determined by importing elements from finite element models, multibody simulation models and measurements. An interface between the simulation program and a control design tool is developed. Using this interface, three control laws, a skyhook-type controller, a fuzzy-logic controller, and a state feedback controller, are developed in the control design tool and exported into the simulation environment. These control strategies have been selected because they have been shown to be effective in semi-active automotive and truck suspension control. The control parameters are optimized using a multi-objective parameter optimization. In a further step, the performance of the three control strategies is compared with respect to the improvement of vertical accelerations in the time- and the frequency-domain. The dependence of the control performance as a function of system parameters, regarding both varying aircraft speed and aircraft weight, is assessed, and limitations due to realistic actuation restrictions are discussed.

The investigation will concentrate on rolling. Semi-active control of the touch-down, while feasible, will not be touched. The study concentrates on the semi-active control of the nose landing gear only. Because of its location a the long distance from the center of gravity and the main landing gear, vibrations of the rigid body modes (especially the pitch mode) as well as elastic fuselage and symmetric wing modes can be influenced and damped effectively. While a control of the main landing gears could also be envisaged, especially since much of the excitation is induced via those gears, they are subject to high inner sliding and stick friction, often due to strong bending because of high leg inclination angles. It is, therefore, an open question whether control of the main landing gears will lead to reduced accelerations or loads at all.

The semi-active control concept has been selected because it offers a good compromise between complexity and efficiency, i.e. it combines low additional weight with a good control performance. Furthermore, semi-active shock absorbers can easily be designed fail-safe. Fully active systems require a lot of additional equipment because of the necessary high pressure reservoir, leading to a weight penalty and reliability concerns.

The thesis is structured according to this analysis strategy: the presentation of the work will start with an overview of landing gear requirements and configurations, also highlighting the above-mentioned design conflict between touch-down and rolling (chapter 2). Conventional passive landing gear concepts as well as a proposed design for a semi-active landing gear will be discussed. This chapter will also point out why a semi-active solution has been given preference over a fully active one. Afterwards, modern landing gear design and simulation methods will be discussed, especially the use of multibody simulation which will play an important role

in this investigation. The most important software tools used including the interface between multibody simulation and control design tool will be presented.
In chapter 3 the aircraft and landing gear model will be discussed in detail. The most important equations for the force laws necessary for the simulation of the system dynamics will be given as well as the used configurations, the excitations used for design and evaluation, and the criteria for the optimization of the control parameters. The two-mass model and its role in aircraft suspension design will be introduced. Finally, an analysis of the aircraft model with respect to observability and controllability will be performed.
In chapter 4 the control design is performed. The possibilities for suspension control are discussed, the theoretical approach to the three selected control laws is given as far as necessary for the work, followed by a discussion of the restrictions imposed by the semi-active approach. The design process of the controllers and the optimization of the respective control parameters are shown at the end of the chapter.
The performance evaluation is the topic of chapter 5. A simulation of a full aircraft model is performed, first for the design point, then for different aircraft speeds and aircraft weight configurations. The semi-active approach is compared with a possible fully active design. The results are evaluated with respect to time and frequency criteria. Technical aspects of the implementation, as actuator force level and response time, are discussed. Finally, the control concepts are compared by regarding not only their respective performance but also their design and implementation effort. Open questions which arise during the work will be addressed at the end.

2 Landing Gear Development as an Integral Part of Aircraft Design

2.1 Aircraft Landing Gears: Requirements and Configurations

2.1.1 Landing Gear Requirements

Aircraft landing gears fulfill the tasks of absorbing the vertical energy of the touch-down as well as providing a smooth ground ride before take-off and after landing. However, they perform a number of further duties which are less evident. Jenkins [43] and Young [104] have given a detailed presentation of these requirements which are summarized in [57]. The most important factors influencing the landing gear design are described in the following paragraphs.

System weight is an important aspect in aircraft development. The landing gear accounts for 3 to 6% of the maximal takeoff weight. A subsequent major reduction in landing gear weight will be hard to realize because the landing gears are one of the few non-redundant load-paths in an aircraft, and any reduction in reliability from current fail-safe standards is not acceptable [10]. Considering the progress in aircraft light-weight structural design and fuel efficiency the relative weight share of the landing gears can thus be expected to increase further.

The position of the landing gears must be such that the aircraft will not tip over under static and dynamics loads. Another important factor for the design is the number and properties of the tires as airfield compatibility has become an important factor in the design of landing gears. The number of tires depends on aircraft weight, maximum force per tire and maximum tire size, and is dictated by pavement bearing strength which may vary from airport to airport. Large civil transport aircraft as the A340, Boeing 747 and MD 11 reach loads of over 20 tons per tire on the main landing gears.

During flight the landing gears of practically all modern transport aircraft are retracted. This requires restrictions on the landing gear positioning as these parts have to be stored in a limited space and must not collide with other systems. For this reason, landing gears often possess complicated kinematical layouts of the retraction mechanism for the storage in nacelles in wings and fuselage. Landing gears are usually retracted to the front so they can be released in case of a hydraulic failure and being pushed into position by the air flow, Figure 2, [101].

Since landing gears have to carry the aircraft weight and have to absorb the energy of the landing impact, the fuselage has to be strengthened in the vicinity of the attachment points. Load alleviation is therefore also of importance for the dimensioning of the fuselage, especially at the attachment points and at the rear of the aircraft. For aircraft with a high maximum landing weight the bending moment resulting from the landing impact is often the critical design case for the rear fuselage [59]. Therefore, comfort improvements obtained by the application of the results of this study must not result in higher attachment loads.

Other load cases besides touch-down and rolling are also of great importance. On many airports aircraft are towed, either by push-rods or by special trucks. Cornering exerts high lateral

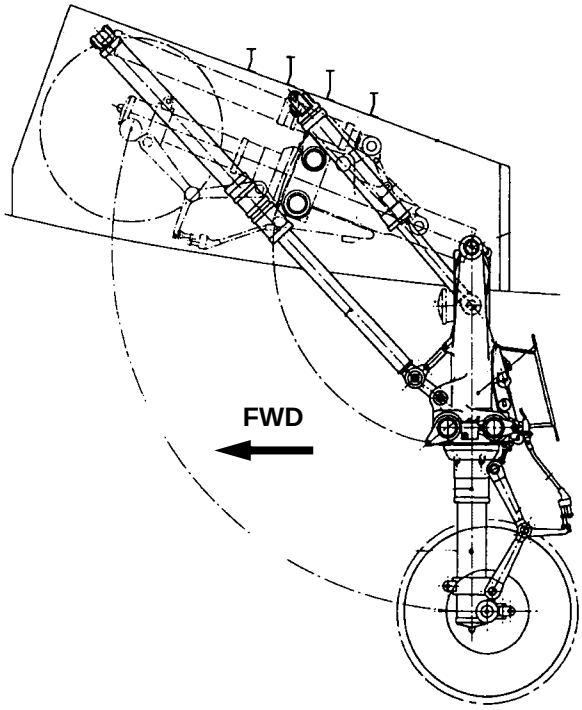

Figure 2: A300 nose landing gear

loads on the landing gears. These factors often lead to higher forces than those obtained at touch-down, especially in lateral and horizontal directions, and have to be taken into consideration as design loads [112].

All requirements mentioned so far have to be met with a system that is one of the few aircraft parts which have no redundancies. And, as airlines look as well at acquisition costs as at DOCs (direct operational costs), the landing gear should be inexpensive and require minimum maintenance.

The great number of requirements can only be fulfilled if comprehensive trade-off studies concerning space availability, weight considerations, and structural (stress-) evaluations are performed. Since a large number of engineering disciplines are involved in the suspension development, an integrated design of airframe and landing gears is essential for modern aircraft.

2.1.2 Landing Gear Configurations

Landing gears have developed from the simple skids of the first aircraft into the sophisticated and rather complex systems they are today. Originally, the spring function of the suspensions consisted only of the leg elasticity or solid springs [104]. In the years after the first world war the oleo-pneumatic shock absorber became popular because it provided high efficiency by combining the desired spring and damping characteristics in a relatively small unit. At that time, the landing gear configuration with two main landing gears and a tail wheel was common, the most prominent example being the DC 3, see Figure 3a, [56]. In the thirties, the retractable landing gear was introduced for reasons of reduced aerodynamic drag. Since the

generation of aircraft of the fifties the landing gear configuration of large transport aircraft has remained principally the same - a steerable nose landing gear and two, or more, main landing gears [14], one of the earlier aircraft with landing gears of that type being the Lockhead L-1049G Super Constellation, see Figure 3b, [56]. Other possible landing gear systems include floaters, skids, skis, track-type gears, and air cushions. They are applied in specialized aircraft but have found no wide usage [81], [90].

a) tail wheel landing gear configuration: DC 3

b) nose wheel tricycle landing gear configuration: L1049G

Figure 3: Common landing gear configurations

The nose wheel tricycle landing gear configuration has some important advantages when compared to the tail wheel type gear. First, the fuselage is level when the aircraft is on the ground, increasing visibility for the pilot at take-off and at ground maneuvers. Second, the center of gravity is located in front of the main landing gears which leads to a pitching moment of the aircraft at touch-down, automatically reducing lift. Furthermore, the aircraft is stabilized and the pilot can utilize the full brake power [10]. On the other hand, aircraft with tail-wheel landing gear types have an initial angle of attack, allowing a shorter take-off distance.

A major disadvantage of the conventional landing gear layout, though, is the fact that the requirements mentioned in section 2.1.1 restrict the designer’s choice of landing gear location and layout. With aircraft becoming larger and the number of main landing gears increasing to

three or even four, substantial limitations in the designer's freedom occur [10]. The available envelope within which the landing gear has to be located to produce the ideal loading and stability characteristics may no longer be large enough to place the increased number of main landing gears in the fuselage and the wings. A good example is the A380 where the accommodation of four main gears with four- and six-wheel-bogies poses a demanding design challenge.

2.2 Conventional, Active, and Semi-Active Landing Gears

2.2.1 Conventional Landing Gears

Practically all modern transport aircraft are designed with retractable landing gears in nose wheel tricycle configuration. The main landing gear is equipped with disk brakes and a multi-tire combination on one or several axles. In the latter case the axles are connected to a bogie. In many cases the shock absorber acts in the (vertical) translational degree of freedom of the landing gear (cantilevered gear, Figure 4a, [74]); in another type of gear, the shock absorber acts across a landing gear angle (articulated gear, Figure 4b). A number of nose landing gears with

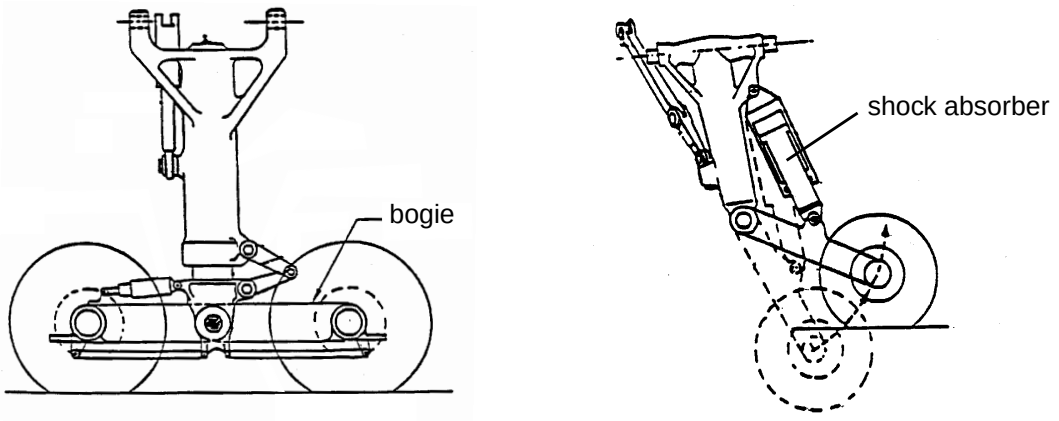

a) cantilevered main landing gear b) trailing edge (articulated) main landing gear

Figure 4: Shock absorber configurations

the shock absorber in the translational degree of freedom are designed with a small trail to stabilize the wheel while taxiing. An example is the A300 nose landing gear in Figure 2, which is of the same configuration as the nose landing gear used in this work.

Almost all commercial transport aircraft today are equipped with an oleo- (i.e. oil-) pneumatic shock absorber, often simply called the "oleo" to absorb and dissipate vertical kinetic energy, see Figure 5, [101]. An oleo has a high weight efficiency when compared to other shock absorber types. It consists of a chamber (1) filled with gas (mostly dry air or nitrogen) which is compressed during the stroke and provides the characteristics of a progressive spring, and an oil volume which is pressed through orifices between main chamber (2), gas room (1) and recoil chamber (3) at compression and expansion to account for the damping of the stroke

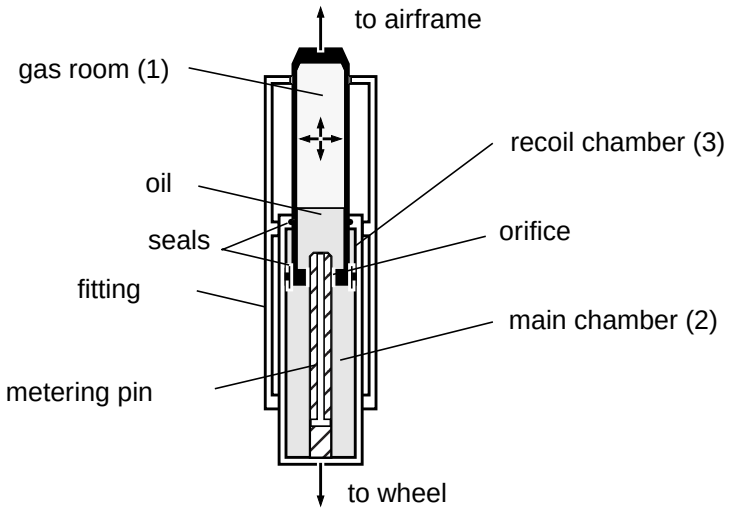

Figure 5: The passive oleo

motion. Friction is introduced by two phenomena, the pressure of the seals on the metal of the fittings (“seal friction”) and the strong bending moments, especially at touch-down (“bending friction”) and can account for more than 10% of the total force in the oleo (for a mathematical representation of friction models see section 3.3.4).

This layout leads to a relation of force over stroke during the landing impact shown in Figure 6 [104].

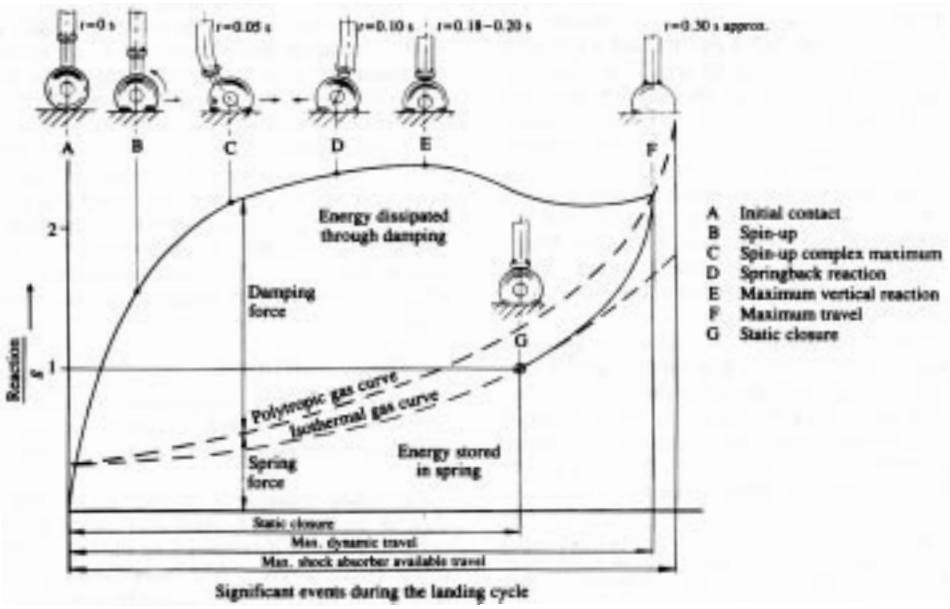

Figure 6: Characteristic force diagram for landing impact

The areas under the load-stroke curve in that figure correspond to the energy generated by the respective forces. The spring force increases with stroke, storing energy. The oil damping and the friction forces dissipate energy until the system comes to rest at the static closure point. Figure 7a shows the same process as a function of time for a fixed-orifice oleo. From these considerations follows that the peak force for a landing impact in the shock absorber theoretically reaches a minimum if the area under the load-stroke curve for a hard landing impact (i.e.

an impact where the peak force is greater than the static force) has the shape of a rectangle; in the load-time curve, the two peaks of the total force should converge into a single one. For a soft landing, in the load-stroke curve the optimum is a force sloping to the static point. Since a rectangular force level is neither technically feasible nor desirable, as it would lead to a force step, the oleo is optimized to a steep force slope after ground contact, see Figure 7b.

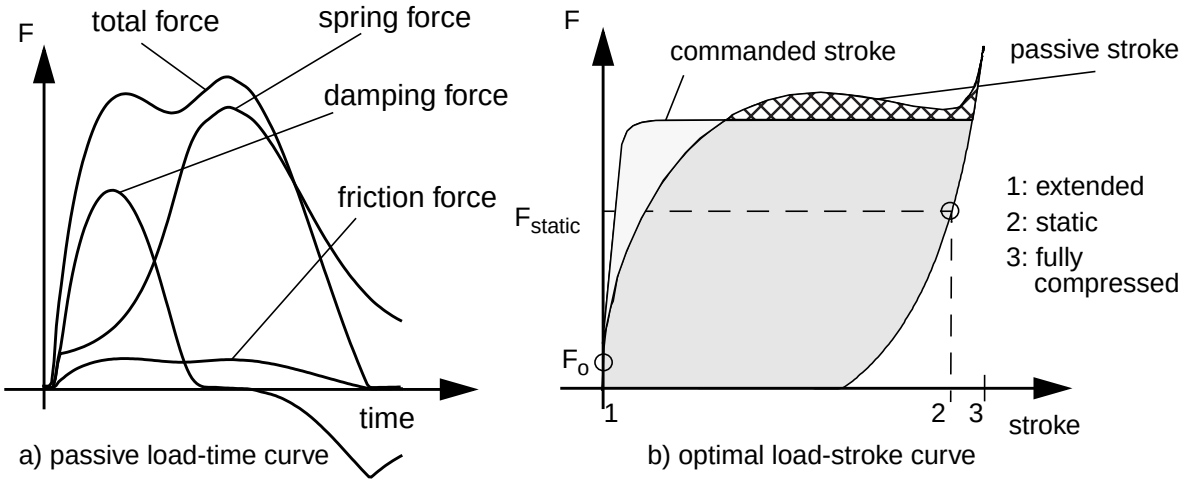

Figure 7: Passive Load time curve and optimal load-stroke curve for landing impact

The conventional technical solution for such a shaping of the force slope by a variation of the damping factor is the use of a “metering pin”, which changes the orifice cross section and thus the damping factor as a function of stroke, reaching efficiencies of 80% to 90% [10]. It can be seen from these considerations that the performance of the shock absorber will be better if the full oleo stroke can be used. This in turn leads to relatively soft damping factors because of the high stroke velocity at landing impact.

Next to the efficient absorption of the energy of the landing impact the oleo should provide a comfortable ground ride. This poses two problems: first, at taxiing the aircraft is in or is close to a static equilibrium. Therefore, the air spring operates in the range of a steep curve slope, especially for the maximum take-off weight, leading to a very hard suspension. This hard suspension is necessary because aircraft weight variations during the boarding of passengers or while loading freight should not result in substantial gear deflections. Second, the damping required to successfully encounter oscillations has to be considerably larger for taxiing than for landing because the oleo stroke velocity at taxiing is significantly smaller than at touch-down.

Aircraft designers have been aware of that design-conflict for many years and have proposed a number of measures [12]. A standard solution is the use of a double-stage air spring or a taxi valve, i.e. a spring-supported valve that changes the damping coefficient as a function of stroke velocity, see Figure 8, [58]. For low stroke velocities, i.e. at taxiing, the valve closes at P_1 and high damping factors are achieved. At touch-down, i.e. at a high stroke velocity, the oil flow opens the valve at P_2, thus reducing the damping factor. The so-called rebound coefficient d_{exp} can be set separately from d_1 and d_2 and is selected such that the aircraft does not jump up, i.e. rebound, in the case of a hard landing.

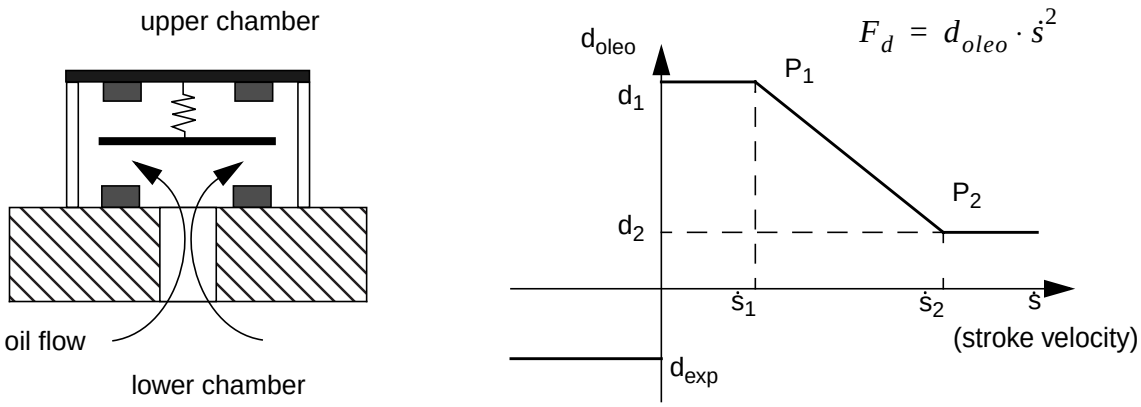

Figure 8: Taxi valve - passive system for improved ground ride

For the rolling aircraft a further aspect is of importance. Strong friction forces are induced, especially in landing gears with a large inclination angle towards the vertical aircraft axis, by the resulting bending moment which cause the oleo to stick even while the aircraft is rolling. Measurements show that aircraft main landing gears can lock for several seconds during taxiing. In this case all the suspension deflection is provided by the tires only [57]. Although sticking due to friction, sometimes called “sticktion”, has a strong influence on the ground dynamics, reliable data about this phenomenon are difficult to obtain - the reasons being that either the effect is not sufficiently understood or the data are kept proprietary by the landing gear manufacturers (or both) [57].

2.2.2 Landing Gears of Variable Characteristics

Conventional landing gears as they have been described above are suspensions with fixed spring-damper characteristics. Those passive systems are restricted to generating forces in response to *local relative* motion, e.g. upper and lower strut of the shock absorber. In order to obtain an improved performance with respect to comfort and loads, the suspension characteristics can be made adaptable to aircraft parameters as well as to environmental conditions, e.g. the quality of the runway. Active systems may generate forces which are a *function of many variables*, some of which may be remotely measured, e.g. vertical acceleration, aircraft weight, and forward speed. Active suspensions are already state-of-the-art and are applied in a number of automotive and railway applications.

Basically, two different active suspension strategies exist. A first type is an a-priori setting of spring or damper characteristics according to the expected runway quality and aircraft weight prior to touch-down, and keeping those suspension characteristics constant during roll. This variant, sometimes also called “adaptive suspension“, has been examined by Somm, Straub, Kilner in 1977 [88] who used a gas spring with an adaptive pressure which was used for military aircraft landing on unpaved runways. Another variant of this suspension type are those suspensions of luxury cars which can be switched between sportive and comfortable operating modes. A second type is the feedback of vehicle motion and, consequently, a suspension control. The

basic sensor and control layout is similar for most systems and has already been described in the seventies and eighties by Corsetti and Dillow [12], Karnopp [48], and Hedrick [33]: a sensor at the vehicle measures acceleration and velocity of the sprung mass as well as the suspension deflection, and, via a control law, results in a change of suspension characteristics.
Several ways to classify suspension systems can be found in the literature. A common way of classification is by the bandwidth of the actuators. Prokop and Sharp [76], for example, distinguish between

- very slow active systems, the actuator cut-off frequencies of which are lower than the natural frequency of the body resonance (i.e. frequency range less than 1 Hz), e.g. load levelers and adaptive spring settings;
- slow-active systems, which show cut-off frequencies between the body and wheel natural frequencies of the system (i.e. frequency range between 1 Hz and 10 Hz), e.g. actuators for pitch and roll control; systems like these can be realized by pressure variations of a gas spring, e.g. Citroën Xantia [29], [13], or adjustable mechanical devices, e.g. Delft Active Suspension, DAS [95];
- and fast-active systems, with actuation bandwidth beyond the wheel-hop natural frequency, i.e. frequency range above 10 Hz, e.g variable dampers operating at high bandwidth [80].

In the course of this work the term “active suspension” will always be used for the fast systems. The complete suspension can consist of an arrangement of passive and active components. The active parts can be used in parallel with or as a substitute for passive elements, see Figure 9. Most technical solutions put the actuator in parallel to conventional components, Figure 9a. This is done for reasons of safety, i.e. to guarantee vehicle stability in case of actuator failure, and to reduce the load on the actuator. Furthermore, a certain amount of inherent damping, e.g. by friction, is present in most cases anyway. For control design purposes, however, it can also be of use to neglect the passive damping, Figure 9b, or to see the actuator as a combination of all suspension parts, Figure 9c.

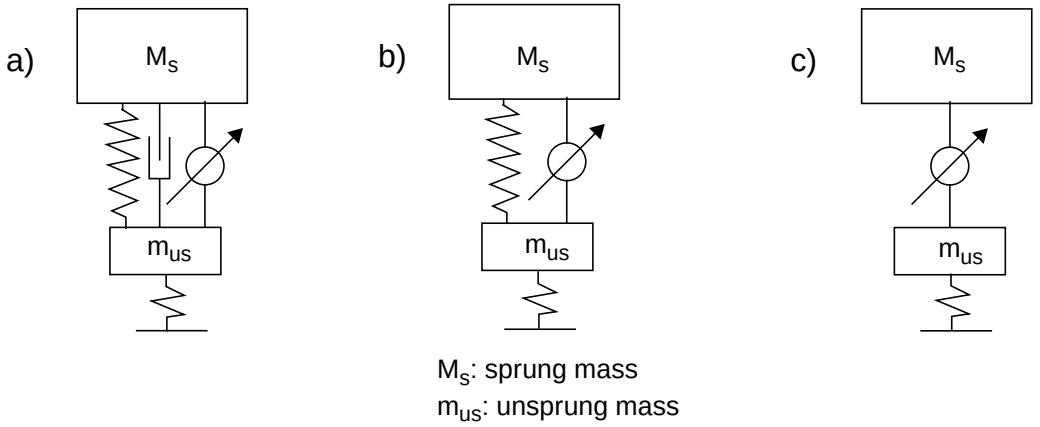

Figure 9: Possible arrangements of components for active and semi-active suspensions

An improved performance can be achieved by the application of so-called preview sensors which scan the runway for obstacles and rough patches and enter this additional information into the control loop [85]. Sensors using optical, ultrasound and radar technology are may be applied, however, they pose problems concerning practical application (dirt, accuracy) and interpretation of data, e.g. how can a water-filled pot-hole be distinguished from the runway, how a cardboard box from a stone... [40]. A good compromise for road vehicle suspensions is to use the motion of the front axle as preview for the rear axle [85]. This strategy is not applicable to aircraft since the tracks of aircraft main gears are so wide that the information from the nose gear would be of little benefit for potential main landing gear control.

Even optimal suspension control has its limits. First, a suspension realizing an optimal frequency isolation between passenger and road or runway input would require an unlimited working space. Second, the wheel-hop natural frequency cannot be damped easily since in practice it is difficult to measure the tire deflection. Third, energy consumption limitations apply. Even though extreme opposite standpoints in respect of energy consumption are possible [85], conventional solutions with electro-hydraulic actuators require a substantial amount of energy since actuation occurs by virtue of high pressure oil flowing into the actuator and a corresponding volume of oil has to be exhausted to tank (atmospheric) pressure (see next section).

Figure 10 gives an overview of the suspension layouts discussed above. This work will be restricted to the control of semi-active suspensions in the range of 1 to 10 Hz without preview.

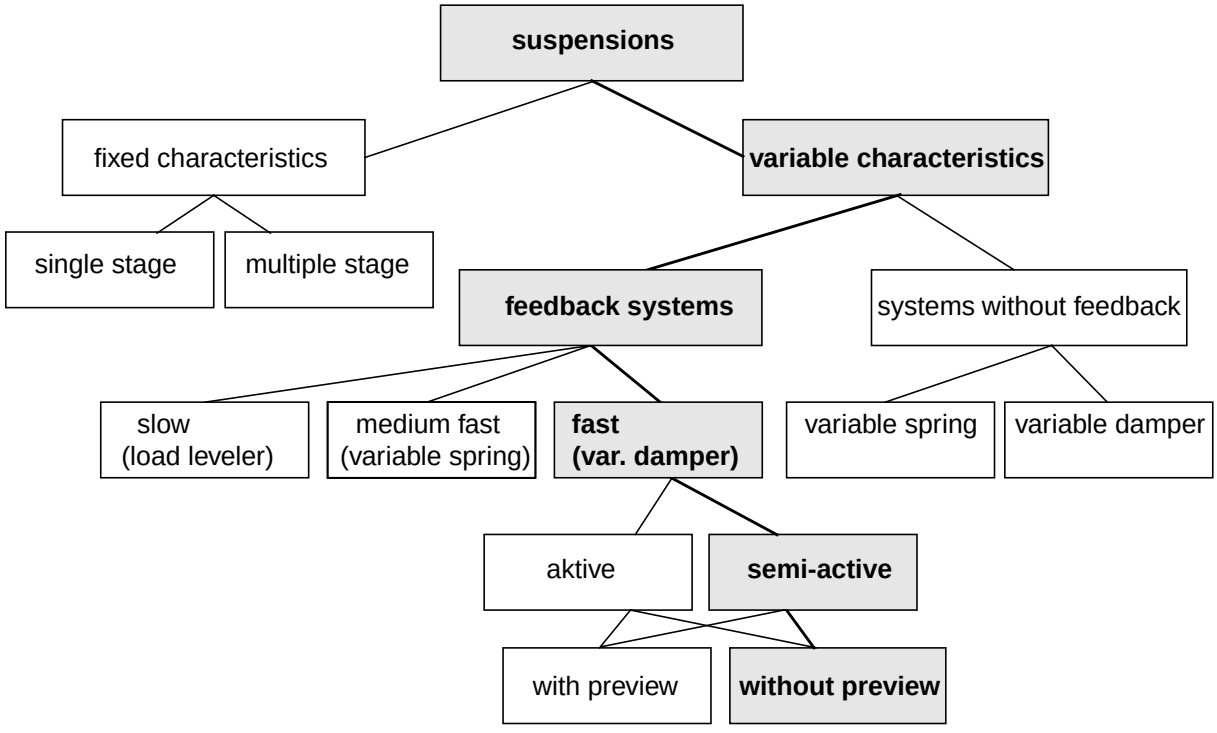

Figure 10: Suspensions of variable characteristics

2.2.3 Semi-Active Landing Gears

As mentioned in section 2.2.1, requirements for the dynamic behavior of shock absorbers are different, even partly conflicting, for landing and rolling. Since certification demands the shock absorber layout for a hard landing, landing gears are optimized towards that goal. However, even this optimization is only valid for a single operational point, i.e. sinking speed and aircraft weight.

Active (“fully active”) and semi-active shock absorbers promise improvements to this conflict. Figure 11 exemplifies the differences between those concepts.

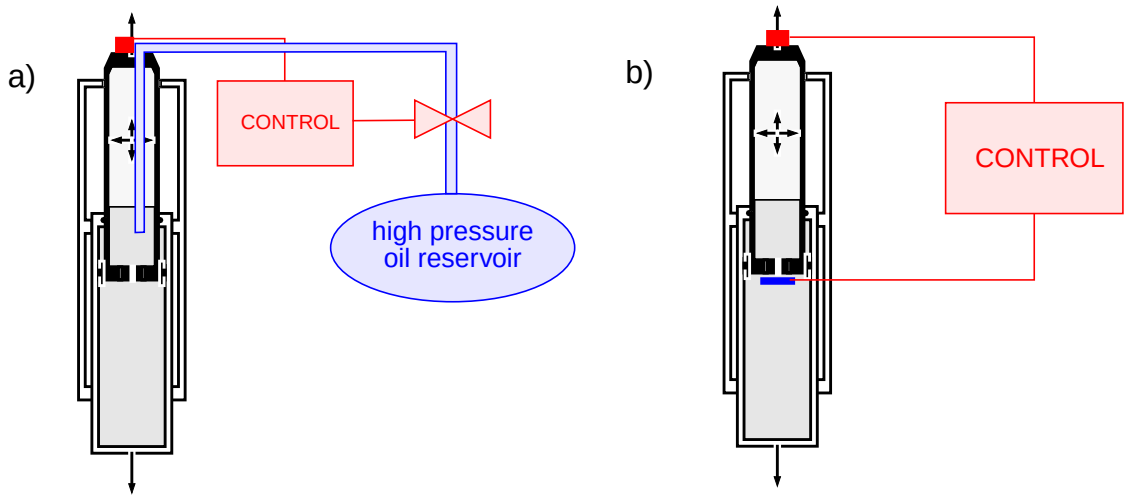

Figure 11: Active (a) and semi-active (b) damper

In active shock absorbers oil is pumped from a pressurized reservoir into the oleo and out of it, responding to the commands of the controller, Figure 11a, [101]. The principle of the semi-active oleo consists of regulating the energy dissipation by a controllable orifice, Figure 11b, [101]. Thus, the semi-active control is also known as “active damping” [8]. Contrary to the fully active systems the semi-active oleo requires no external energy supply other than for the control valve. Semi-active dampers are state-of-the-art in railway and automotive applications [94].

As for a passive damper, the applicable force in a semi-active damper depends on the sign of the stroke velocity across the damper, see Figure 12. Since, contrary to the fully active actuator, the damper can only dissipate energy, not every control command can be applied and only forces can be produced which lie in the first and third quadrant of the force-stroke velocity plane, i.e. a positive force F_d in the sense of Figure 12 can only be supplied while the oleo is compressing, a negative force can be supplied by an expanding oleo. If the controller commands a negative force during oleo compression, the best that can be done is to generate only a compression force as small as possible, in other words, to open the orifice completely. The requirement to be able to switch from force generation to near zero force generation in a very short time makes the semi-active damper an inherently highly nonlinear device.

A controller with a semi-active control scheme is often designed as if it was a fully active sys-

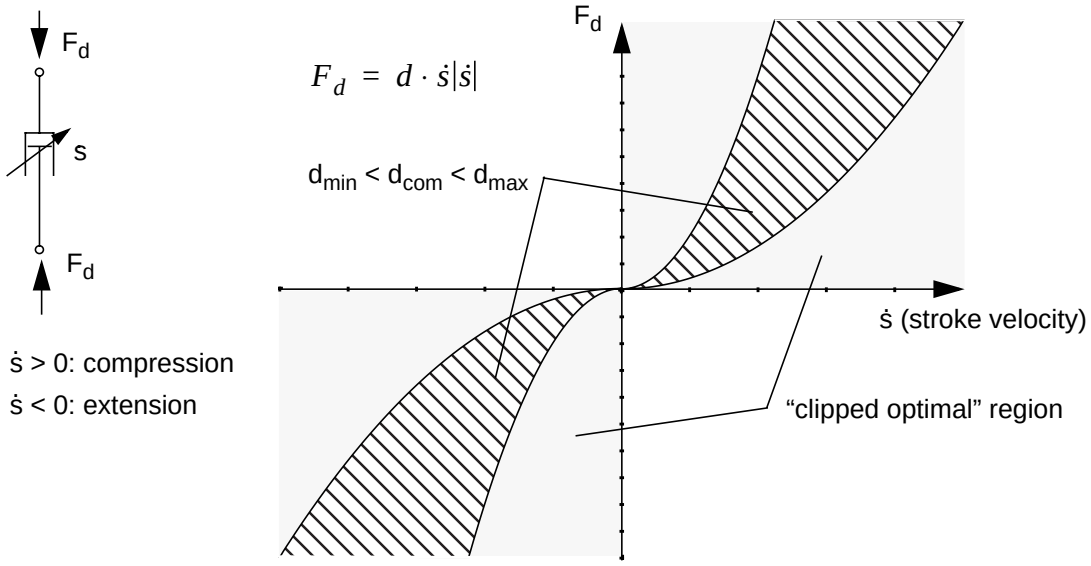

Figure 12: Principle of semi-active damping for an oil shock absorber

tem. Control commands that lie in quadrant 2 and 4 of Figure 12 are then set to zero. This is known as a “clipped optimal” approach. It will be shown in this work, however, that a purely clipped optimal design strategy, i.e. operating the semi-active oleo with the same parameters as found for the fully active controller, is only sub-optimal.

Another restriction to the clipped optimal assumptions is the fact that a technical semi-active damper has a minimum and a maximum orifice size for the oil flow, resulting in a respective minimum and maximum controllable damping coefficient. Therefore, a clipped optimal scheme has to be replaced by a realistic, limited system setting boundaries for the commands and operating with separately adapted gains.

The use of fully active landing gears has been investigated in several studies [26], [39]. No system has actually been introduced on a production aircraft since the performance improvements have not justified the increased system complexity and the additional weight encumbrance. Semi-active landing gears, however, are not considerably heavier than passive systems and less complex than their active counterparts, and are therefore better suited for aircraft applications. In addition, a semi-active oleo needs only little energy to operate a valve in order to vary the orifice cross section whereas a fully active system requires a substantial amount of energy to build up the high pressure oil supply. Very important is the fact that semi-active landing gears can fulfill the important requirement of a fail-safe design. At power loss or malfunction the characteristics of a semi-active oleo are identical to the characteristic of a non-optimized passive fixed-orifice oleo. Table 1, [101], gives an overview of advantages and disadvantages of the different shock absorber concepts.

passive	**semi-active**	active
low weight	**low weight**	high weight
satisfactory performance only for design point	**good performance over wide operational range**	good performance over wide operational range
medium complexity	**medium complexity**	high complexity
fail-safe	**fail-safe**	fail-safe?

Tabelle 1: Comparison of different landing gear concepts

2.2.4 Control Actuators

All control schemes for suspension control require an actuator in the landing gear leg. Fully active oleos have been built and tested by Howell et al [39] and by Freymann [26] as additional hydraulic pressure sources connected to the oleo by supply pipes. While Freymann uses the upper chamber for oil exchange, the lower oleo chamber is used by Howell et al, see Figure 13, [39], [26]. Otherwise, both test actuator set-ups are similar, feeding back for control purposes the information of an acceleration sensor at the top of the landing gear, a linear potentiometer for the measurement of the oleo stroke and a pressure gauge for the measurement of the hydraulic pressure in the actuator. Servo valves are used to regulate the oil flow.

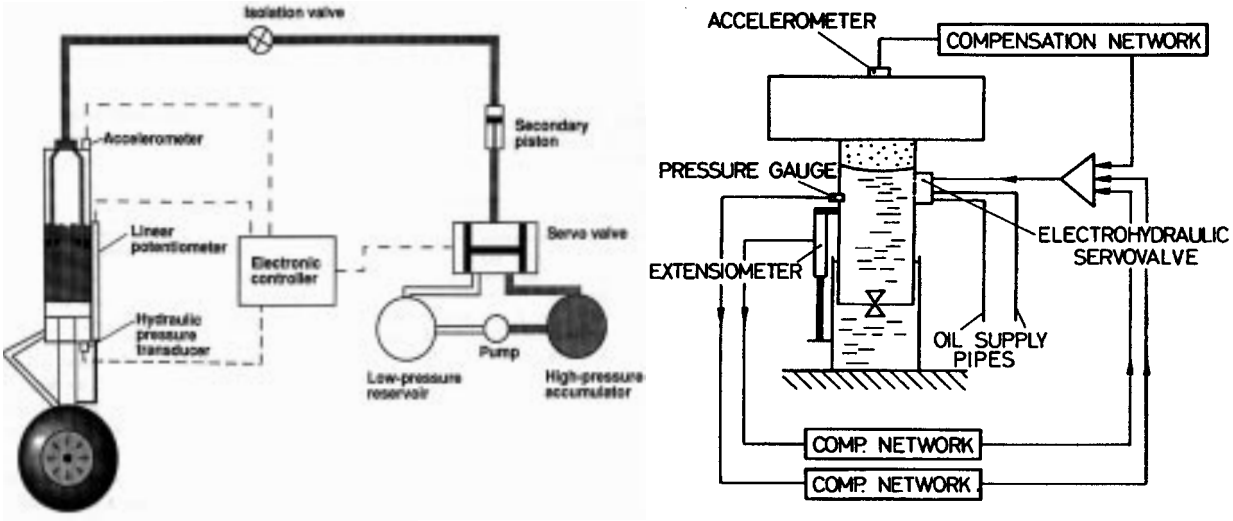

Figure 13: Active landing gear control

The dynamic response of the actuators is of special interest for the evaluation of the control performance. While in [39] no comments are made concerning the actuator response time since the test rig was used for drop-test evaluation and dynamic response was no prime topic, Freymann notes a significant delay between actuation signal and pressure build-up in the oleo.

According to [26], the reason for this delay is that a large volume of hydraulic oil has to be inserted into the upper oil chamber of the oleo in order to compress the gas enclosed in the reservoir before a significant pressure is built up. A phase angle of 90˚ at 0...5 Hz was observed by the author.

Besinger et al [2] investigated the dynamic behavior of a semi-active damper. Using a car shock absorber on a hardware-in-the-loop test rig, transition responses for switching of a semi-active damper were recorded. For the given set-up, a response time of approximately 5 ms between the applied control signal and the damper force response was recorded. The time for the damper force to reach its steady state level results in an additional 10 to 15 ms, almost independent of the velocity across the damper, indicating that the force transients are governed by a stiff linear compliance. Causemann and Irmscher of Sachs Boge reported similar response times for their automotive by-pass shock absorber design [9]. For a semi-active truck damper a time delay of approximately 5 ms after application of the control current in a phase of adaptation due to electrodynamics, valve dynamics and oil compressibility could be measured. The time to full adjustment was 35 ms for closing and 15 ms for opening [94]. The semi-active landing gear test rig built up by Liebherr Aerospace consists of a helicopter nose landing gear with a modified oleo also equipped with a by-pass system based on a commercially available servo-electric valve with a cut-off frequency of 20 Hz [107]. The performance of active and semi-active control as a function of the actuator response time is investigated in chapter 5.1.3.

Force control of a semi-active landing gear can be achieved in two ways [2] - open loop response, where the damping coefficient is selected for a given demanded force and damper velocity using a look-up table, and force feedback control where the damping rate is adjusted according to the error between measured and desired damping forces. Open loop control requires relatively simple instrumentation to measure the velocity across the oleo; however, the performance of the suspension is subject to changes in damper characteristics due to temperature variations and wear. Force feedback requires more complex instrumentation since the damper force needs to be monitored continuously, e.g. by pressure gauges in the upper and lower oleo oil chambers, but it offers the advantage of being insensitive to changes in damper characteristics. It is shown in [2] that the open loop control displays a faster dynamic response than the force feedback scheme. In the case of the studies performed in this theses an open loop control is assumed. The commanded damping force is transformed into a commanded damping orifice cross section, using pre-set values for the mechanical properties of the system, e.g. for oil density. It is one of the important open points to verify in practical tests whether this assumption can remain valid for the whole operational range.

2.3 Modern Landing Gear Design: Concurrent Engineering and Multi-body System Simulation

2.3.1 Landing Gear Design as a Part of the Aircraft Design Process

The landing gear design is one of the fundamental aspects of the aircraft design [14]. A number of engineering disciplines are involved since the quality of a landing gear concept depends on the efficiency of the overall system integration.

The traditional landing gear design process has been described in textbooks by Conway [11] and Currey [14]. This process is based on experience and, in its early phase, based upon geometric considerations, i.e. questions of landing gear configuration and its integration into the fuselage and the wings.

At the start of the design process the possible range of the aircraft center of gravity has to be determined. This information is required not only for flight mechanics but also to position the landing gear according tol ground stability, maneuverability and clearance requirements. The design has to make sure that the vector sum of weight and applied forces under static and dynamic conditions will not result in a point outside the triangle determined by the nose and the main gears. The aircraft is in danger of tipping over if the distance between center of gravity and the connecting line between the main landing gears is very small, an example being the Boeing 727 which is mostly parked with the rear airstairs down [10]. At some aircraft this constraint has led to main landing gears which are strongly tilted backwards, resulting in high oleo friction (see chapter 3.3.4). On the other hand, the center of gravity should not be located too far to the front in order to allow the aircraft to rotate at take-off. In most aircraft about 85% to 92% of the weight is distributed on the main landing gears [10] which is also of advantage for a short stopping distance; in most cases only the main landing gears are equipped with a brake. The track of the main landing gears is limited by the fact that the aircraft has to be able to make a curve of 180˚ on the runway.

Another important aspect are the mission requirements. A military transport aircraft able to start on short unpaved runways will require a different suspension layout than a civil transport aircraft operating from international airports.

As mentioned in section 2.1.1, flotation requirements, i.e. the number and size of tires for an aircraft of a given mass, are essential for aircraft operation on airports. The certification rules for encumbrance of paved runways can be found in the Aircraft-Pavement Classification Number (ACN-PCN) [110]. The ACN of a certain aircraft determines whether an aircraft is cleared to operate out of an airport with a given PCN. As a consequence, for an Airbus A320 (199 tons MTOW) six wheels are sufficient, an A340 (275 tons MTOW) needs 12 wheels, and the planned A380 (up to 550 tons MTOW) will probably be equipped with 22 wheels. Additional wheels, however, mean higher landing gear mass; one wheel of an A340 including tire and brake, for example, weighs about 350 kg. Only static tire loads are considered for certification purposes, no criterion for dynamic loads exists yet. However, studies performed on trucks indicate that improved suspension layout can also lead to reduced dynamic pavement loads [94].

In a further step, the shock absorber is designed. The most important considerations concerning the shock absorber design have been discussed above in chapter 2.2.1. A load analysis follows as landing gear loads are decisive for much of the fuselage. While the wings and the wing spar frame are dimensioned by gust loads the fuselage aft section is often dimensioned by the bending moment resulting from the impulse of the landing through the main landing gears [59]. Finally, the retraction mechanism has to be designed and a first weight estimation can be given.

Many decisive criteria like number of tires and brakes for flotation analysis as well as the shock absorber design must be defined considering international standards and design regulations as the above-mentioned ACN-PCN [111] and the FAR/JAR 25 [112]. This makes the landing gear one of the key systems in the pre-design, as a change of configuration will be difficult and costly late in the development phase. Two examples for such a late change in the design have been the third main landing gear on the fuselage of the DC-10-30 and the A300, where the wheels were placed further apart on the bogie which was mainly necessary to fulfill the runway load requirements of New York LaGuardia Airport [10].

Since the design and production of a large aircraft requires enormous manpower and often extremely specified know-how, aircraft and landing gears are often designed by different companies. After the specification of the requirements and the basic geometrical data the development and production of the landing gear is given to a specialized company which develops the gears according to the airframer's specification and the certification requirements.

At present, the main certification requirements for the landing gear design are formulated for the whole aircraft and for the single landing gear. The ground load requirements for the whole aircraft can be found in FAR/JAR 25.471 ff. The manufacturer has to prove that the aircraft is able to withstand a landing at the following conditions:

- The aircraft is in a steady state prior to touch-down.
- The landing is symmetrical, i.e. no roll and no yaw angle.
- The descend rate is 10 ft/s = 3.05 m/s at maximum landing weight (MLW).
- The horizontal speed is V_{l1} (= stalling speed V_{s0} at sea level, about 70 m/s for an A340).
- Calculations have to be performed for minimum pitch angle, "three-point landing", and for maximum pitch angle, "tail-down landing".
- as well as for critical (extreme for and aft, vertical and lateral) aircraft centers of gravity.
- The descend rate is 6 ft/s (= 1.83 m/s) at a landing with maximum take-off weight (MTOW).
- Aircraft lift may be assumed to exist throughout the landing impact; no bottoming of any of the energy absorbing elements may occur.
- A dynamic response of the structure must be covered by an analysis at a limit descent velocity of 10 ft/s for the complete flight structure.

The landing itself gear has to fulfill the requirements of FAR/JAR 25.721:

- The limit load factors of FAR/JAR 25.721 must not be exceeded. This must be shown by energy absorption tests, either with a complete aircraft, or with a complete landing gear in a drop test from 18.7 in (for MLW) and 6.7 in (for MTOW) with an equivalent substitutional mass.
- Additionally, the landing gear must be able to withstand a landing at a vertical velocity of 12 ft/s (= 3.66 m/s, drop test from 27 in) at a horizontal velocity of zero; in practice, sink speeds of this magnitude rarely occur due to ground effect and flare-out of the aircraft prior to landing.

Next to simulation and excessive calculations with finite element models of the landing gears the manufacturers perform a number of practical tests. As seen above, drop-tests are mandatory, as well for verification of the loads as for fine-tuning of shock absorber parameters.

In the landing gear simulation and at the drop-test the aircraft is usually represented as a substitutional mass. Lift is simulated by simple force laws in the simulation and with auxiliary means, e.g. aluminum bee-hive structures at the test rig [90]. It is evident that the dynamics of the airframe are included only inadequately which can lead to unwanted influence of the structural elasticity on the loads and, vice versa, of unexpected influence of the landing gear dynamics on the natural frequencies of the aircraft. However, there are only a few certification requirements for rolling, most of them concerned with braking and turning [112].

It should be mentioned at this point that another decisive factor for loads and dynamics is the aircraft tire. Modeling the tire characteristics is a science for itself. Tire models vary depending on load direction (vertical and lateral models) and frequency range of interest (low frequency: e.g. touch-down, braking, turning; high frequency: e.g. shimmy). In 1941, von Schlippe and Dietrich [84] have analyzed the shimmy motion of the aircraft and have described the interaction of tire and landing gear leg stiffness with tire forces analytically. Pacejka [71] uses a similar tire model based on the stretched string concept and developed simple derivatives representing first order lag with a relaxation length and a gyroscopic couple coefficient as parameters. For the description of steady state slip characteristics empirical expressions have been developed by Bakker and Pacejka [1], using trigonometric functions; this model is known as the “Magic Formula”. Recently this model has been extended to dynamic tire forces. The tire model of Moreland [68] is also frequently used in aircraft landing gear dynamics research. Reference [72] gives an overview of tire models used in vehicle dynamics analysis.

Independently from the theoretical approach, tire models have to be validated by measurements on drums or test trucks. Results differ widely between test methods and, even if the same methods are applied, between tires of the same type from different production batches. Additionally, tire properties depend on tire pressure, wear, and external conditions like temperature and road or drum surface properties. Also, while a lot of testing dating back to the fifties has been performed for radial tires [87], only few validated theoretical models of bias tire exist even though they have been successfully used on aircraft for many years. Thus, in many cases today’s tire models are sufficient for simulations giving trends, but many questions are still open to research, if precise results are expected from simulations [57].

The conventional landing gear layout process is well understood and has been proven to lead to satisfactory designs in most cases, even though a number of last-minute modifications have been necessary for production aircraft [10]. However, newly developed aircraft will depend on more integrated design approaches for light and reliable designs, especially if novel aircraft concepts are concerned for which classic approaches might not applicable and no comparable experience is available. This will be the case for the Airbus A380, for a potential Supersonic Civil Transport Aircraft [81] and especially for blended wing-body configurations.
An essential element of new design methods will be an exchange of models and simulation results between the involved disciplines and manufacturers at all design stages to identify problems of system integration that might lead to expensive re-design late in the development due to unsufficient load prediction or unexpected fuselage vibrations. Aspects of such integrated design methods are discussed in the next sections.

2.3.2 Multibody Simulation in the Concurrent Engineering Process

At the development of a new aircraft, engineers of several disciplines are involved, under pressure of decreasing development time and of limited financial resources. As manufacturers as well as civil and military customers try to incorporate multidisciplinary design methods in the conceptual design phase [36], a more systematic approach needs to be introduced. A number of projects and programs aim at providing the designer with tools to automate the multidisciplinary analysis. Examples of this development are the programs MIDAS and MEPHISTO of Daimler Benz Aerospace Airbus [78], [79], and the more landing gear oriented package presented by Chai and Mason [10].
Modeling and computer simulation have become tools in all engineering disciplines. The most widely used are computer aided design (CAD), finite element analysis (FEA), flight dynamics, control design (often called CACE - Computer Aided Control Engineering), and computational fluid dynamics (CFD). A mediating role between these disciplines is taken by the multibody simulation (MBS) approach. It aims at the simulation of the total aircraft dynamics and offers a good compromise between “fast”, “robust”, and “exact” simulation [83].
All those methods can be summarized by the term “computer aided engineering” (CAE). However, the models used in the engineering fields differ considerably depending on application and the complexity of the task. As an example, in “classical” flight mechanics the aircraft was often represented as a point mass (the coupling of flight mechanical and structural oscillations, of course, today demands a more detailed modeling). Contrary to that, the methods of the finite element analysis and computational fluid dynamics decompose structure and surface of the aircraft in millions of small computational units, a development that has been made possible by the powerful improvement of computer hardware and software in the last decades. In addition, modern CAD programs allow the design of a virtual prototype before a single component is in production. However, this large versatility of models requires an enormous, sometimes redundant modeling effort, and makes it difficult to exchange the obtained results [32], [83], [93].

Furthermore, the advent of microelectronics into mechanical engineering led to a close interaction between mechanical and electronical components. This combination of the two “classical” disciplines, mechanical and electronical engineering, led to a new discipline, called “Mechatronics” [52]. In these kind of systems the dynamics are not only determined by properties of the mechanical components but also of the control design.

For mechatronic systems an integrated design of mechanical structures and control is indispensable. Multibody simulation is well suited for this procedure and is therefore an important tool in the concurrent engineering process. Multibody simulation allows model simulation and analysis using the know-how of all engineering disciplines mentioned above. To be able to perform these tasks, the program needs intelligent bi-directional interfaces to tools of neighboring disciplines like CAD, FEA, and CACE which allow a continuous comprehensive data exchange. Multibody simulation is suitable both for the pre-design and for the analysis of existing systems, and can be applied for stability and comfort analysis, aircraft response on certain maneuvers, for ground and gust loads, and for life-time prediction. A further help for the design process is the possibility to perform parameter studies on a complex simulation model and to optimize free parameters (“design-by-simulation”). Finally, an MBS program is used to calculate system response in a large number of critical operational cases automatically which is of advantage for certification cases. A multibody simulation tool which fulfills these requirements is an essential part of the integrated design process.

During the development of an aircraft it will frequently be the case that the modifications of one engineering group will lead to a change in the configuration and, therefore, to a change of the complete system dynamics. Modifications can have influences on other components, as an example will illustrate: a modified landing gear can result in increased loads at the attachment points between landing gear and structure and enforce a recalculation of the dimensioning of the structure. The example presented in section 2.3.3 shows that it is not sufficient to make fixed assumptions about the system at an early point - a concurrent model exchange among all related disciplines has to become the rule. Only in this way the effects of local changes on the whole aircraft can be assessed.

Concurrent engineering methods are developed in national and international projects by industry and research. In the field of aeronautics the EU-program ENHANCE (ENHanced AEro-Nautical Concurrent Engineering) [106] has to be mentioned, on a national level the Flexible Aircraft Project [59], and on an industrial level the Airbus ACE (Airbus Concurrent Engineering) program [65].

This thesis is a contribution to the concurrent engineering process, particularly to the integrated design of aircraft and landing gears. Much of the modeling work is based on experience gained in the Flexible Aircraft Project. In this project, the DLR played the role of an intermediate between airframer and landing gear manufacturer who are interested in airframe loads (respectively landing gear loads) and certification. Using the model expertise of the specialists, i.e. an finite element model of the structure supplied by the airframer and a landing gear model supplied by the landing gear manufacturer, DLR developed methods and software to help at the

exchange of know-how, models and results between the partners (see Figure 14, [59]). Multi-body simulation played an important role at this project as the central analysis tool for the calculation of ground loads for touch-down and taxiing. In a case study for the functionality of the process, a conventional two-stage passive shock absorber has been optimized for touch-down and taxiing and has been evaluated against a semi-active nose landing gear oleo.
Initial results of the thesis, i.e. the development of interfaces and a preliminary evaluation of a semi-active nose landing gear, have been included in the integrated design process to be used in projects such as the Flexible Aircraft and ELGAR.

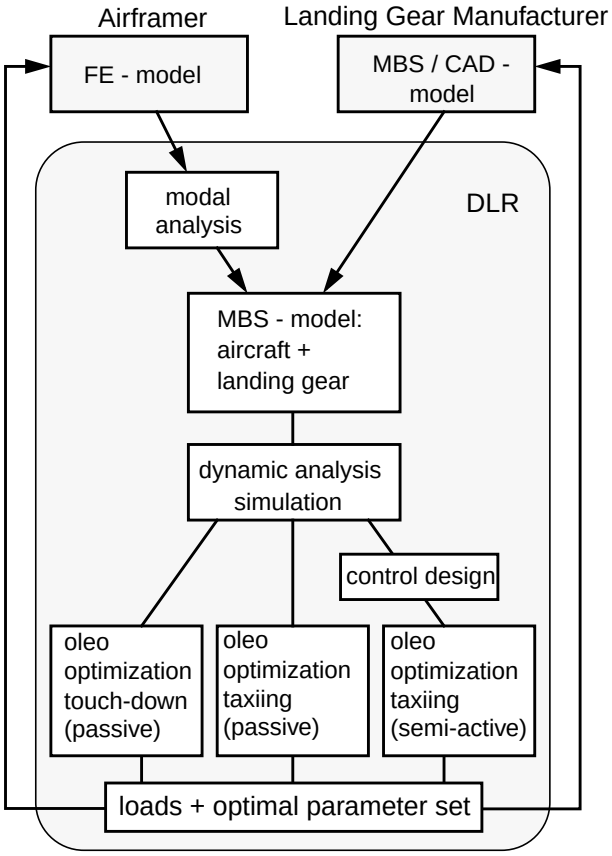

Figure 14: “Flexible Aircraft“: an application of the integrated design process

2.3.3 Simulation in Landing Gear Design

The discussion in the section above shows that simulation plays an important role in aircraft development and is essential for landing gear design. Simulations are used to assess the interaction of subsystem dynamics and to perform ride quality studies as well as “what-if” analyses. Simulation of vertical motion, e.g. the drop tests of landing gears and full (usually rigid) aircraft models, are performed to obtain the design loads which are necessary for the configuration of the landing gear structure and the oleo layout. Of great importance are also simulations of the lateral landing gear motion to assess the lateral landing gear stability against shimmy [57]. All these simulations also a part of the certification process.
In this context it is important to choose the appropriate model complexity for the given analy-

sis purpose. Traditionally, for the computation of landing gear dynamics, rather simple models as two-mass models or rigid body models have been used. However, the choice of the model complexity can have a strong influence on the validity of the results. Simplified models are valid in certain ranges only. The simulation presented in Figure 15, based on a realistic problem, exemplifies this observation: a high-speed taxi over a double (1-cos)-bump (see section 3.4) has been simulated with two models of a large transport aircraft. The first model represents mass and moments of inertia for a rigid body aircraft, the second model includes the structural dynamics of fuselage and wings up to 20 Hz. The rolling velocity is 60 m/s, the distance between the bumps 21.2 m, their height 3.8 cm. Regarding the results it can be seen that the vertical cockpit acceleration calculated with the rigid model are only one third of the accelerations predicted by the flexible model. This is due to the fact that the first fuselage flexible mode is excited by the bumps and dominates the system response. This behavior has been observed at existing aircraft which might hit a certain critical frequency at any bad runway [37]. The example shows that the use of simple models, which are sufficient to satisfy the certification rules according to FAR 25, can lead to misleading predictions and thus to a poorly tuned suspension. It is therefore important to select a model as simple as possible but as complex as necessary.

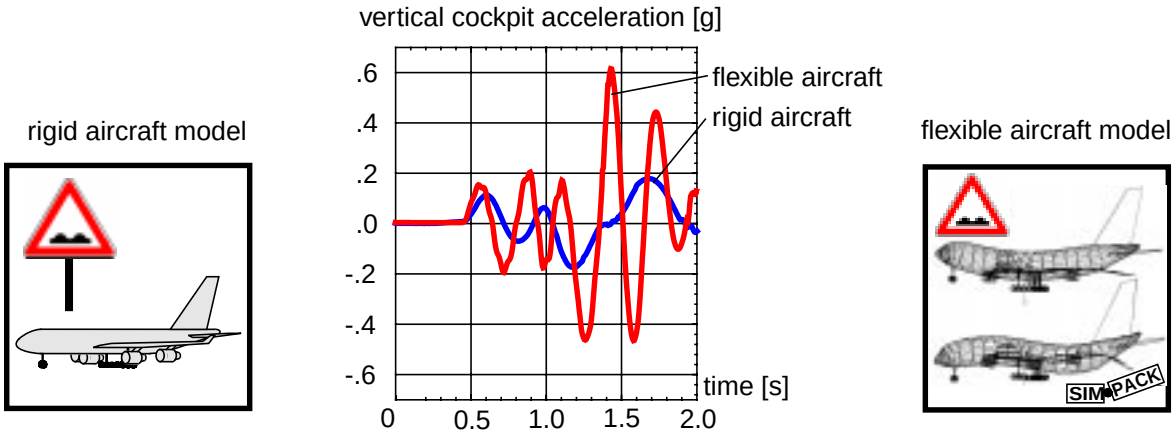

Figure 15: Simulation results for a rigid and an elastic aircraft model, taxiing over two sinusoidal bumps at a speed of 60 m/s

A number of simulation packages have been developed in recent years which are used for the purpose of landing gear simulation. The origins, aims, and usage of the programs are distinct, resulting in different approaches to the modeling of landing gear dynamics.

Three software packages based of different modeling philosophies which are used in the simulation of aircraft on the ground have been described in [57]. MECANO is based on the finite element code SAMCEF, SD-Approach is a tailor-made package for the simulation of aircraft ground dynamics, SIMPACK is based on a multibody simulation approach. Also other codes exist for these applications, [49], [27], among those the commercial multibody codes DADS [62] and ADAMS [25]. In this thesis, SIMPACK, as the central MBS simulation software of DLR has been selected for modeling and simulation.

2.3.4 Methodology of Simulation, Control Design and Analysis

This thesis has three central parts - aircraft and landing gear modeling (chapter 3), control design (chapter 4), and performance evaluation (chapter 5). The following section provides an overview of the chosen approach. The software packages which have been used will be presented in detail below.

Modeling and Data

As the central tool for the complete process cycle from modeling to analysis of the control law performance the multibody simulation tool SIMPACK is chosen. The integration of the complete model as well as analysis and optimization of control parameters were performed inside this tool.

A major model basis is a condensed finite element model of the fuselage and wings of a large transport aircraft which has been supplied by the aircraft manufacturer. This airframe model is transferred into the simulation by the pre-processor FEMBS, see section 3.2.1. The simulation model of the landing gears has been set up by the landing gear manufacturer in ADAMS and has also been transferred to SIMPACK, section 3.2.2. Force elements describing the physical properties of the shock absorber are taken from SIMPACK library elements or are user-coded, section 3.3. The tire model is also based on a SIMPACK library element which has been modified by a comparison with measured data supplied by the airframer. The runway data have come from the same source; data for two runways profiles are available which can be used directly in the simulation, section 3.4. All modeling information, i.e. MBS elements, elastic data, runway profiles, are stored in a central project data base.

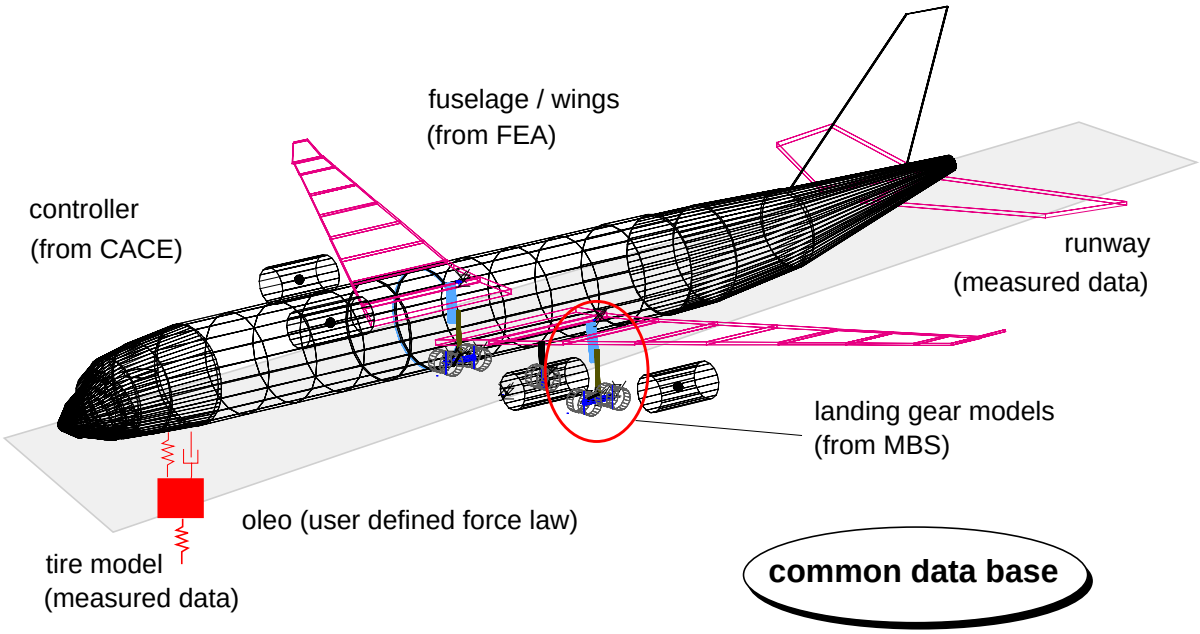

Figure 16: Aircraft model data sources

Control Layout

The control design is performed by using SIMPACK and MATRIXx in parallel. Design models of different complexity are derived from the full model which are transferred via the SIMAX interface, section 2.3.5, to MATRIXx's SystemBuild simulation environment.
The controllers are set up and tested completely in MATRIXx. After the design, controllers are exported as force elements from MATRIXx, section 4.3. Using this interface, complex control structures can be implemented in SIMPACK.
A special contribution by the author to the process used in the thesis is the development of the SIMAT interface which enables the transfer of models and controllers between MATRIXx and SystemBuild on the one side and SIMPACK on the other side, see section 2.3.5.

Multi-Objective Optimization:

As a final part of this investigation the optimization of the control parameters using the SIMPACK full model for different load cases and speeds with the program SIMPACK-MOPS is performed. Because of the strong nonlinearities in the semi-active suspension (see section 3.3.3) and the quasi-stochastic nature of the excitation (see section 3.4), the final sets of control parameters have not been derived by linear control design methods but rather by multi-objective parameter optimization [44]. This optimization method finds a "best compromise" between several conflicting criteria. The algorithm tries to reduce all criteria such that no further criterion can be improved without deteriorating the others. Here, optimization is based on time integrations of the mechanical system. Those time integrations for simulation and evaluation are performed in the multibody simulation (MBS) tool where all nonlinearities and excitations can be modeled in detail; furthermore, the highly optimized integrators of the MBS tool allow rather short integration times. The optimization part, minimization of criteria and modification of the model, is done in a multi-objective parameter optimization (MOPO) tool coupled to the MBS tool. The free system parameters are varied by the MOPO routines within their given limits until an optimal compromise between the criteria is found; for details see section 4.3.2.

Software Tools

As we may see from the procedure, several commercial software packages have been used in the course of this thesis for modeling, simulation and control design. The applied programs will be presented briefly in this section.
SIMPACK is the central MBS simulation program of DLR. It is applied in the areas of air- and space technology, vehicle system dynamics and robotics. SIMPACK has developed from a typical multibody code to an extensive simulation and analysis package for mechatronic systems with a number of interfaces to other programs of the integrated design [52], [83]. Basis of SIMPACK is a multibody formalism which generates the equations of motion. Systems are described in relative coordinates. The result is a set of ordinary differential equations (ODEs) or, in the case of kinematic loops, differential-algebraic equations (DAEs). For analysis in the

time domain SIMPACK offers a number of different integrators which are optimized for the use in numerical simulation of mechatronic systems. For all time simulations performed in this thesis, an integrator based on ODASSL, a standard solver for differential-algebraic equations [5], has been used. This integrator is a variable step size, variable order solver based on backward differential formulae (BDF) with root functions which has been adapted to the structure of multibody systems.

Beyond the solvers for time-integration a number of additional numerical analysis methods being part of the program have been applied, in particular for linear system analysis, the linearization, eigenvalue calculation, and frequency response analysis.

The model set-up is performed using elements from the library of bodies, joints, and force elements. Additional user elements, describing the complex suspension force characteristics, have been defined using FORTRAN and C subroutines. For the simulation of mechatronic systems SIMPACK includes a library of elements for the realization of control loops which has also been used; for sensitivity and design calculations parameter variation allows the modification of up to three parameters in a loop which has been applied for parameter range checks prior to the optimization runs. Results of the simulations can be visualized in a 3D-animation or in form of data plots.

SIMPACK is included in the concurrent engineering process by its intelligent, bi-directional interfaces, see Figure 17. Flexible structures are included in the multibody simulation via the pre-processor FEMBS (see section below). The interfaces to MATRIXx have been used for control layout and have been extended as part of this thesis.

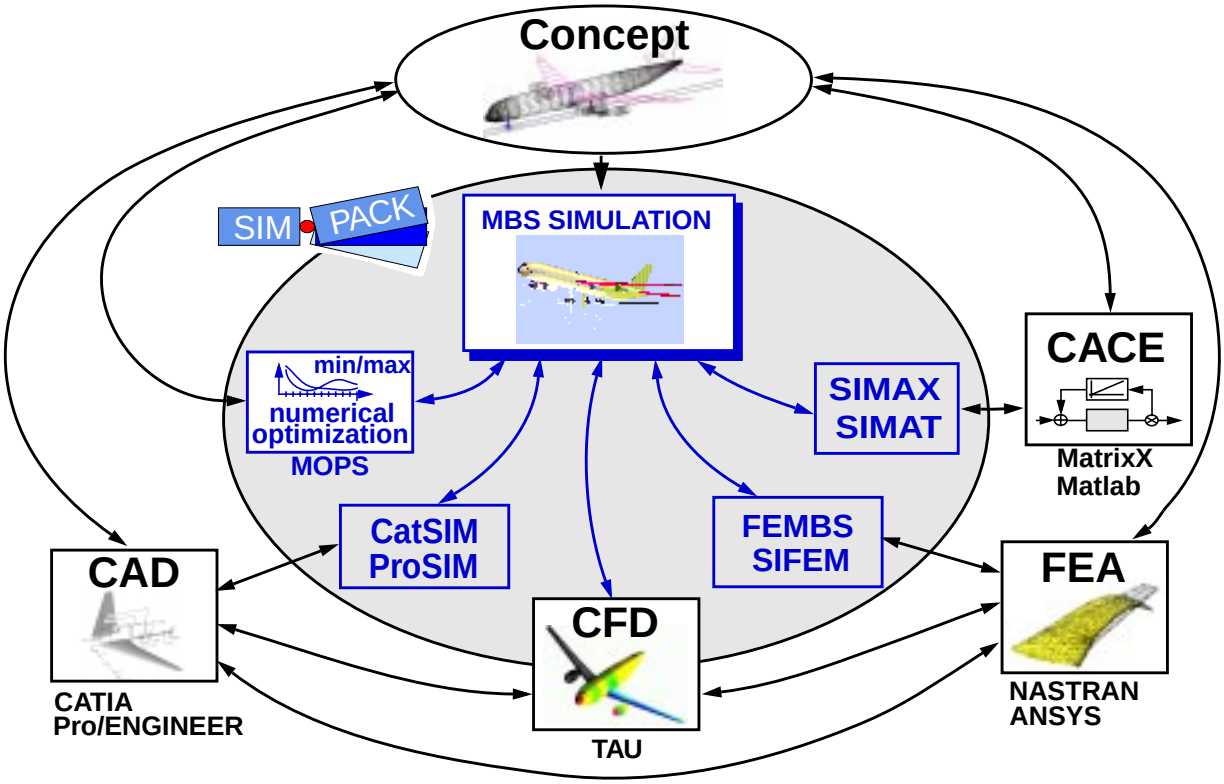

Figure 17: SIMPACK in the Concurrent Engineering Process

SIMPACK has been selected for the work of this thesis because it allows fast analysis also for complex models because of its built-in optimization routines, and because of its well-established interface to NASTRAN. Furthermore, SIMPACK made it possible for the author to develop the interface to MATRIXx which was important for the control design.

SIMPACK-MOPS is used for a multi-objective parameter optimization of SIMPACK models. This tool is based on the optimization program MOPS, also a development of DLR, which has originally been implemented within the ANDECS control engineering design environment, [30], [44]. The parameters to be optimized can be design parameters (e.g. attachment locations), free parameters in force elements (e.g. a spring stiffness) or control elements (e.g. control gains). The application of multi-objective parameter optimization is an important part of the concurrent engineering process; with MOPS, parameters of those different types mentioned above can be optimized simultaneously, while standard control design methods deal only with control parameters. Furthermore, the optimization can consist of several different models or operational cases of a model at a time ("multi-model" approach). Wentscher [101] has used an earlier implementation of SIMPACK and ANDECS-MOPS for the optimization of control parameters in his simulation of an A300 semi-active nose landing gear. In [101] and [102] a detailed description of the optimization methodology is given.

NASTRAN is a finite element program which is used by many aircraft manufacturers. Specifically, the aircraft structural model which has been used as a basic component of the simulation model was available in NASTRAN. Structures that have been set up in NASTRAN are transferred by model reduction in the pre-processor **FEMBS** into flexible bodies in the multibody simulation. FEMBS was developed at the DLR and can process models of the commercial FE-programs NASTRAN, ANSYS, ABAQUS and MARC. The output of the modal reduction process is the description of the flexible data in the Standard-Input-Data (SID) format for MBS programs [97]. Since the elasticity plays an important role in the investigations described here, a short description of the modal approach for the introduction of structural elasticity into the MBS equations is given in chapter 3.2.1.

MATRIXx is a tool for control design and system analysis which forms a design chain with its block-oriented simulation environment SystemBuild and the code generation tool AutoCode. The package is similar in structure and complexity to MATLAB / Simulink which is no coincidence since both programs evolved from the same roots, the original Matlab by Little and Moler (cf. [54]). MATRIXx offers analysis methods in the time and the frequency domain as well as many basic control design functions. MATRIXx / SystemBuild offers different interfaces for model import and export; this data exchange to and from SIMPACK can be performed via the interface **SIMAX** [60]. Since this interface has been developed by the author for the controller design in this work, the interface will be described in detail in the next section. *Remark: Since the work presented here has been finished The MathWorks, distributor of MATLAB, has also become the distributor of MATRIXx. MATRIXx will be supported until 2003 but further development is not to be anticipated.*

2.3.5 The Interface between MBS Simulation and Control Design Environment

The exchange of models and data between the MBS dynamic simulation and the control design tool has been essential for this work. SystemBuild offers a large library of pre-defined control elements for the control loop design, whereas only very simple mechanical plant models are pre-defined. Complex mechanical models usually require a lot of user-specific programming. Thus, a more effective way is to build up plant and controller in different, specialized environments, each one best suited for the respective purpose, and to transfer models from one environment to another by the means of interfaces. SIMAX, the interface between SIMPACK and MATRIXx, allows different levels of model and data exchange according to the complexity of the given task.

a) Model Transfer from SIMPACK to MATRIXx

Linear System Interface

SIMPACK models can be linearized and exported in the form of linear system matrices in a MATRIXx-readable format. The model is represented in the following form:

$$\begin{aligned} \dot{x} &= Ax + Bu \\ y &= Cx + Du \end{aligned} \tag{2.3.1}$$

where x can consist of rigid-body motion states, states of elastic bodies (in modal formulation, see section 3.2.1), and states of force elements; the input u can be any kind of excitation, prescribed motion or external force. Inside SystemBuild the model can be used directly in a state-space block. The interface allows a very fast model export, is platform independent and universal. Restrictions are, as the name suggests, the limitation to linearized models and the one-way data transfer of the MBS environment to SystemBuild. This interface has been used as a first modeling approach in the design of all controllers developed in this thesis. It was already available in the standard SIMPACK distribution for MATLAB and has been adapted for the use with MATRIXx.

Symbolic Code Interface

Models with non-negligible nonlinear effects can also be exported in a platform independent way in the form of so-called *Symbolic Code*. While generally the Symbolic Code is capable of exporting any kind of mechanical system, only models described by ordinary differential equations (ODEs) can be used by the SIMAX Symbolic Code Interface. Here, the model has the following form:

$$\begin{aligned} \dot{x} &= f(x, u) \\ y &= f(\dot{x}, x, u). \end{aligned} \tag{2.3.2}$$

SIMPACK generates model dependent, portable FORTRAN code which can be connected to the SystemBuild UserCode Block interface. With a suitable converter the symbolic code can also be transferred into C to be used in a Hardware-in-the-Loop environment. However, the

code is model dependent, i.e. if the multibody system is modified, the FORTRAN code must be generated, compiled, and linked again. Furthermore, no re-transfer of simulation results into SIMPACK is possible. The link between the symbolic code and SIMPACK has also been established for this thesis and has been used for preliminary parameter studies inside System-Build.

b) Communication between SIMPACK and MATRIXx

Function Call Interface

The maximum communication between SIMPACK and MATRIXx can be reached by the use of the Function Call Interface which allows to include SIMPACK in MATRIXx in its full functionality. The interface also works using the SystemBuild UserCode Block, forming one simulation module from MATRIXx and SIMPACK routines. The numerical integration is performed in MATRIXx which calls SIMPACK subroutines for the right-hand-side of the equations of motion. The interface is restricted to models which can be described by ordinary differential equations (equation (2.3.2). While in MATRIXx only the elements selected for the y-vector as defined in that equation are visible, all the results of the SystemBuild simulation, including the graphical animation of the multibody system, can afterwards be plotted and animated in SIMPACK. It has to be noted, however, that for the Function Call Interface both MATRIXx and SIMPACK have to be available on the same platform since a common executable is formed. Furthermore, for large systems, the integration might become slow when compared to a simulation purely inside SIMPACK because the MATRIXx integrators are not optimized for the solution of mechanical models.
The interface was developed for this thesis but was only used for simulation of the two-mass model because the integration times turned out to be unacceptable with the complex aircraft model. Here, the IPC-Co-Simulation Interface was used instead.

IPC-Co-Simulation Interface

If SIMPACK and MATRIXx are available on the same or on different platforms, a combined simulation can be performed using co-simulation via inter-process communication (IPC). In that case, each package forms its own executable which communicate by the means of sockets, i.e. a network link providing a two-way communication channel between processes, either user-programmed or based on commercial or public-domain IPC libraries [60]. Data exchange is performed in discrete time steps. Since all MBS model components are solved inside SIMPACK, taking advantage of the optimized integrators, no restrictions to modeling apply. The interface is capable of using models in the differential algebraic equation formulation (DAE):

$$\begin{aligned} 0 &= f(\dot{x}, x, u) \\ y &= f(\dot{x}, x, u) \end{aligned} \tag{2.3.3}$$

where x includes rigid body states, elastic body states, force element states, holonomic con-

straints and other algebraic equations to determine additional auxiliary conditions (e.g. for the on-line determination of accelerations and of friction forces). As in the Function Call Interface all simulation results are available for post-processing in both MATRIXx and SIMPACK. Restrictions are that due to sequential (“step-by-step”) co-simulation stability can often only be reached by very small communication intervals and, for some cases, is not even theoretically guaranteed [61].
As mentioned above, the IPC-Co-Simulation Interface was used for a coupled time simulation of MATRIXx and SIMPACK where the complex mechanical model of aircraft and landing gears could be solved by the SIMPACK internal integrator while the defined control structure remained inside SystemBuild.

c) Transfer of Control Structures from MATRIXx to SIMPACK

All the interfaces described above can be used to make an MBS model available for control design. However, once a control structure is established, it is essential that the complete model can be simulated in the MBS environment for evaluation and optimization purposes. For this reason, two ways have been developed to export a defined control loop from MATRIXx to SIMPACK.

Inverse Symbolic Code Interface

After a control design concept is set up in SystemBuild, any chosen parameters can be defined as free parameters and the control structure can be exported. For this kind of model export, MATRIXx offers the module “AutoCode” which generates portable C code from SystemBuild models. This code can be used as a user-defined control force element and connected to the multibody simulation via the SIMPACK programmable interface, the so-called “UFEL” (User Force ELement). However, the MATRIXx module “AutoCode” is separately licensed which can lead to considerable additional costs. The Inverse Symbolic Code Interface has been implemented for this thesis and used here for the export of the skyhook controller.

MBS Syntax Interface

Not all elements defined in MATRIXx/SystemBuild can be exported as AutoCode. State space systems, which are, among other applications, are needed to define a Kalman filter, belong to that group. Furthermore, sometimes the result of a MATRIXx calculation is only a gain matrix for which the AutoCode export would be too cumbersome. In this case it is possible to save the results of the control design in the syntax of single SIMPACK force elements. An element thus defined is then placed in the data base from which the simulation model is assembled, a process which has been automated by the author for the state feedback controller design by the development of special MATRIXx script files.
All interface possibilities described above are summarized in Figure 18.

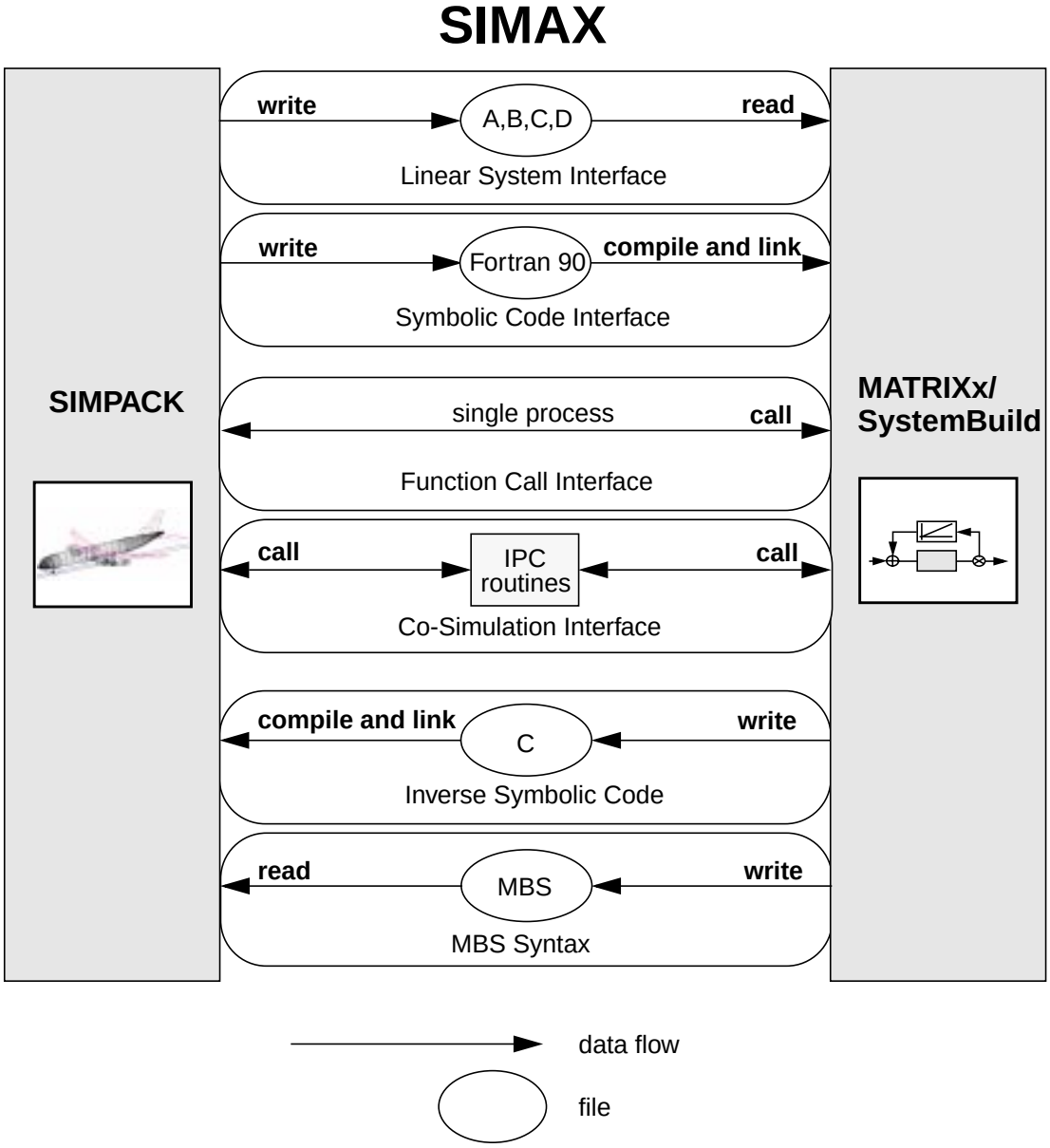

Figure 18: Interfaces between multibody simulation and control design tool

3 Modeling of Aircraft and Landing Gears for Simulation and Analysis

The simulation model of an aircraft suited to perform comfort and load analysis is complex, the data originating from a number of sources. This chapter describes the model set-up, the data used and their origin. The methods and physical background for the models of the components which make up the aircraft, e.g. fuselage, shock absorber, tires, are described as well as the excitations, the sensor locations, and the methods for the performance evaluation. Finally, a model analysis concerning observability and controllability with respect to the potential locations of sensors and the actuator, i.e. an active or semi-active landing gear, is performed.

3.1 Model Set-Up

3.1.1 The Aircraft as a Multibody System

The aircraft model has to be complex enough to cover all important system dynamics in the frequency range of interest, but at the same time as simple as possible to allow a fast analysis in the time domain. Important criteria for shock absorber design are the vertical acceleration at several aircraft locations, e.g. at cockpit and center of gravity, as well as the forces in the landing gear and its attachment points to the aircraft structure.
Since in this study only rolling is investigated, the main criterion for optimization is the improvement of passenger and pilot comfort. The decisive frequencies for vibration comfort studies lie in the range of approximately 1 to 8 Hz. To represent the aircraft dynamics, it is necessary to model fuselage and wings as flexible bodies. Basis for this example is a finite element model supplied by the aircraft manufacturer. Due to the symmetric excitation and the frequency range of interest only the most important symmetric eigenmodes up to 16 Hz and additionally three static modes are selected and included via modal reduction to be used in the MBS simulation. The elastic model and the process of its introduction into the multibody model is described in detail in section 3.2.1. The landing gears are rigid body models (section 3.2.2) with nonlinear force laws for shock absorbers and tires. The respective force laws can be found in chapter 3.3.
The complete multibody aircraft model consists of five components,

- the airframe structure, comprising fuselage and wings,
- the nose landing gear,
- two main landing gears and
- the center landing gear.

Figure 19 shows a topology map of the multibody model.

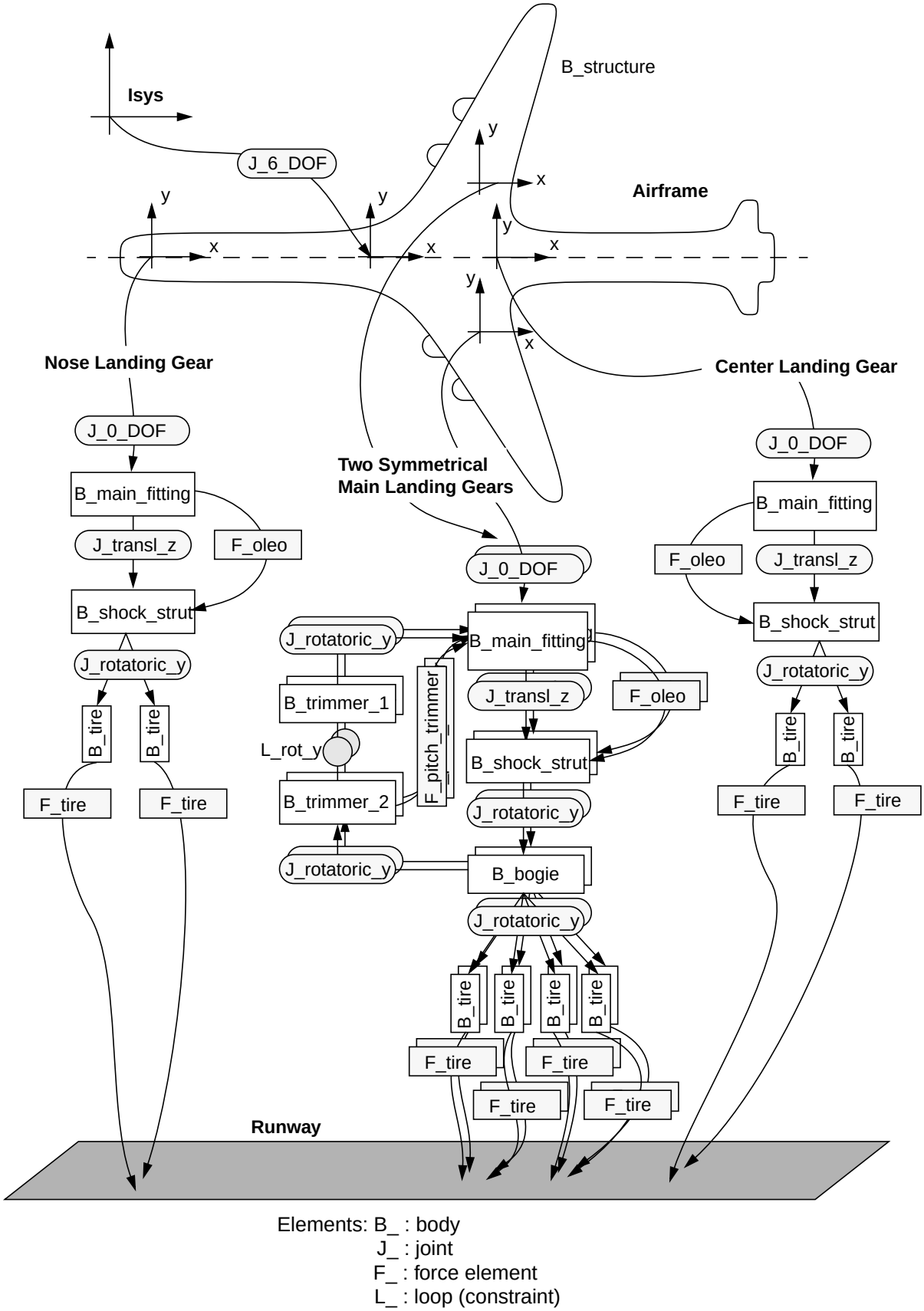

Figure 19: Topology map of the aircraft multibody model

3.1.2 Model Simplification for the Control Design Process

The rather detailed nonlinear simulation model resulting from the modeling process described so far is too complex for the early phases of the control design. Therefore, three different stages of model complexity have been used in the control design process:

“Evaluation Model”: The complete and detailed model as described in section 3.1.1 is used for evaluation purposes, especially for the analysis of the active and semi-active control law performance presented in chapter 5.

“Design model”: For control layout and optimization (chapter 4) simplifications have to be applied to reduce the time necessary for the optimization procedure. First of all, the kinematics of the rolling aircraft is linearized in good accordance to the nonlinear model. Since no braking is investigated, tires can be reduced to point followers without slip and without a rolling degree of freedom for the wheel. Additionally, the complicated kinematics of the main landing gear are simplified, and a rigid attachment of the landing gears to the airframe is used. Finally, only the lowest three symmetric elastic eigenmodes of the airframe are taken into consideration. Thus, the design model for rolling can be brought down to the 20 most important degrees of freedom.

“Two-Mass-Model:” A final simplification step is the so-called “two-mass” or - as it is called in the automotive industry - “quarter car” model. It consists of a single landing gear leg including shock absorbers, wheel and tires, and point mass substituting the respective aircraft weight. For a closer explanation of the two-mass model see section 3.2.3.

For the control design a “bottom-up” strategy is used. The basic control structure and starting values for the free parameters are selected using the “two-mass”-model. The tuning of the structure and the parameters is performed using the design model, and finally the results are evaluated using the evaluation model.

3.1.3 Equations of Motion

An elastic mechanical multibody system consists of bodies which can be rigid or elastic, and which are connected with joints or interacting via forces. While bodies have masses and moments of inertia, the connecting elements are assumed to be massless. The kinematics and dynamics of a tree-structured system with additional kinematic loops can be represented by a set of second-order differential equations in minimal coordinates with additional algebraic constraints. Such a system of differential algebraic equations (DAEs) can be represented in the so-called descriptor form:

$$\dot{p} = T(p)v(t), \tag{3.1.1}$$

$$M(p)\dot{v} = f(p, v, t) + G^T(p)\lambda, \tag{3.1.2}$$

$$0 = g(p), \tag{3.1.3}$$

$$0 = G(p)v = \frac{\partial g(p)}{\partial p}T(p)v = \dot{g}(p, v), \tag{3.1.4}$$

$$0 = G(p)\dot{v} + \dot{G}(p, v)v = \ddot{g}(p, v, \dot{v}), \tag{3.1.5}$$

using the generalized mass matrix M (of size $n_p \times n_p$), the vector of position coordinates p, velocity v, and acceleration $\dot{v}$. The kinematic equation of motion (3.1.1) describes the relation between position and velocity coordinates with the help of a coefficient matrix $T(p)$ (also of size $n_p \times n_p$). The loop closing joints are represented by a set of n_z constraints $g(p)$. These constraints are formulated, according to the numerical solution method, not only on position, but also on velocity and acceleration level, $\dot{g}(p, v)$ and $\ddot{g}(p, v, \dot{v})$, equations (3.1.3) to (3.1.5).
In the dynamic equation of motion (3.1.2), applied forces $f(p,v,t)$ and constraint forces $G^T(p)\lambda$ have to be considered. The constraint forces consist of the constraint Jacobian $G(p)$ ($\partial g/\partial p$, size $n_z \times n_p$) and the Lagrange multiplicators λ.
The most extensive amount of computational effort is taken up by the solution of the dynamical equation of motion. Two basic strategies exist:

- algorithms which explicitly calculate the mass matrix M, which then has to be inverted; the computational effort increases quadratically with the number of bodies in the system;
- O(N)-algorithms: at these recursive algorithms the computational effort increases only linearly with the number of bodies [4], [83] because the dynamic equation of motion is generated directly in the form

$$\dot{v} = h(\lambda, p, v, t) = M^{-1}(f(p, v, t) + G^T\lambda). \tag{3.1.6}$$

One of the significant properties of the O(N) algorithm is the fact that because of the recursive nature of the strategy the inversion of the mass matrix M is avoided. As a consequence, however, the matrices M, f, and G are not directly available during the computation.
The O(N) algorithm for the automatic generation of the equations of motion used by SIMPACK cannot be outlined here but is described in detail in [83]. The equations of motion for the elastic aircraft include the following elements:

- rigid body motion of the airframe and the landing gears, including wheels and bogies;
- linear elastic deformation of the airframe;
- applied forces of air springs, dampers, friction, tires;
- algebraic states for the loop-closing conditions for pitch dampers in the main landing gears;
- algebraic states for the constraint forces in the main landing gears for the calculation of bending friction.

The mathematical approach for introducing the equations for elastic bodies into the multibody system will be given in chapter 3.2.1. The equations describing the applied forces will be presented in detail in chapter 3.3.
The nonlinear equations of motion have been used in all time integrations performed for this thesis. For the linear system analysis and for the aircraft model which is needed as basis of the model-based Kalman filter and state feedback controller design a linearized aircraft model has been derived. The differential equations are linearized inside SIMPACK by the following two-sided differential quotient

$$A]_{ij} = \frac{f_i(x_j + \Delta x_j) - f_i(x_j - \Delta x_j}{2\Delta x_j} \tag{3.1.7}$$

to the standard linear system

$$\Delta\dot{x} = A\Delta x + Bu(t)\,. \tag{3.1.8}$$

3.2 Airframe and Landing Gears

3.2.1 Airframe Model

The description of the airframe is based on a finite element (NASTRAN) model which had been prepared by the airframer for flutter studies and which was expanded with attachments for the landing gears in the course of the Flexible Aircraft Project [59]. In this model, the airframe is represented as a beam structure comprising fuselage, wings, and empennage. The engines are represented as concentrated masses with predefined moments of inertia. Three different load cases have been available which had been cleared for use by the aircraft manufacturer for the Flexible Aircraft Project:

- maximum take-off weight (MTOW = 250 t),
- maximum landing weight (MLW = 190 t),
- operational weight empty (OWE = 150 t).

The expanded flutter model consists of 555 grid points and 352 elastic modes representing structural elasticity in the frequency range of up to 100 Hz. For the simulation of ground dynamics and comfort analysis, however, only the low frequency modes of fuselage and wings are of interest and a lower model complexity is desirable to reduce computation times for the multibody simulation and the optimization of control parameters. As shown later in Figure 35 (chapter 3.5.2), the frequencies of interest for vibration comfort studies lie in the range of approximately 1 to 8 Hz. However, to detect possible deterioration of comfort at higher frequencies and to fulfill Shannon's theorem (the frequency of the measurements has to be at least twice as high as the highest frequency to be evaluated, [101]), elastic modes up to 16 Hz are considered in the model.

Thus, during the transformation process from NASTRAN to SIMPACK a further model reduction is performed by the selection of specific modes according to the following strategy: a modal analysis is performed inside NASTRAN with the complete expanded flutter model, supplying all natural frequencies and mode shapes of the complex model. From those results, 90 grid points (of the available 555 points) are selected in the pre-processor FEMBS for use in the multibody simulation program. The grids are chosen to be fairly uniformly distributed over wings and fuselage to be able to visualize the elastic deformation of the structure; additionally, three grid points are selected as attachment points for each landing gear, respectively. Furthermore, a set of elastic modes is chosen. The selection of modes is based upon the influence of each mode on the overall system dynamics in the frequency range of interest. Since all excita-

tion cases are symmetric the following airframe modes have been chosen for the simulation:

- symmetric fuselage bending modes up to 16 Hz,
- symmetric wing bending modes up to 16 Hz,
- wing torsion modes, excited largely by pitching of the engines.

All antimetric modes up to 16 Hz and all modes above 16 Hz have thus been neglected.

The grid points are not only useful to visualize the elastic deformation; in addition, at each of the 90 selected grid points on the elastic body, kinematic measurements (displacement, velocity, acceleration) can be obtained during integration. These measurements are necessary for controller feedback as well as for evaluation of the results. A list of the locations selected for the sensors placement can be found in section 3.5.

The elastic deformation is included in the equations of motion (3.1.1) - (3.1.5) by means of the modal approach. According to that method, any deformation of a flexible structure can be represented if a sufficient number of free eigenmodes are included into the model. For this purpose the spatial motion of the elastic body is split into a global motion *s(t)*, characterized by the movements of a body reference frame, and its (small and linearized) elastic deformation which is expressed by the displacements *u(r,t)* of all body points with respect to the body reference frame, with *r* remaining constant, see Figure 20:

$$r_P(t) = s(t) + r + u(r, t) \; . \tag{3.2.1}$$

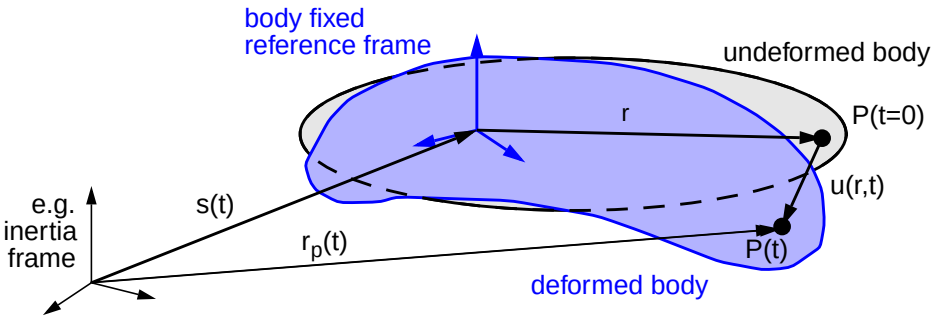

Figure 20: Separation of global motion and deformation

The global motion of the airframe has six degrees of freedom relative to the inertial system. For the representation of the elastic motion, the location and time dependent body deformation vector *u(r,t)* is split by a separation function, often referred to as “Ritz approach” [16], into a location dependent displacement matrix $\Phi(r)$ and the corresponding time dependent vector of elastic modes *q(t)*:

$$u(r, t) = \Phi(r)q(t) \, . \tag{3.2.2}$$

The displacement matrix consists of mode shapes resulting from eigenvalue and static load analyses. The eigen- and static modes as well as the stiffness matrix are computed in FEA; additionally, geometric stiffening effects, e.g. due to centrifugal forces, are included. FEMBS enables the user to select only those modes which are necessary to represent the body flexibility for the individual load case. Finally, the equations of motion of the multibody system are expanded by n_q additional states *q(t)* describing the elastic deformation, including additional

rows and columns in the mass matrix, the gyroscopic terms, the stiffness matrix, and the external forces. A detailed representation of the specific elements of the expanded “elastic” equations of motion can be found in [97].

As mentioned, any deformation of a flexible structure can be represented by the modal approach if a sufficiently large number of free modes are included in the model. Calculations performed in the process of the model set-up, however, showed that the free modes up to 16 Hz chosen for the airframe model were not able to correctly represent static aircraft bending on the landing gears, and a great number of additional higher eigenmodes would be necessary to approximate the static deformation, leading to an unreasonably large multibody model. To overcome this problem of the “classical” Ritz approach working with free modes, two static modes of the aircraft on the landing gears have been included in addition to the eigenmodes, see Figure 21. For the determination of those modes, the finite element model of the aircraft is supported on the landing gear attachment points and a static analysis is performed in the finite element program. The resulting deformation is called the static mode and added to the free modes for simulation of the multibody model. Structural damping can be included and has been chosen to be 1% for all modes; discussions with the airframer shows this value to be sufficiently exact for low frequency excitations [59].

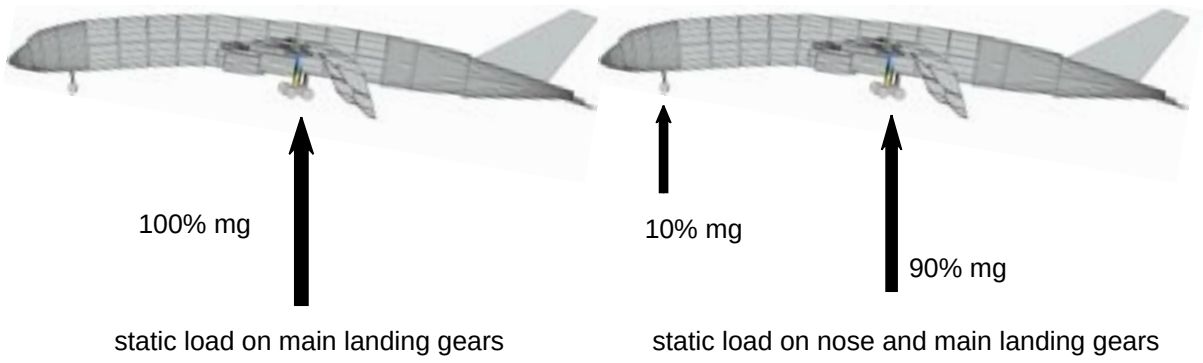

Figure 21: Calculation of static modes of the flexible aircraft model

3.2.2 Landing Gear Models

Figure 22 shows the graphic display of the simulation model of nose landing gear, main landing gear, and center landing gear. The models consist of the main fitting, the shock tube, and two or four wheels, respectively. The shock absorbers (oleo) are located between shock tube and main fitting. The main landing gears include an additional bogie tilted 15° during the approach shortly before touch-down. It is fixed at that angle by the pitch trimmer. At touch-down, the shock tube starts to contract into the main fitting only after the pitch trimmer has been totally compressed; this kinematic solution leads to a two-stage suspension characteristic. All landing gears have one translational degree of freedom for the shock absorber and one rotational degree of freedom for each wheel. The main landing gear pitch trimmer is described by two additional degrees of freedom, one for each link, as well as a kinematic constraint between the two links and a force acting between pitch trimmer and main fitting.

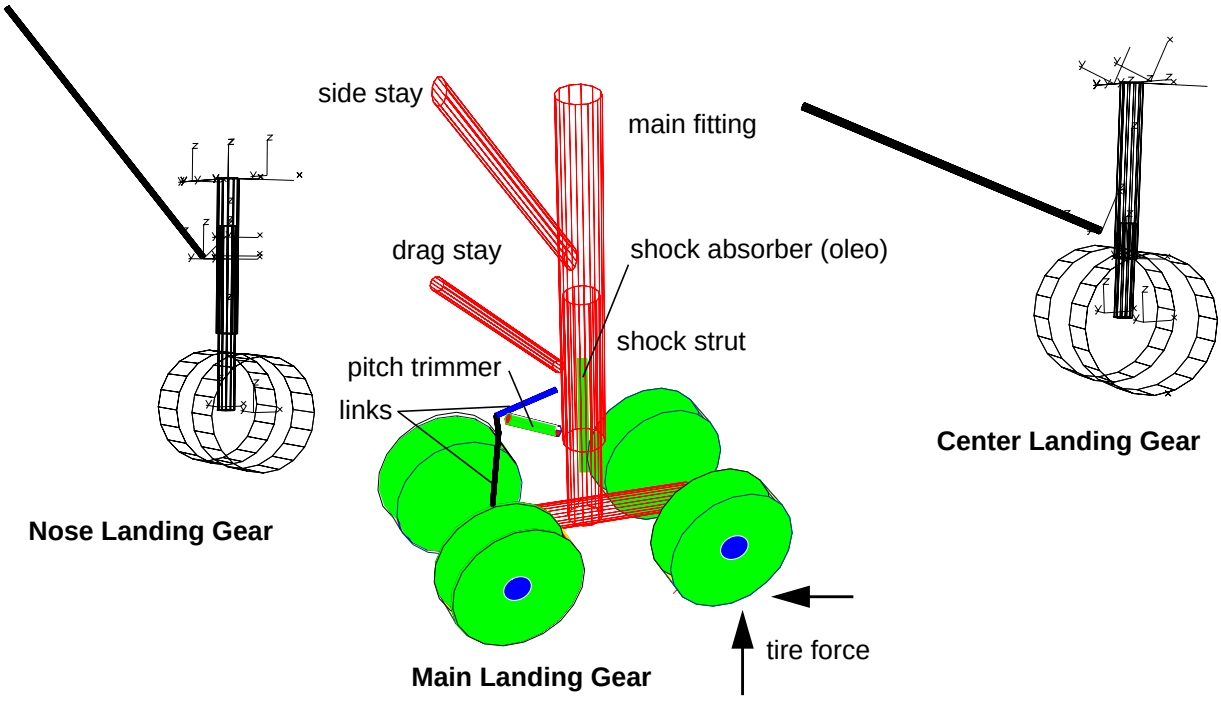

Figure 22: Landing gear simulation models

The landing gears are modeled as rigid bodies, a modeling of the flexibilities, however, could be achieved by either replacing the rigid by flexible bodies or by including springs as substitutional stiffness [19]. However, a rigid landing gear is sufficient for the model described here as the modeling of landing gear flexibilities becomes necessary for calculations of gear walk at touch-down and for stress and life-time analysis, and is of small importance for comfort analysis at taxiing. For the design model, however, a completely rigid landing gear model has been used, and the attachments to the airframe were also assumed to be rigid. Main fitting and drag stay, as well as side stay for the main landing gear, have been modeled as one body. The landing gears are connected to the attachment points of the airframe by flexible couplings.

The following masses have been used in the simulation model: the mass of the nose landing gear sprung mass, i.e. main fitting and drag stay, is 340 kg, the mass of the unsprung mass, shock tube, wheels and tires, is 400 kg. The main landing gear sprung mass (main fitting, side stay and drag stay) is 1300 kg, the unsprung mass (shock tube, bogie, wheels and tires) is 2500 kg. The sprung mass of the center landing gear is 575 kg, the unsprung mass 525 kg.

The oleo design is described in section 2.2.1, the oleo force elements as well as the tire force element are described in section 3.3.

3.2.3 The “Two-Mass Model”

Basic studies for ground vehicles are often performed using reduced models, such as the single-track (“half-car”) model for longitudinal and lateral dynamics [77], or two-mass models for suspension design. A two-mass model consists of a single full suspension including shock absorber, tire, and suspension mass, the so-called “unsprung mass”, supporting a substitution

point mass, the so-called “sprung mass”, which is equivalent to part of the total vehicle body mass. From automotive applications with its typical two-axle, four wheel configuration, where this model is frequently employed, the much-used term “quarter car model” is derived [47], [54]. In aircraft design such a model is applied for the design and certification of landing gears, especially in the form of landing gear drop tests.

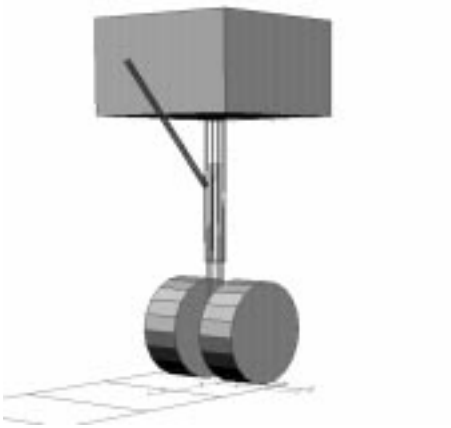

Figure 23: Two-mass model of nose landing gear

The advantage of the two-mass model is its simple set-up; the model is reduced to the essential suspension elements. The model has proven to be sufficient for many basic considerations concerning suspension design; its use is justified when the excitations are mainly vertical, no pitch and roll motion has to be considered and as long as only rigid body motion is concerned. Thus, it is a good test-bed for new concepts. On the other hand, no predictions about vehicle behavior can be made if vehicle pitch and roll are important, or if elastic deformations of bodies are involved.

Using two-mass models for aircraft suspension design, there are some basic differences between the models for rolling and those used for touch-down. The most evident difference is the change of the equivalent mass. At the suspension design for rolling (both for cars and aircraft) the value for the substitution mass is equal to the static mass resting on a single suspension leg. For cars, this would be roughly one quarter of the total body mass (hence the name “quarter car model”), for aircraft the weight on the legs differs considerably between nose landing gear and main landing gear (as an example, the static mass on an A340 nose landing gear is approximately 16 tons, on a single A340 main landung gear it can be as high as 100 tons for MLW). For touch-down calculations, on the other hand, certification requirements demand the equivalent mass for the nose landing gear to be considerable larger than the static mass to account for an additional force resulting from the forward pitching moment of the aircraft at touch-down. Furthermore, a variation of the static mass for both nose landing gear and main landing gear has to be made if the drop test is performed without taking aerodynamic lift into consideration [112].

A second difference is the value of the friction in the landing gear oleo. Whereas for touch-down usually a net friction force of 10% of the total force level is assumed [59], resulting from

seal friction and from the strong leg bending at ground contact and the resulting tire spin-up (see Figure 28), the model has to include stick friction effects when rolling is concerned (see section 3.3).

The two-mass model of the nose landing gear used for this work is set up as follows: tire and oleo are the same as for the complete aircraft (sprung mass: 0.4 tons, see section 3.2.2), the equivalent mass is 16 tons (8.5% of the total aircraft mass for MLW). Note that for touch-down simulations as performed in the Flexible Aircraft project [59] the equivalent mass for the same case would have to be 30 tons. A topology diagram of the model can be seen in Figure 24.

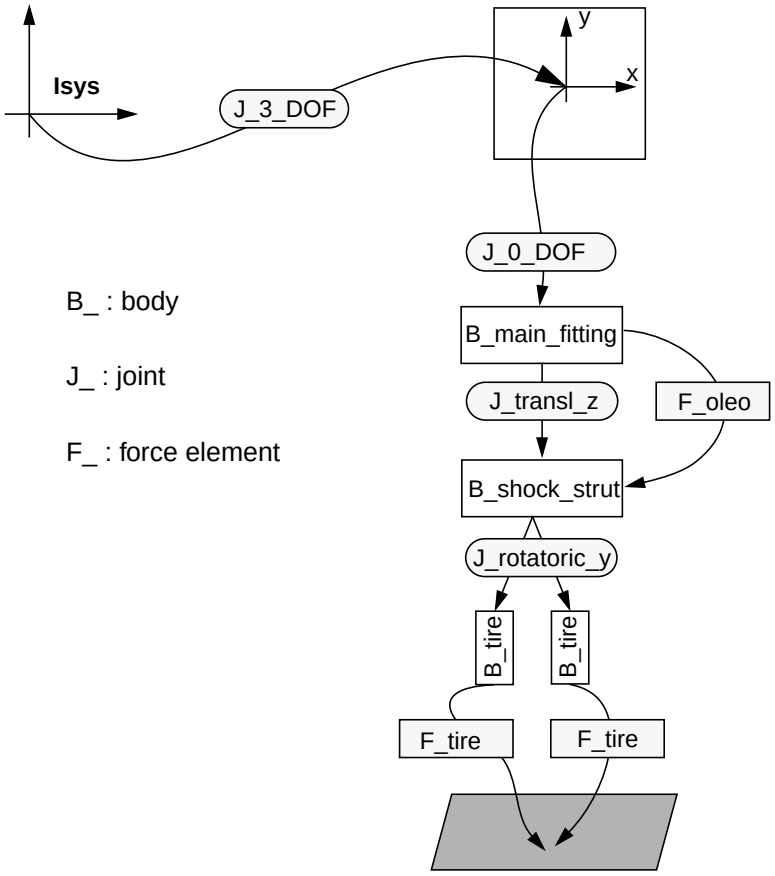

Figure 24: Topology map of two-mass model for nose landing gear

Considering the advantages and limits of the two-mass model, the following restrictions have to be kept in mind. For a active and semi-active landing gear control, aircraft pitch and fuselage and wing elasticities play an important role. Therefore in this work the model will only be used for proof-of-concept studies for the applicability of the control concepts investigated. A short comparison in section 5.1.4 will show up to which point a two-mass model is sufficient for the layout of aircraft landing gears.

3.2.4 Frequency Analysis of the Simulation Models

For the linear analysis in section 4.1 and the calculation of the linear system matrices needed for Kalman filter and state controller design, see section 4.2.3, the aircraft is linearized according to equation (3.1.3) with respect to the static ground position in the MLW configuration.

Table 2 lists the natural frequencies of the aircraft evaluation model together with the corresponding degrees of freedom.

No.	natural frequency [Hz]	natural damping [-]	corresponding mode
1/2	.6628E+00	-.2263E-02	AC pitch
3/4	.8731E+00	-.2263E-02	AC heave
5/6	.1193E+01	-.2880E-01	1st vertical wing bending
7/8	.2397E+01	-.7511E-01	wing torsion
9/ 10	.2737E+01	-.8431E-01	1st fuselage bending
11/ 12	.3031E+01	-.8878E-01	fuselage bending, engine lateral
13/ 14	.4041E+01	-.1275E+00	inner engine vertical
15/ 16	.4378E+01	-.1385E+00	both engines vertical
17/ 18	.6747E+01	-.2165E+00	2nd fuselage bending
19/ 20	.7056E+01	-.2261E+00	2nd wing bending
21/ 22	.8772E+01	-.2852E+00	3rd fuselage bending
23/ 24	.1107E+02	-.3760E-03	MLG vertical
25/ 26	.1107E+02	-.3760E-03	MLG vertical
27/ 28	.1110E+02	.0000E+00	bogie torsional
29/ 30	.1110E+02	0000E+00	bogie torsional
31/ 32	.1123E+02	-.3810E+00	high fuselage mode
33/ 34	.1346E+02	-.4827E+00	fuselage fore/aft
35/ 36	.1428E+02	-.5274E+00	high fuselage mode
37/ 38	.1591E+02	-.1360E+00	CLG vertical
39/ 40	.1518E+02	-.3272E-03	NLG vertical

Table 2: Aircraft natural frequencies for MLW

The two-mass model has only vertical degrees of freedom with the natural frequencies given in Table 3.

No	natural frequency [Hz]	natural damping [-]	corresponding mode
1/2	.8188E+00	-.3000E-03	aircraft heave
3/4	.1675E+02	-.1100E-02	landing gear vertical

Table 3: Natural frequencies for two-mass model

Figure 25 shows the bode plots of three models:

- the aircraft on the landing gears with the fuselage represented by the full expanded flutter model (the plot is limited to frequencies up to 30 Hz),
- the aircraft evaluation model on the landing gears with the fuselage represented by the selected modes up to 16 Hz, Table 2,
- and the two-mass model, Table 3.

The input is a symmetric vertical excitation of the main landing gears, output is the vertical acceleration at the cockpit. It can be seen that the reduced model represents well the system dynamics in the frequency range of interest (up to 16 Hz), proving that the choice of modes from the finite element model is valid. The natural frequencies of the two-mass model meet the modes of aircraft heave and nose landing gear vertical motion.

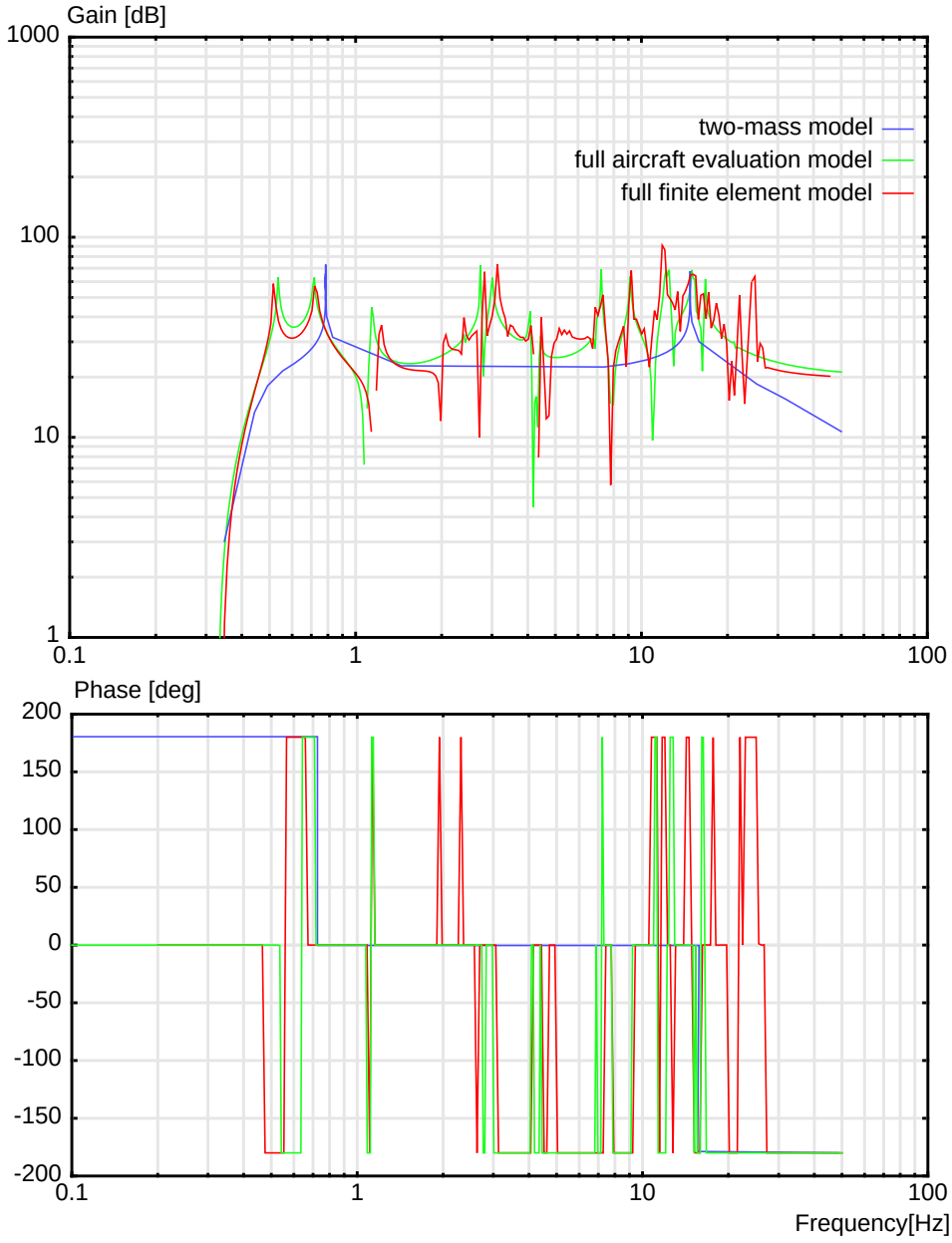

Figure 25: Bode plots of aircraft FEA model, evaluation model and two-mass model

3.3 Force Elements in the Simulation Model

The force elements describing the landing gear characteristics have been modeled in detail for this thesis, including all important linear and nonlinear effects because they determine the landing gear dynamic behavior and are, therefore, essential for comfort evaluation.
While the equations of the physical phenomena as such are valid independently from the exact aircraft type and can be taken from standard textbooks (e.g. [14], [82]), the parameters for the force elements are usually proprietary. The data used in this work are those which were prepared for the Flexible Aircraft Project [59].

3.3.1 Oleo: Gas Spring

The gas spring is represented by a law of polytropic expansion [19]

$$F_f = F_0\left(1-\left(\frac{s}{s_m}\right)\right)^{-n\cdot c_\kappa} \tag{3.3.1}$$

with spring force F_f, pre-stress force F_0, oleo stroke s, oleo gas length s_m, polytropic coefficient n ($1 \le n \le \kappa$), and a correction factor c_κ. The pre-stress force F_0 can be calculated from the initial pressure in the fully extended oleo. The correction factor c_κ, typically between 0.9 and 1.1, allows the adjustment of the curve to measured data. The minimum and maximum stroke limits are modeled by stiff springs. The center landing gear is equipped with a two-stage gas spring, both branches modeled according to equation (3.3.1), but with different coefficients F_0, s_m, and c_κ. In reality the spring curves for static and dynamic compression differ approximately by 10%, because the static curve represents the isothermic case, n=1, whereas the dynamic curve describes a polytropic process (see Figure 26). In the simulations of the rolling aircraft, only the dynamic curve is used.

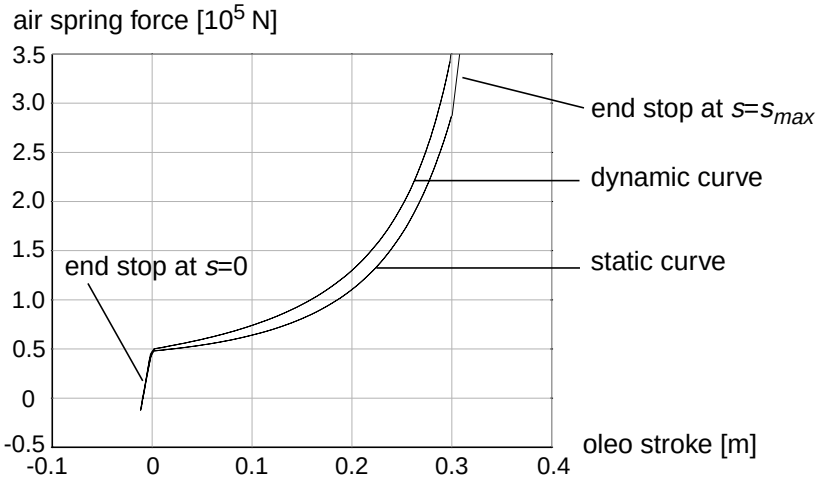

Figure 26: Dynamic and static air spring curves

3.3.2 Oleo: Passive Damper

The properties of the passive damper are determined by the laws describing the flow of a viscous fluid, e.g. oil, through an orifice. Bernoulli‘s equation solved for the force on the oleo piston ([66], p. 41) yields

$$F_d = \mathrm{sgn}(\dot{s}) \cdot d \cdot \dot{s}^2 \tag{3.3.2}$$

with oleo stroke velocity $\dot{s}$, oleo damping force F_d, and damping coefficient d.
The damping coefficient is constant for a fixed orifice oleo (see Figure 27). By the means of one-sided valves, however, d can be changed considerably for compression (d_{comp}) and rebound (d_{exp}). Furthermore, d can become a function of landing gear stroke with the help of a metering pin, or of the landing gear stroke velocity with a spring supported plate (see chapter 2.2.1). Thus, a different damping coefficient can be achieved for touch-down and for rolling in order to improve the comfort at rolling.
All those possibilities have been implemented in the simulation model of the oleo. The comparison of passive and semi-active oleo is performed based either on the fixed orifice oleo defined in the Flexible Aircraft Project [59] or on the taxi valve passive design, Figure 8.

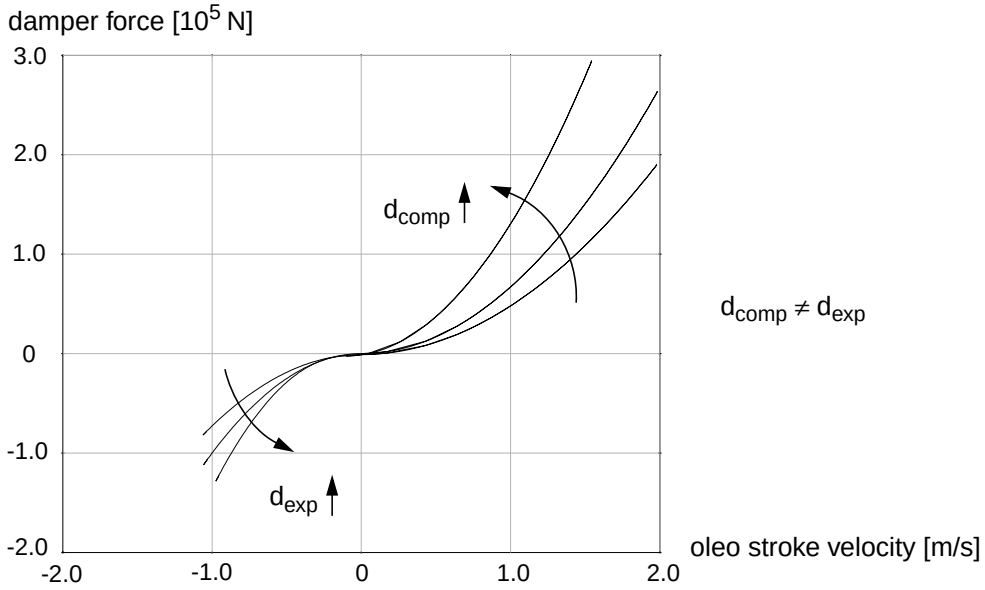

Figure 27: Damping force curve of a passive shock absorber

3.3.3 Oleo: Semi-Active Damper

The basic layout of the semi-active oleo is that of the passive oleo. As for the passive damper described above, the applicable force in the semi-active damper depends on the sign of the stroke velocity across the damper. The main difference is that the semi-active oleo is not restricted to working along a quadratic relationship between stroke velocity and damping force, but can operate in a field limited only by minimum and maximum damping, Figure 12.
For general active suspension control, the output is not a damping factor but a commanded force

F_{com} as a direct function of the system dynamics, resulting from measurements or the state vector, and can be positive or negative. The oleo, however, has to work with an (always positive) damping factor. This requires first a check of the applicability of the control force at a given time. The force can only be applied if it has the same direction as the current stroke velocity. Second, the force has to be transformed into a damping factor according to equation (3.3.2). Third, minimum and maximum damping factors have to be regarded if the control law is not considered to be “clipped optimal”:

$$d = \begin{cases} F_{com} / \dot{s}|\dot{s}| & \text{if} \quad \operatorname{sgn}(F) = \operatorname{sgn}(\dot{s}) \\ d_{min} & \text{if} \quad \operatorname{sgn}(F) \neq \operatorname{sgn}(\dot{s}) \end{cases}$$

where

$d_{min} < d < d_{max}$ in general

$d_{min} = 0$ for clipped optimum (3.3.3)

It can be seen that for a semi-active control law, contrary to a fully active control law, a measurement of the stroke velocity is always required.

For the application in a real damper the damping factor has to be converted to a corresponding commanded orifice cross-section. According to [19], the commanded orifice cross section can be calculated from the commanded damping coefficient using the following equation

$$a_{com} = \sqrt{\frac{\rho A_g}{2\alpha_D^{\,2}} \cdot \frac{1}{d_{com}}}, \tag{3.3.4}$$

with the commanded damping factor d_{com}, commanded orifice cross section a_{com}, oil density $\rho = 0.87\text{g/cm}^3$, oleo gas room cross section A_g, oil discharge coefficient $\alpha_D = 0.8$ (for the given case).

For the performance evaluation a time constant of approximately 25 ms [94] for the controlled valve was assumed which is taken into consideration by the use of a first-order low pass filter. The influence of the actuator response time on performance has also been investigated, see section 5.1.3. The weight of the actuator is assumed to be negligible when compared to the aircraft sprung and unsprung masses.

3.3.4 Oleo: Friction

Two types of friction play a major role when regarding the oleo, seal friction and bending friction. *Seal friction* F_{DS}, i.e. the friction force exerted by the oleo seals being pressed against the walls of the oleo, is a function of the pressure difference in the oleo chambers and thus of the oleo stroke velocity, and it is of importance mainly for the landing impact. An exact friction model is not available and so, in accordance with calculations done at the landing gear manufacturers, friction at the landing impact is approximated by a load factor

$$F_{DS} = 0.1 \cdot (F_f \pm F_d) \tag{3.3.5}$$

where F_f and F_d result from (3.3.1) and (3.3.2), respectively.

The *bending friction* force F_{DB} has its origin in the bending of the part of the shock tube that slides in the main fitting. It is of main importance at touch-down, especially for the spin-up of the wheels and for tilted landing gears. The force law can be described by Coulomb friction

$$F_{DB} = \mu \cdot (F_{N1} + F_{N2}). \tag{3.3.6}$$

A value of $\mu \approx 0.01$ (steel on steel, greased) can be assumed. The normal forces F_{N1} and F_{N2} necessary for the friction calculation can be taken from the simulation, Figure 28. However, when using relative coordinates with the O(N) - formalism, F_{N1} and F_{N2} are results of the evaluation of the right-hand-side of the equation of motion and, at the same time, needed as input for the calculation of the friction force F_{DB}. Therefore, the force element has to be solved iteratively by using an additional algebraic equation and cannot be used in this form within an ODE formulation. For time simulation in SIMPACK, however, a solver for differential algebraic equations (DAEs) is available and has been used in this work. For the linearized model, bending friction has been neglected.

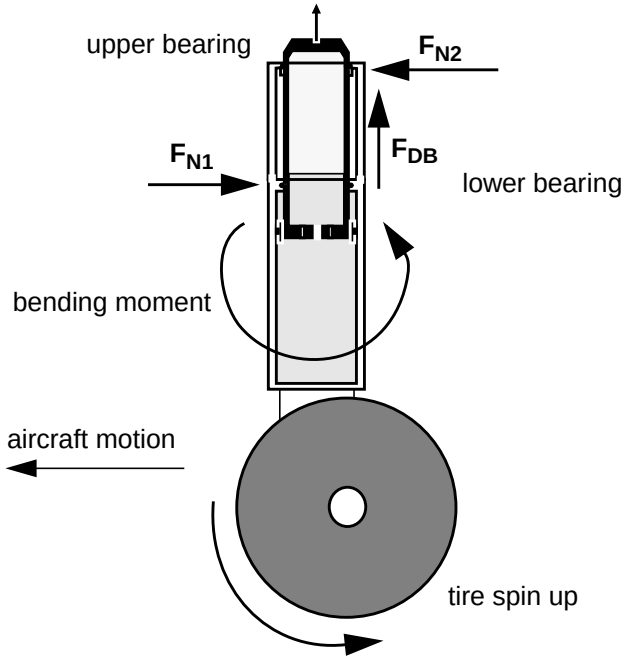

Figure 28: Bending friction

Stick friction is of great importance especially for the main landing gears. At taxiing, the gears often remain in stick mode for several seconds, leaving the tires as the only flexible suspension element between airframe and runway. This is one of the most important reasons why semi-active shock absorbers show the most potential when used at the nose gear and not at the main gear; main gears seem to stick significantly longer than nose gears during ground ride due to their inclination angle. Stick friction in landing gears has not been covered widely in past publications. However, the subject is of major importance for future research concerning dynamic control and the implementation of a semi-active damper at the main landing gears for taxiing.

3.3.5 Tires

The tire connects the wheel to the runway when the aircraft is on the ground. The simulation force element measures the height of the wheel axis with respect to the excitation. This rolling radius r_r is subtracted from the nominal tire radius r_{nom} to determine the tire deflection d_z:

$$d_z = r_{nom} - r_r . \tag{3.3.7}$$

The wheel is modeled as a separate body with a rotational degree of freedom. The longitudinal motion of the body with respect to the runway is used to calculate tire slip and torque on the wheel.

The vertical force F_z is calculated first. It is a function of the tire deflection d_z. Using a third-order polynomial we find

$$F_z = c_1 d_z + c_2 d_z^{\,2} + c_3 d_z^{\,3} \tag{3.3.8}$$

where c_1, c_2, and c_3 are selected to match measured tire data. A linear spring can be simulated by setting c_2 and c_3 equal to zero and providing the spring coefficient in c_1.

For longitudinal forces the slip calculated in the main tire element is used. It is defined as the ratio between the horizontal velocity of the wheel contact point and the axle forward velocity,

$$slip = \frac{v_x - r_r \Omega}{v_x} \tag{3.3.9}$$

where Ω denotes wheel spin and v_x the wheel axle forward velocity.

The friction coefficient μ_{RW} of the runway is a function of slip. An approximation of the functional relation between μ_{RW} and slip is displayed in Figure 29. Typical values for μ_1 and μ_2 range from 0.4 to 0.9 for dry runways, depending on the runway type.

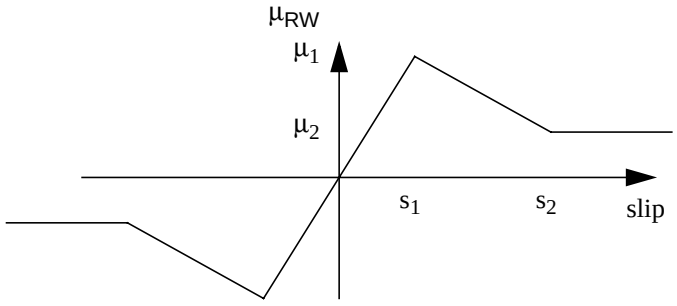

Figure 29: μ_{RW} as a function of tire slip

The friction coefficient μ_{RW} is needed to calculate the longitudinal tire force F_x which is a function of the vertical tire force F_z and μ_{RW}

$$F_x = \mu_{RW} \cdot F_z . \tag{3.3.10}$$

The resulting torque T_y on the wheel is calculated using the effective rolling radius $r_{r,eff}$ which can be set to a constant value or, if desired, can be calculated during the simulation using the equation

$$r_{r,eff} = r_{nom} - (d_z/3) \quad . \tag{3.3.11}$$

The torque T_y is then

$$T_y = r_{r,eff} \cdot F_x. \tag{3.3.12}$$

This approach is able to simulate rolling with braking as well as the landing impact and tire spin-up. It is sufficiently complex for a qualitative approach as the work of this project has been restricted to straight aircraft motion without curving or non-symmetric load cases.
The tire model is a so-called point follower. The contact patch is either neglected or represented by a filter “smoothing” the runway. This is no restriction for this work since the given runway excitations contain no sharp-edged obstacles.

3.4 Runway Excitations

For the evaluation of the semi-active landing gear the aircraft rolls over different excitations at different velocities and for load cases. The complete envelope (empty aircraft to fully loaded aircraft, slow taxiing to fast rolling) will be covered.
There exist not many comprehensive comparisons of airport runways. Still a valuable work in this area is the study of W.E. Thompson [92], who in 1958 supplied a method for representing runway data as elevation plots and power spectral densities (PSD) for comparison purposes and, using these methods, compared measured data of 34 runways from different NATO countries. The PSD plots in his study confirm that over a large frequency range the PSDs of the runway elevations are almost parallel to each other. A similar observation for roads lead to the standard road description given in [67]. It should be noted, however, that runways often will not fit into standardized road spectra because of their short length when compared to roads for ground traffic.
Two runways have been selected for the investigations in this thesis because they represent typical cases of rough runways:

- “San Francisco old”: a standard runway for landing gear design and certification, consisting of a measured runway profile (elevation as a function of runway length, with a length of 1259 m, Figure 30).

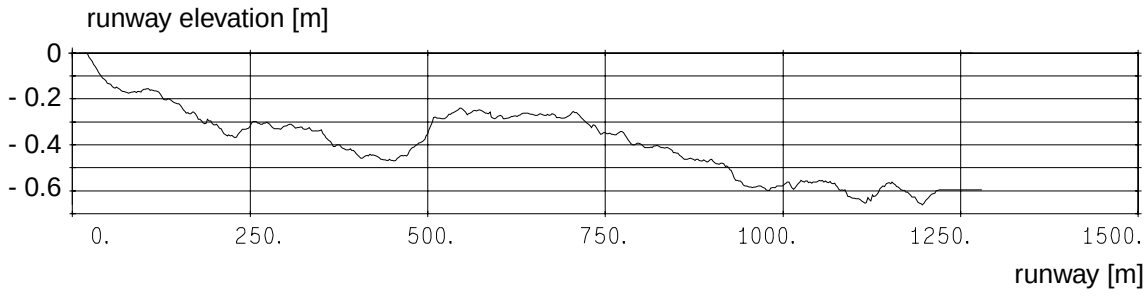

Figure 30: Plot of “San Francisco old” runway

- “Rough Runway”: an example of a runway of bad quality, also consisting of a measured runway profile (elevation as a function of runway length, with a length of 2495 m, Figure 31).

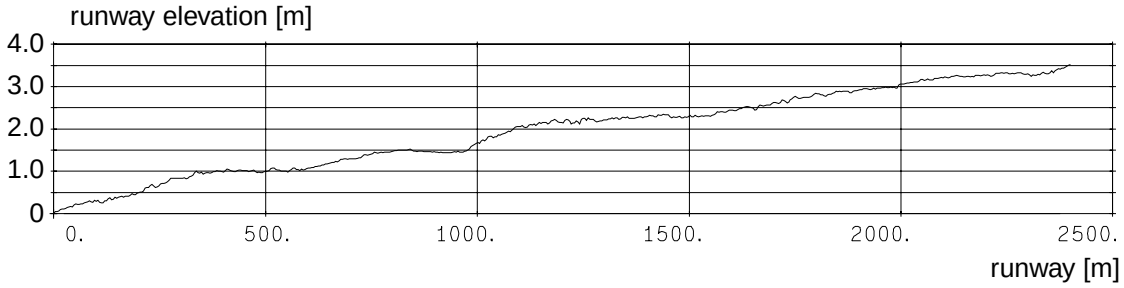

Figure 31: Plot of the “Rough Runway“

The runway elevations are available as measured data. Due to their representation as value pairs the runways have different cutoff frequencies (the highest frequency contained in the runway data) as a consequence of the different spacing of the value pairs. San Francisco has been recorded in two-feet steps (approx. 0.62 m), whereas the rough runway has a spacing of 0.5 m. At the regarded aircraft speeds, though, this difference has no effect since at a speed of 60 m/s, at which most evaluations have been performed, a spacing of 0.5 m is equivalent to a cutoff frequency of 120 Hz, a spacing of 0.62 m is equivalent to 96.8 Hz, both values being well above the frequency range of interest for comfort evaluation.

As will be shown in section 5.1, San Francisco runway and the Rough Runway have not only a different roughness but also different frequency contents, leading to distinct aircraft responses. Figure 32 shows the power spectral densities (PSD) of the measured runways.

Of further interest is the control performance as a function of runway roughness alone, keeping the frequency content constant. For this purpose, the amplitude of the profile of the Rough Runway was multiplied by factors varying from 0.25 to 2.0, leading to a parallel vertical shift of the PSD-representation. The results of this investigation are presented in chapter 5.2.3.

Some specific test cases, e.g. Figure 15 or the comparison of the semi-active oleo with a two-stage passive nose landing gear suspension in section 5.2.6, have been performed with a so-called “double cosine”-bump, Figure 33. Excitations of this kind are used in the simulation of aircraft ground dynamics as they can be tuned to specific natural frequencies of the aircraft by adjusting the wavelength of the bump. Here, the wavelength is chosen to be equivalent to the first natural frequency of the fuselage. However, in this work the bumps are only used for comparison of simulations, not for optimization purposes, because semi-active controllers optimized on such a single input will lead to other results than optimizations on (quasi-) stochastic runways as they are used in this thesis.

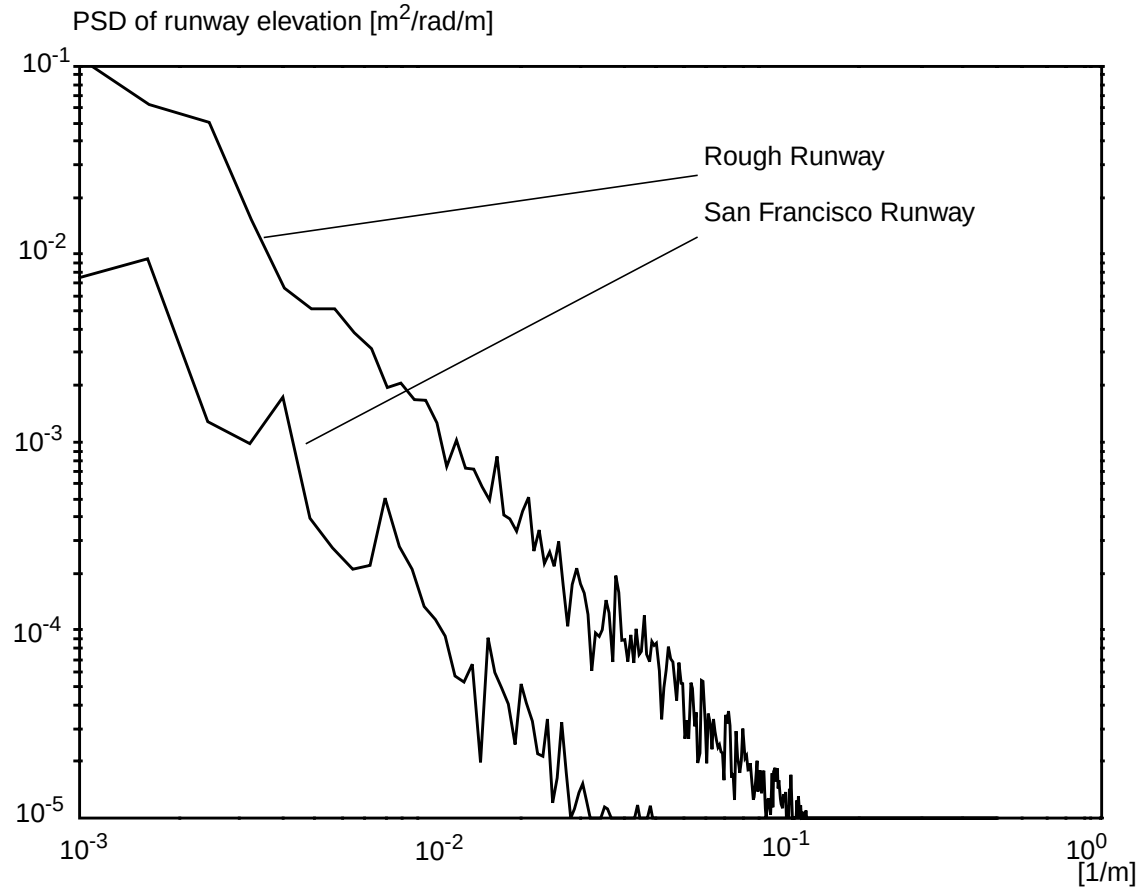

Figure 32: PSD of “San Francisco old” and “Rough Runway”

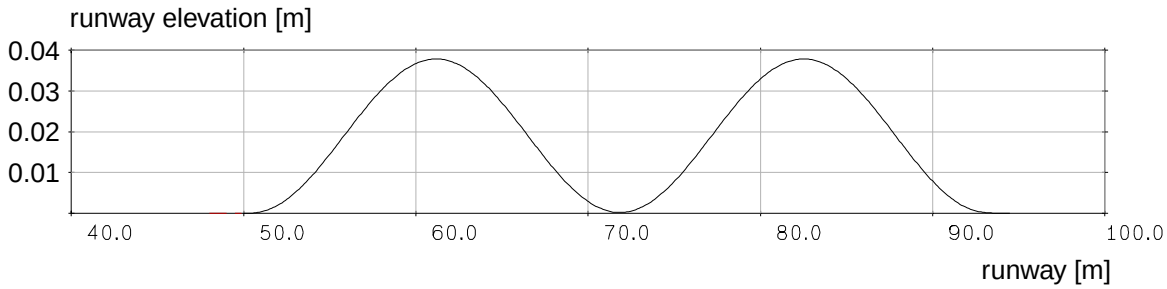

Figure 33: Plot of the “double cosine”-bump

Some assumptions for all excitations apply:

- The runways are assumed to be rigid and the tire contact point follows the runway profile directly. However, the tire is not constrained to remain in contact with the runway, so lifting of the tire (wheel-hop) is allowed.
- The runway profile is two-dimensional, being of constant elevation along its width. Thus, on a straight run, all tires on all legs meet the same input, separated by a time lag which is a function of the current speed and the position of the wheels at the aircraft.

3.5 Quantities of Interest and Criteria

3.5.1 Sensor Locations

The work presented in this thesis is mainly concerned with the improvement of both passenger and pilot comfort. Therefore, the acceleration at the cockpit and in the passenger section is of special interest for the analysis. For model evaluation purposes and as potential control inputs the resulting accelerations at the top of the nose landing gear, the center of gravity, the rear bulkhead, and the wing tips are taken into consideration, too. Additionally, for the application of a semi-active actuator the controller needs information whether the shock absorber, at a given time, is being compressed or expanded. This can be determined by the sign of the relative velocity between main fitting and shock strut which can be measured.

As mentioned in section 3.2.1, kinematic measurements in the simulation model can be obtained between arbitrary locations of the model. It is, therefore, possible to measure any relative acceleration, velocity, and displacement. Eleven prominent locations on the aircraft have been selected as sensor locations for the simulation which will serve as potential sensors for the control laws and provide input for the performance evaluation during the optimization, see Figure 34. However, all applied forces and working values of the force elements are accessible during the simulation, allowing to monitor also those parameters of interest which are no input to the optimization, e.g. the loads at the landing gear attachment points.

While in the simulation all values mentioned can be directly obtained, in reality only some can be measured directly, others must be deduced from these measurements. The vertical cockpit velocity can be acquired by the integration and filtering of an acceleration signal (see e.g. [63]), and the sign of the oleo velocity can be obtained by either differentiating a displacement signal between shock strut and main fitting or by measuring the pressure difference in the oleo chambers.

3.5.2 Analysis Criteria

The evaluation includes analyses in the time as well as in the frequency domain. In the study, time domain evaluation consists mainly of direct comparison of time plots of vertical acceleration by the means of root-mean-square (RMS) and maximum values (peak criterion). To assess the influence of certain frequencies, power spectral density (PSD) plots of passive and controlled aircraft are compared.

The *root-mean-square* (RMS) of acceleration as an important criterion is defined as follows

$$c_{i,\,RMS} = \sqrt{\frac{1}{t_e - t_0}\int_{t_0}^{t_e} \ddot{z}_i - \ddot{z}_{m,\,i}{}^2 dt}\,, \tag{3.5.1}$$

with vertical acceleration $\ddot{z}_i$ at sensor i, reference value for acceleration evaluation $\ddot{z}_{m,\,i}$ (for RMS generally: $\ddot{z}_{m,\,i} = 0$), RMS criterion $c_{i,\,RMS}$ for sensor i, as well as start and end of time integration t_o and t_e.

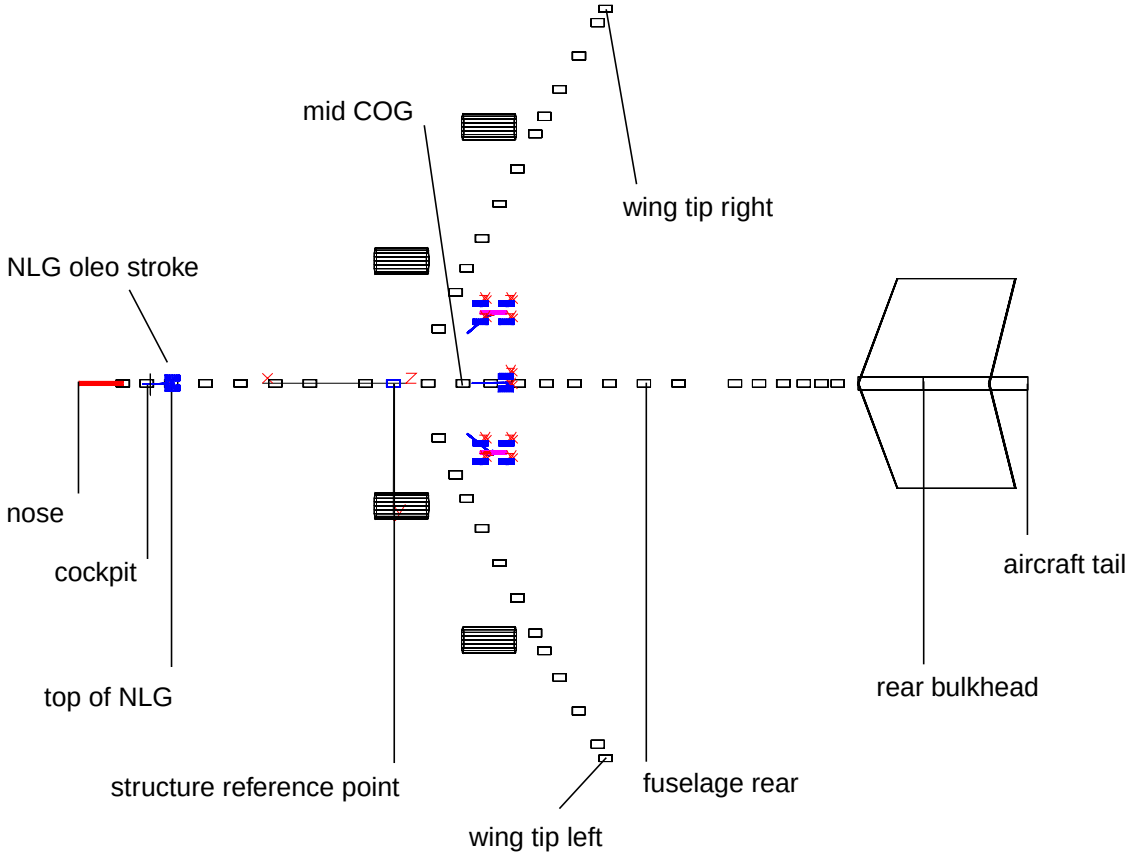

Figure 34: Sensor locations in the simulation model

The RMS criterion alone is not sufficient for optimization because a small RMS value can result either from desired low values of $\ddot{z}_i$ over the complete simulation time or from an undesired high value of $\ddot{z}_i$ in a slim peak only. To avoid second case, the *maximum criterion*

$$c_{i,\,max} = max(abs(\ddot{x}_{z,\,i} - \ddot{x}_{m,\,i})) \tag{3.5.2}$$

is used additionally, where $c_{i,max}$ denotes the maximum absolute deviation from the mean acceleration.

The *power spectral density S(ω)* (PSD) describes the density distribution of all harmonic frequencies that make up the process to be analyzed. It can be symmetric (double-sided) or one-sided, depending on definition, and is a real function defined as the Fourier transformation of the autocorrelation function. The discrete values of the time response of the aircraft simulation are subject to a PSD analysis according to the following definition [54], [69]:

The *autocorrelation function R(τ)* is a characteristic of the noise process, e.g. a time series of accelerations $\ddot{z}_{z,\,i}(t)$. It describes the statistic dependence of values at different time points, e.g. the dependence of $[\ddot{z}_i(t_1) - \ddot{z}_{m,\,i}]$ at time t_1 on the value of $[\ddot{z}_i(t_2) - \ddot{z}_{m,\,i}]$ at time $t_2 = t_1 + \tau$:

$$R(\tau) = \lim_{T \to \infty} \frac{1}{T} \int_{t_0}^{t_e} \ddot{z}_i(t)\ddot{z}_i(t+\tau)dt - \ddot{z}_{m,\,i}^2, \tag{3.5.3}$$

$T = t_e - t_0$, with the mean value

$$\ddot{z}_{m,\,i} \;=\; \lim_{T \to \infty} \frac{1}{T} \int_{t_0}^{t_e} \ddot{z}_{z,\,i}(t)\,dt. \qquad (3.5.4)$$

Finally, the double-sided PSD $S(\omega)$ of the time series $\ddot{x}_{z,\,i}(t)$ is defined as the Fourier-transformation of the autocorrelation function $R(\tau)$:

$$S(\omega) \;=\; \frac{1}{\alpha} \int_{-\infty}^{\infty} R(\tau) e^{-j\omega\tau} d\tau. \qquad (3.5.5)$$

The factor α depends on the definition of the Fourier-transformation used. In the filter applied for this work it is $\alpha = 2\pi$ following the definition of [69].

Since *comfort* for the human body is frequency dependent, the frequency range between 4 and 8 Hz is of special interest [105]. Special care has therefore to be taken that improvements at lower frequencies (e.g. aircraft pitch and heave) do not degrade performance in the range most relevant for comfort. The relationship of comfort and frequency for vertical vibrations is displayed in Figure 35.

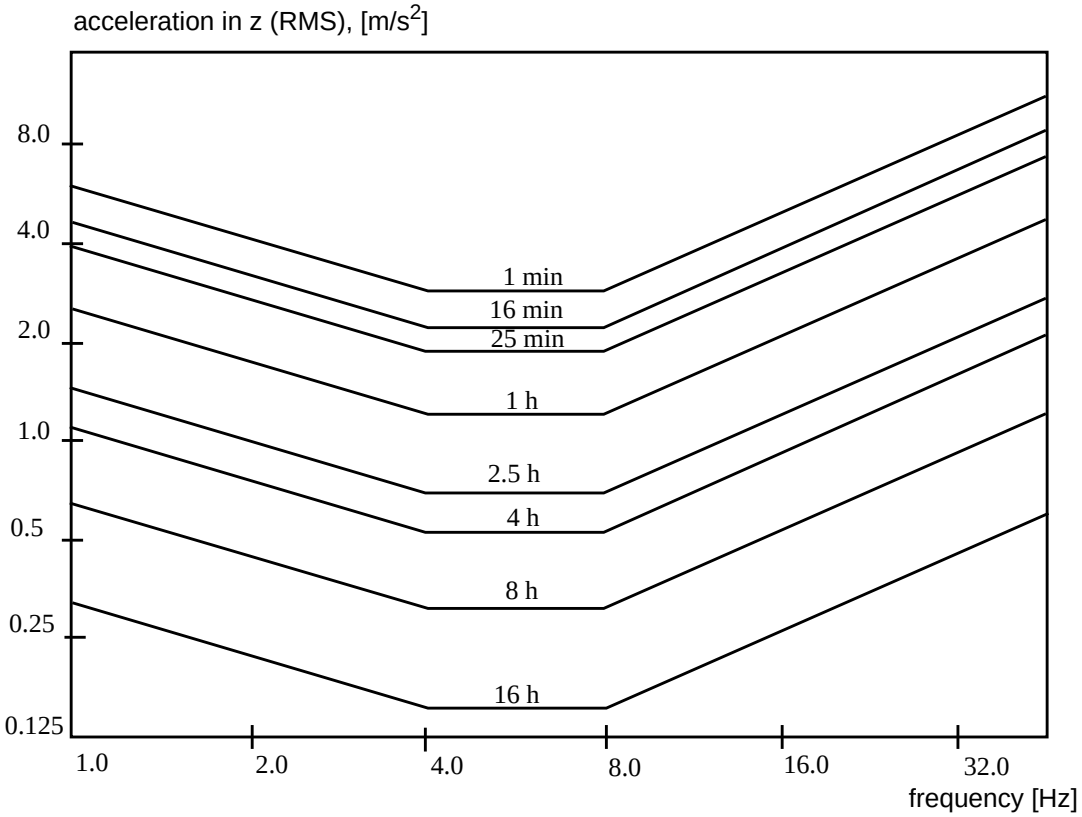

Figure 35: Fatigue-decreased proficiency boundary

4 Design and Optimization of a Control Concept

In this chapter an analysis of the aircraft in terms of controllability and observability if performed. The control concepts investigated in this work, i.e. the skyhook controller, the fuzzy controller, and the state feedback controller, are illustrated as far as necessary for the understanding of the studies. The method of multi-objective optimization is discussed and the strategy for the design and optimization of the control laws is presented. Finally, the optimized control parameters are given.

4.1 Aircraft Model Structural Analysis

4.1.1 Observability and Controllability

An aircraft with an active nose gear can be considered as a plant with one control input (in the following called *u*), the controllable oleo orifice. Sensors are installed along fuselage and wings to measure the oscillations of these bodies giving a plant output (in the following called *y)*. For the application of an active or semi-active shock absorber it is of interest whether the system, i.e. the rigid and elastic aircraft eigenmodes, is observable and controllable by a single sensor or a set of sensors, and whether the elastic modes are controllable by an actuator at the nose landing gear. For this investigation, the actuator can be regarded as working only in one coordinate direction applying a force on a given point on the structure.
For reasons of cost and system complexity a minimum number of sensors is desired. Special interest is furthermore focused on the question whether a single sensor in the cockpit area suffices to supply all necessary information since this location is the position of an inertia platform already equipped with an acceleration sensor.
The *Kalman criteria* for observability and controllability [54] are a direct way to investigate observability and controllability for systems given in state space form:
A system is completely controllable if

$$\mathrm{Rg}(Q_S) = \mathrm{Rg}[B \;\; AB \;\; A^2B \;\; .... \;\; A^{n-1}B] = n \tag{4.1.1}$$

and completely observable if

$$\mathrm{Rg}(Q_B) = \mathrm{Rg}[C^T \;\; A^TC^T \;\; (A^T)^2C^T \;\; .... \;\; (A^T)^{n-1}C^T] = n \tag{4.1.2}$$

However, the Kalman criteria only provides a qualitative statement as to whether the full state vector is controllable or observable. In practical applications, some states might be more ‘strongly’ observable or controllable than others with a given set of sensor and actuator locations. Thus, further quantitative deductions are necessary. They can be made using the *Hautus Criteria* [75]. According to those criteria, a system is completely controllable if

$$(\lambda_i E - A^T)x_i = 0 \Rightarrow B^T x_i \neq 0,\; i = 1 \ldots n\;, \tag{4.1.3}$$

and completely observable if

$$(\lambda_i E - A^T)x_i = 0 \Rightarrow Cx_i \neq 0,\ i = 1 \ldots n \ . \tag{4.1.4}$$

For the application of this method, the system has to be subject to a *modal transformation* as shown in [54]. This requires the calculation of the modal matrix T made up of the eigenvectors and the transformation of the state vector x into modal coordinates $\underline{x}^{mo}$:

$$x^{mo}(t) = T^{-1}\, x(t) \tag{4.1.5}$$

This linear relation transforms the state-space equation

$$\begin{aligned} \dot{x} &= Ax + Bu \\ y &= Cx \end{aligned} \tag{4.1.6}$$

into the form

$$\begin{aligned} \dot{x}^{mo}(t) &= diag(\tilde{a}_i)x^{mo}(t) + T^{-1}Bu(t) \\ y(t) &= CTx^{mo}(t) \end{aligned} \tag{4.1.7}$$

In this form each modal state x_i^{mo} corresponds directly to an eigenvalue $\tilde{a}_i$. Thus, the elements $b^{mo}_{ik} = (T^{-1} B)_{ik}$ (and their absolute value if b^{mo}_{ik} is complex) indicate the component-wise influence of u_k on x_i^{mo}. Likewise, the elements of $(CT)_{ik}$ are indicators for the observability of the modal state x_i^{mo} by the measurement y_k. A more thorough discussion of observability and controllability aimed at the selection of optimal sensor locations can be found in [31].

4.1.2 Kalman-Criterion

Basis for the structural analysis outlined above is the aircraft model made up of the flexible airframe presented in section 3.2.1 and the landing gears described in section 3.2.2. The wheels on nose landing gear and main landing gear have been selected as excitation input for the observability analysis, the nose landing gear oleo has been selected as control input for the controllability analysis. Output for both cases is the set of sensors presented in section 3.5.
For this aircraft model, the matrices given in equations (4.1.1) and (4.1.2) are of full rank; thus the Kalman criteria indicate that all states are observable by each sensor, including the one located at the cockpit area, and that each state and eigenmode can be controlled by an active nose gear.

4.1.3 Modal Controllability Analysis

The modal analysis gives a more detailed picture. The modal transformation leads to a vector $abs(b^{mo})$, here called “magnitude of controllability”, which is displayed in graphical form in Figure 36. The magnitude of controllability is normalized to the power of ten of the lowest value in the plot. The numbering of the columns correspond to the numbers given to the modes in Table 2, section 3.2.4.
The high values for $abs(b^{mo})$ of all symmetric modes of fuselage and wings, heave and pitch as well as the elastic modes, show that all these modes can be controlled by a semi-active landing gear. The low values for the stroke of the main landing gears (mode 23/24 and 25/26) and the

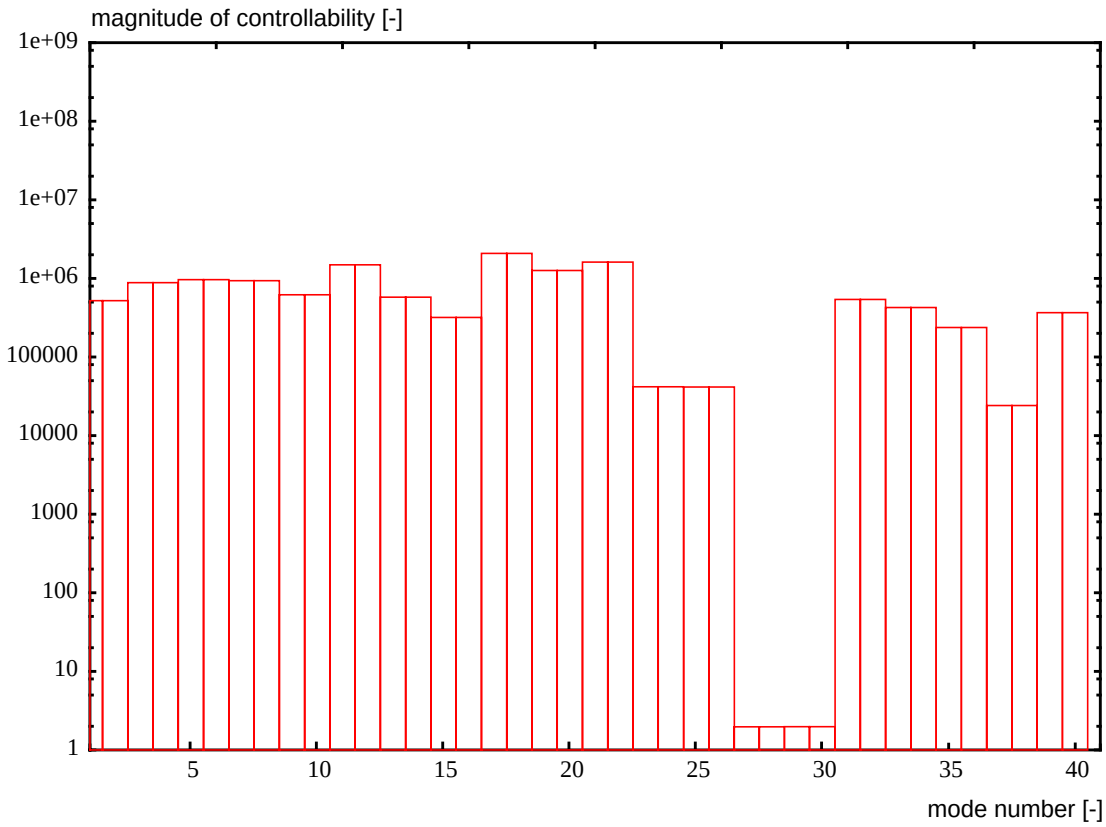

Figure 36: Controllability of aircraft modes by an active nose landing gear

center landing gear (mode 37/38) indicate that neither main landing gear nor center landing gear stroke can be controlled in a suitable way. As was to be expected from the model set-up, especially the bogie pitch (modes 27 to 30) cannot be reached by nose landing gear control with acceptable control effort.

4.1.4 Modal Observability Analysis

A modal observability analysis has been undertaken to evaluate sensor locations along wings and fuselage for their ability to supply information on the oscillations of these bodies. Figure 37 shows plots of the absolute values of $(CT)_i$ for the lowest four fuselage eigenmodes plotted against the length of the fuselage.

The plots indicate that fuselage nose and tail seem to be the sensor locations suited best for the control input of an active or semi-active nose landing gear. For observation of the fuselage and the symmetrical wing eigenmodes the cockpit sensor location gives reasonable results, too. There are, however, regions between 25 and 40 meters at the fuselage ill suited for sensor positioning because a sensor positioned in that range will not be able to provide information on any of the low fuselage bending modes. This it noteworthy since this is the region of the aircraft center of gravity where the acceleration sensors for rigid body motion (the inertia platform) are situated. For potential control of further, possibly asymmetric eigenmodes, sensors at the wing tips are recommended. In essence, these results justify the decision to use the vertical cockpit acceleration as an input for the control laws which will be presented in the next chapter.

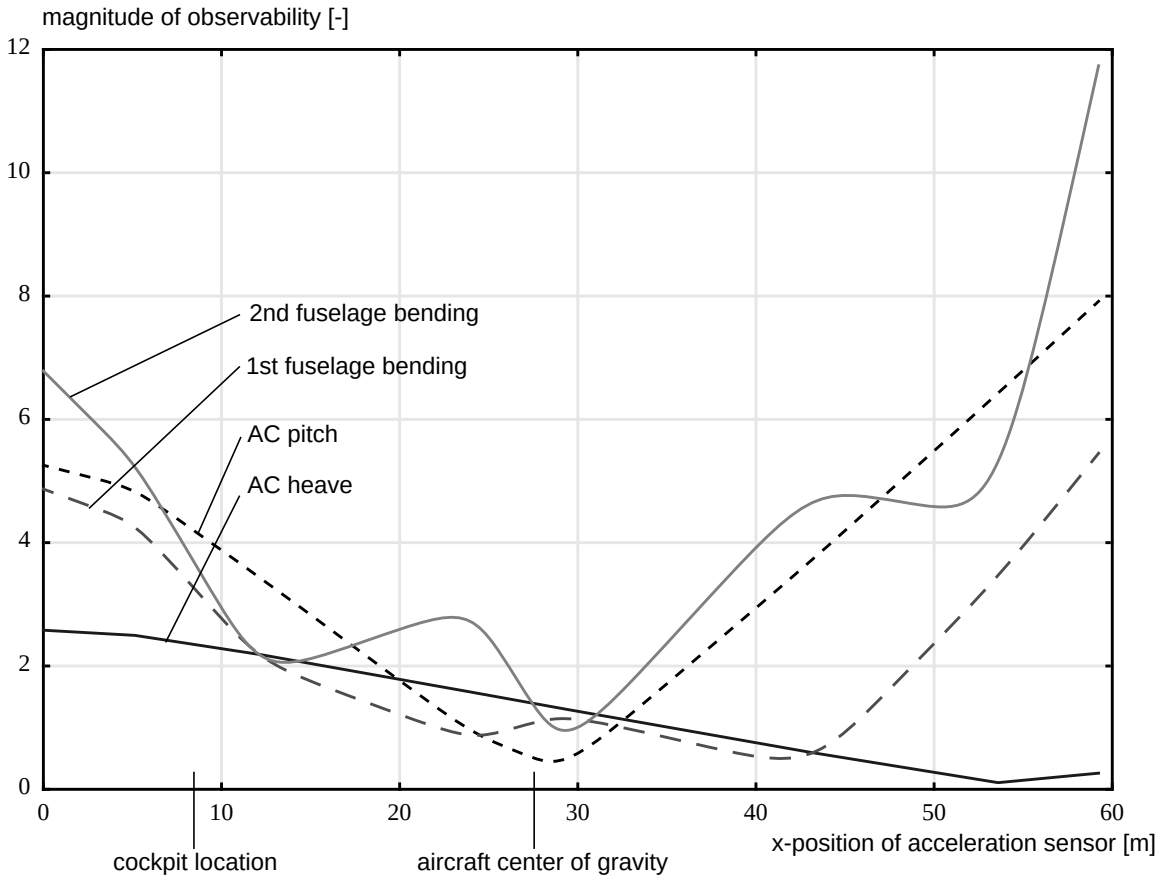

Figure 37: Selected plots of observability of fuselage modes

4.2 Control Algorithms

For the control of the active and semi-active shock absorbers three different control concepts will be designed, a skyhook controller, a fuzzy controller, and a state-feedback controller. These concepts have been selected because they represent different types of controllers, one quite straightforward approach (the skyhook controller), one inherently model based type (the state-feedback controller), and one concept which is not model based (the fuzzy controller). Furthermore, they have been shown to be efficient for suspension control in automotive and truck applications [94]. In the following the basic principles of all control laws will be presented as far as necessary for the understanding of the work.

4.2.1 Skyhook Controller

In the literature several algorithms for active suspension control for ride improvement are proposed. One of the most straightforward, yet effective approaches is the “Skyhook” controller by Karnopp [46]. At this control scheme the actuator generates a control force which is proportional to the sprung mass vertical velocity. The skyhook principle can be shown on a simple, but representative example, as demonstrated in [33] and [54] (see Figure 38).

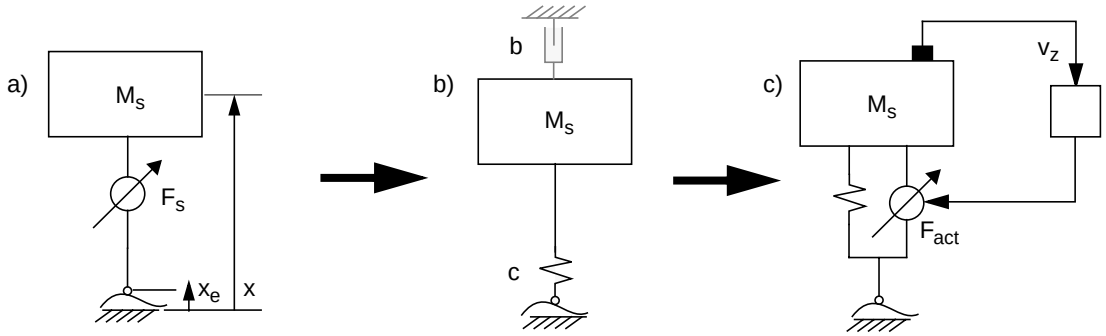

Figure 38: Skyhook control principle

The equation of motion of the one-degree-of-freedom model in Figure 38a is as follows:

$$M_s\ddot{x} = F_s \tag{4.2.1}$$

The system is described with respect to its equilibrium for x_e=0. Although acceleration attenuation is the primary goal of the suspension design, the suspension stroke has also to be taken into consideration. Thus, the goal of optimization is to minimize both the mass vertical acceleration $\ddot{x}$ and the suspension deflection $\delta = x - x_e$, leading to the following performance index:

$$J = E[\ddot{x}^2] + \rho E[(x - x_e)^2]. \tag{4.2.2}$$

Thus, the skyhook controller can be regarded as a special case of a Riccati control design. Equation (4.2.2) leads to an optimization problem, in which the expectation, i.e. the sum of the quadratic deviations of the aircraft acceleration), and of the stroke amplitude (related to the actuation effort), weighed by the factor ρ, has to be minimized. The result yields a suspension force F_s of the following form:

$$F_s = c(x - x_e) - b\dot{x} \tag{4.2.3}$$

This force law could be obtained with a passive system if the mass was connected to the excitation by a spring with stiffness *c*, carrying the static weight, and to the inertial frame by a damper with damping coefficient *b*, Figure 38b. Since the latter would be, for an aircraft, somewhat difficult to build, the solution is to place an actuator parallel to the spring and feed back the vertical velocity of the mass ($F_{act} = -b \cdot \dot{x}$) to simulate a fictitious damper to the inertial frame, giving the “skyhook” control scheme its name, see Figure 38c. As shown in [28], a similar strategy can be used for a two-mass model (Figure 39).

The main advantages of the skyhook damper are its simple implementation and the ease of understanding of the relationship between design and performance. A large number of applications in the literature exist which often make the skyhook approach the reference control law; many of those investigations have used the quarter car model as a basis, see [21], [28], [75], [94].

The performance of a “pure” skyhook controller deteriorates when elastic eigenmodes, as of fuselage and wing elasticities, are significant. In this case a controller with dynamic components might give an improvement. Such a proposition has been made by Wentscher [101] who

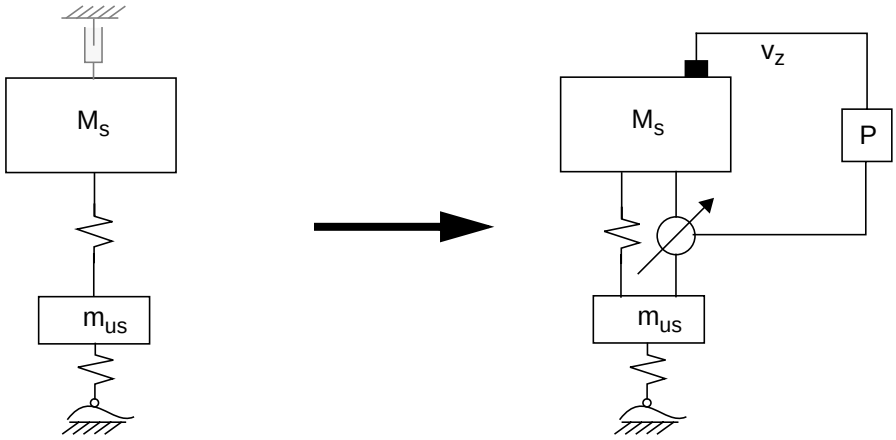

Figure 39: Skyhook control: two mass model

optimized the parameters of a $PIDT_1$-controller for a semi-active nose landing gear oleo using the acceleration on a number of points on the aircraft as criteria for the optimization. A study for the COPERNICUS/SADTS project [94] comes to the conclusion that for reasons of nonlinearities in the damper a piece-wise optimization of control parameters for different working points of the damper (i.e. the gains are a function of the state values) might be of advantage. Several authors point out that the required velocity feedback might be difficult to realize because usually it will be obtained by the integration of an accelerometer signal which would require the use of additional filters [63].

The requirements for active and semi-active landing gear control enforced the use of a modified skyhook controller. First, an additional high pass filter had to be provided to blend out low frequency components of the vertical velocity signal. These signal components result from the aircraft rolling on sloped runways or long bumps. Without a high pass filter the controller will try to compensate (“level out“) the slope, and the actuator will eventually run against its upper or lower stroke limit.

Second, preliminary studies started with the application of a PID-controller, but it showed that the integrational term of the controller, contrary to the differential term, brought no improvement when compared to a purely proportional gain. Thus, finally a PD-controller was used.

Furthermore, for the use with a semi-active actuator the output of the control law has to be treated such that only control demands that can be satisfied by the semi-active shock absorber are passed to the actuator (see chapter 3.3.3). For this purpose, the sign of the oleo stroke velocity has to be known in addition to the commanded force to realize the requirements for the semi-active control according to equation (3.3.3).

The output signal is then scaled by a constant factor K_c to allow the proportional and the derivative gains to remain in the region between zero and one. This step helps the optimization routines to converge on the optimal gains. Finally, an optional limiter gives the user the possibility to chose a minimum and a maximum damping factor. The resulting block diagram of the control loop is depicted in Figure 40.

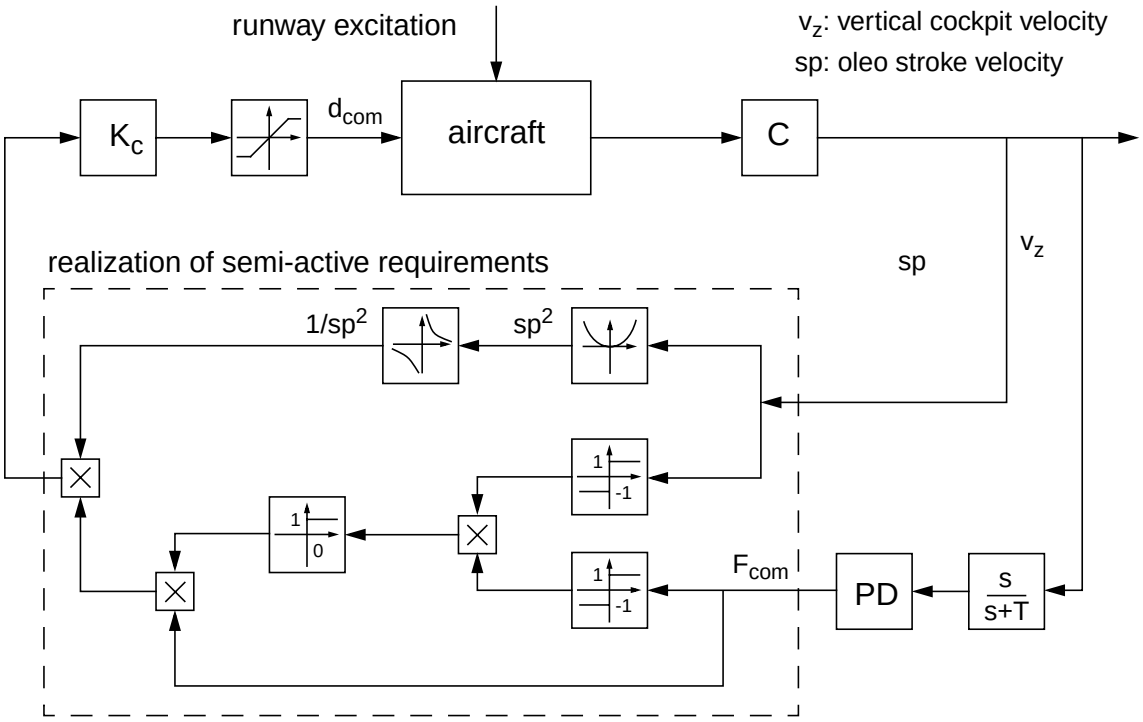

Figure 40: Modified skyhook-controller for semi-active shock absorber

4.2.2 Fuzzy Control

A second control strategy which has been shown to function well with an active and semi-active suspension is the fuzzy logic control [94]. Fuzzy control offers the possibility to include empirical process knowledge and linguistic strategies in the design of controllers [34]. Fuzzy control is of special interest for a plant which is difficult to model, has dominant nonlinear characteristics or is even unknown to a certain extent - all this being at least partially the case for the active shock absorber. The main advantage of the fuzzy controller is its nonlinear transfer function which allows the controller to perform well over a broad range.

The term “fuzzy control” is used for a section of control theory based on “fuzzy logic”, i.e. on the so-called “fuzzy sets” [15]. Fuzzy logic is a general calculation system which is a superset of traditional Boolean logic [35]. The main difference is that in fuzzy logic, contrary to Boolean logic, one element can be a member of more than one given sets. The membership function for an element in a set need not only be “0” (no member) and “1” (member), as in Boolean, so-called “crisp” sets, but can have an intermediate value. Thus, descriptions of values which are difficult to place in discrete sets (very much, a lot, some, a little, very little) can be described better with the help of fuzzy logic than with terms of Boolean logic. To quote a much-used example ([15], p. 20): a room temperature of 18˚ C is difficult to be placed either in the set “cold” or “warm” by a human. It is not in accordance with human experience to set a clear boundary between “cold” and “warm” at 20 degrees. However, using fuzzy logic the temperature could be said to be both “cold” *and* “warm”, e.g. to be 70% “cold” and 30% “warm”, see Figure 41.

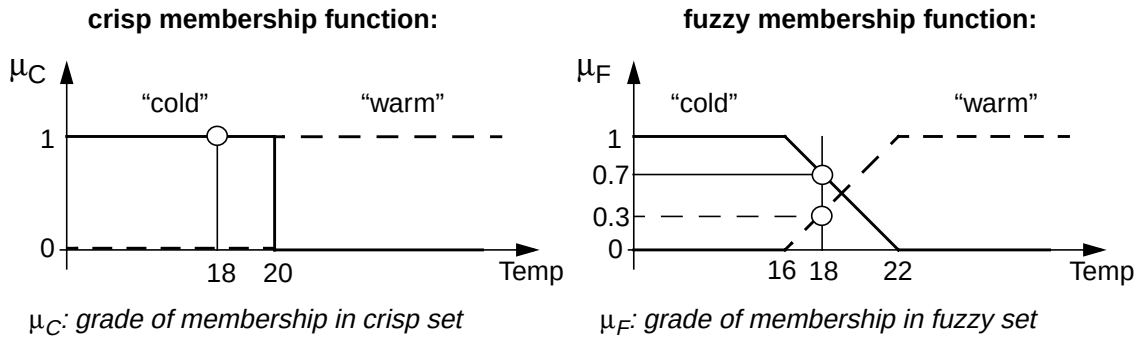

Figure 41: Characteristic crisp and fuzzy membership functions

The control process in a fuzzy system can be divided into four stages [103]:

1. *fuzzyfication*, i.e. the transformation of a crisp value into the description by fuzzy-sets according to linguistic values;
2. *fuzzy implication*, i.e. the individual application of rules on fuzzy sets;
3. *inference*, i.e. the aggregation of the results into a fuzzy output;
4. *defuzzyfication*, i.e. the transformation of a fuzzy output into a crisp control command.

A graphical display of the process is given in Figure 42. The four stages will be described as far as necessary to understand the design of the landing gear controller. A detailed theoretical and practical background can be found in [18] and [96].

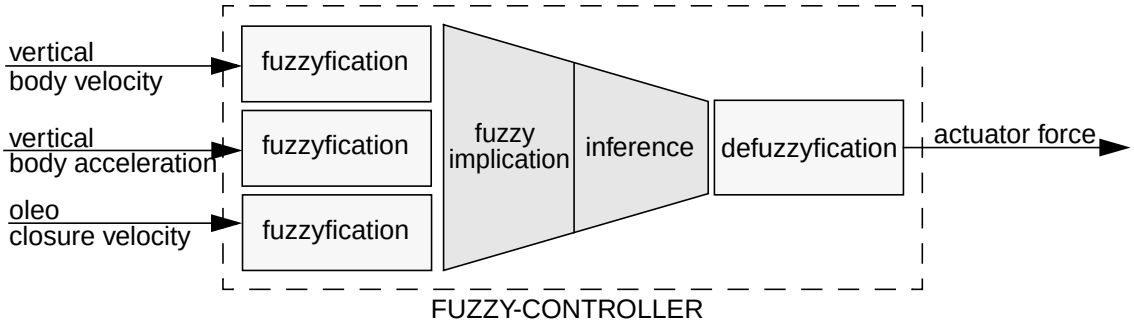

Figure 42: Control process in a fuzzy controller

As part of fuzzification and defuzzification control input and control output are divided into several sections which are assigned linguistic values. Input and output are divided into seven sections: negative large (- -), negative small (-), near zero (0), positive small (+), positive large (+ +), see Figure 43. It is reasonable and done so for the controller developed here, but not mandatory to choose the membership sets is a way that the sum of all membership functions is one. The parameters pv_i, ps_i, pa_i, and pd_i, $i \neq 3$, are design variables for optimization. pv_3, ps_3, pa_3, and pd_3 have been selected to be zero. Although symmetry is no general requirement, the membership function of the vertical cockpit acceleration has been selected to remain symmetric ($pa_1 = pa_5$, $pa_2 = pa_4$) to reduce the number of open parameters.

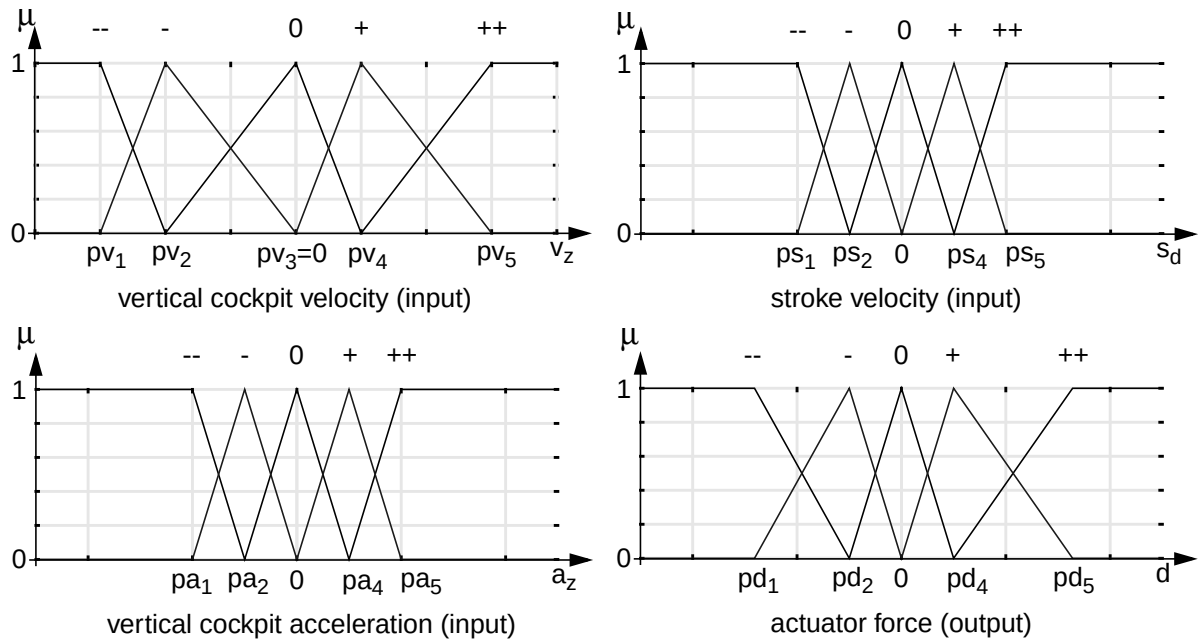

Figure 43: Membership functions of input and output quantities for fuzzyfication and defuzzyfication

As with “conventional” logic, empirical knowledge can be described in the form of rules. The rules consist of an “IF”-part (condition) and a “THEN”-part (consequence). However, while in Boolean logic the values for the consequence can only be TRUE or FALSE (0 or 1), all values in between 0 and 1 are allowed in fuzzy logic. The rules connecting input and output used in this work can be visualized in a matrix as seen in Figure 44.

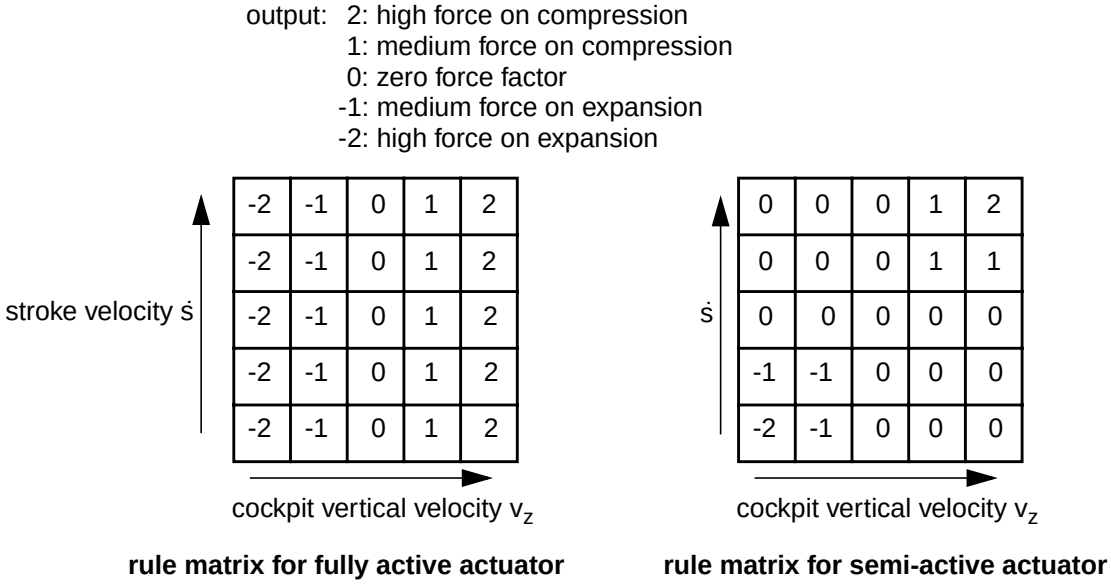

Figure 44: Fuzzy controller rule matrices for active and semi-active actuator

The procedure for the calculation of the crisp output of the fuzzy logic controller rule-base follows the four steps mentioned above, Figure 42:

Fuzzyfication

The first step is the determination of the level of firing of the rules. Here the crisp input x_i is matched with each linguistic label *B*, determining the membership grade μ of x_i in the respective fuzzy set.

Fuzzy Implication

In the fuzzy implication step each rule is evaluated individually to find the corresponding output. As a consequence of the fuzzyfied input, more than one rule can be (and will generally be) applied at the same time. Thus, in a second step the rules have to be aggregated. The most common form for the evaluation of a single rule is the "anding" ("AND-ing", see [103]), i.e. the selection of the maximum of the current membership function values [96]. If *x* belongs to two classes we find

$$\forall x \in X : \mu_{A \cup B}(x) = max[\mu_A(x), \mu_B(x)]. \tag{4.2.4}$$

Rule Aggregation (Inference)

The aggregation of the individual rule outputs is performed using the "oring" ("OR-ing") connective, i.e. the minimum of the individual rule outputs is selected.

$$\forall x \in X : \mu_{A \cap B}(x) = min[\mu_A(x), \mu_B(x)] \tag{4.2.5}$$

Since in the Fuzzy-implication a maximum of the membership values and in the Rule Aggregation a minimum of the rule output is selected, the two steps are sometimes combined and known as the "min-max-inference" [100].

Defuzzyfication

The output obtained by the rule-base cannot be used directly in a controller. To obtain a crisp output from a fuzzy controller a fourth step has to be added. The process of selecting one representative element from the aggregation is called defuzzyfication. The method used here is the Center of Area method. Other methods, e.g. the Mean of Maxima method, can be found in the literature [103]. The Center of Area method defines the defuzzyfied value of a fuzzy set as its fuzzy centroid, written for a discrete membership function as follows [103]:

$$y_f = \frac{\sum_{j=1}^{n} F(y_j) y_j}{\sum_{j=1}^{n} F(y_j)}, \tag{4.2.6}$$

with resulting output (command) of fuzzy controller y_f, output of j^{th} rule y_j, and area of j^{th} rule *F*. The resulting fuzzy controller is deterministic and can be regarded as a static, more-dimensional, nonlinear parameter-field (index array-) controller.

Following the process laid out above, a design of a fuzzy controller for an active and for a semi-active suspension has been performed. A typical plot of a control parameter field for vertical cockpit velocity and stroke velocity for a semi-active shock absorber is shown in Figure 45.

Some differences between the fuzzy controller and the skyhook controller apply for implementation. First, the fuzzy controller does not need to convert a "fully active" control signal to a signal applicable for a semi-active actuator; the stroke velocity enters as an input set and thus the

condition of equation (3.3.3) can already be met in the design of the rule matrix by setting the elements in the 2nd and 4th quadrant of the matrix to zero, see Figure 44. Thus, for the semi-active case, the output of the fuzzy controller (equation (4.2.6)) is already a damping factor, and a transformation according to equation (3.3.3) is not necessary.

The definition of the semi-active requirements by selecting elements for the rule matrix has the additional advantage that contrary to the skyhook controller, the fuzzy controller allows arbitrary transitions of the control force from negative to positive stroke velocity, see Figure 45c, whereas following the clipped optimal approach the force is a function of the sign of the stroke velocity only, not of its value.

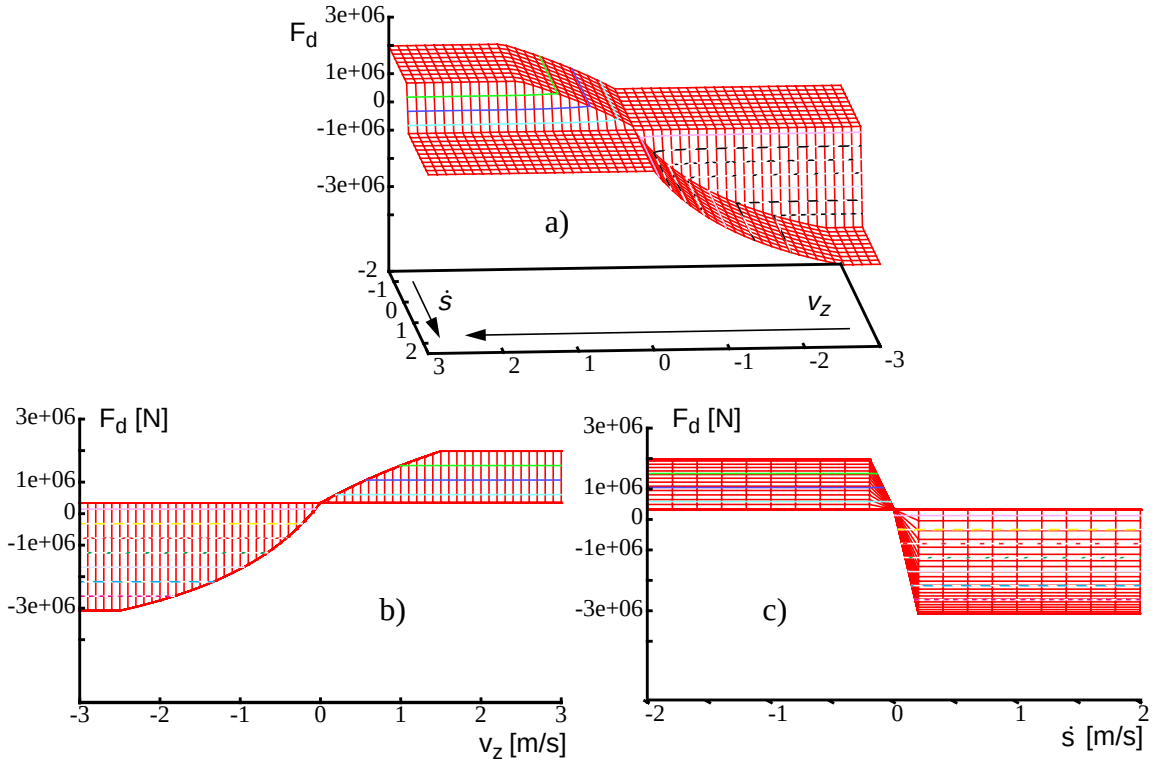

Figure 45: Parameter fields of fuzzy controller for a semi-active damper

4.2.3 State Feedback Control and Kalman Filter

State feedback controllers are a frequently used controller type for vehicle system control. State feedback is a means to control the motion of a system by feeding back the state vector x via a control matrix K,

$$u(t) = Kx(t). \tag{4.2.7}$$

The system performance can thus be modified in a wide range since x contains all information about the process. This control law changes the dynamic matrix A of the system ([54]) to

$$A^* = A + BK \tag{4.2.8}$$

The desired dynamical properties can be obtained by selecting an appropriate gain K. However, the performance of the actuator has to be taken into account as well. The control signal has to

lie within the bandwidth and the force range of the actuator.
For a complex system not all states will be directly accessible. Thus, either the controller works with the feedback of a limited number of states (limited state feedback) or the missing states have to be obtained via a state observer or state estimator. Taking into consideration the stochastic excitation (e.g. runway unevenness) and measurement noise, the optimal estimator has the form of a Kalman-Bucy filter. Controller design and Kalman filter design do not depend on each other, i.e. the controller can be calculated as if all model states were available. The Kalman filter can then be designed independently from the controller (algebraic separation). The necessary equations for the design of a Kalman-Bucy filter and the controller are given in [54] and [24]. Only the equations that have been implemented for the filter and controller design are presented below.

Kalman Filter Design

The state space system including stochastic excitations can be expressed in the following form, separating control input from excitation and sensor noise input:

$$\dot{x} = Ax + B_u u + B_w w \tag{4.2.9}$$

$$y = Cx + v \tag{4.2.10}$$

where w and v are assumed to be zero-mean white noise with spectral densities Q_w and R_v, respectively. The optimal observer for the estimated state $\hat{x}$ has the form

$$\dot{\hat{x}} = A\hat{x} + B_u u + K_k(y - C\hat{x}) \tag{4.2.11}$$

For low measurement noise, K_k will be large and the filter relies on those measurements. For large measurement noise, i.e. low K_k, the filter relies more on its internal system model.
The estimation error $\tilde{x} = x - \hat{x}$ can be described by

$$\dot{\tilde{x}} = (A - K_k C)\tilde{x} + B_w w - K_k y \tag{4.2.12}$$

The error covariance matrix P of the process will reach its minimum for

$$K_{k0}(t) = P_0(t) C^T R_v^{-1} \tag{4.2.13}$$

The optimal P_0 can be obtained by solving the matrix Riccati differential equation

$$\dot{P}_0 = AP_0 + P_0 A^T + B_w Q_w B_w^T - K_{k0} R_v K_{k0}^T \tag{4.2.14}$$

Since $P_0(t)$ is in the general case time dependent, K_k is also a function of time. Such a variable Kalman gain allows the filter to converge to the real state values in minimum time. However, a good estimated starting value P_0 has to be available which is not always easy to obtain. Therefore, often a stationary filter with a constant gain matrix $\overline{K}_{k0}$ and a stationary $\overline{P}_0$ is used. For this case which is also applied in this thesis, equations (4.2.13) and (4.2.14) become stationary with $\dot{P}_0 = 0$:

$$\overline{K}_{k0} = \overline{P}_0 C^T R_v^{-1} \tag{4.2.15}$$

$$0 = A\bar{P}_0 + \bar{P}_0 A^T + B_w Q_w B_w^T - \bar{K}_{k0} R_v \bar{K}_{k0}^T \tag{4.2.16}$$

The spectral densities of the system noise w and the measurement noise v are defined as the expectations

$$E\{w(t)w^T(\tau)\} = Q_w \delta(t-\tau) \tag{4.2.17}$$

$$E\{v(t)v^T(\tau)\} = R_w \delta(t-\tau)\,. \tag{4.2.18}$$

where δ is the Dirac function,

$$\delta(t-\tau) = \begin{cases} \infty & \text{for} \quad t = \tau \\ 0 & \text{for} \quad t \neq \tau \end{cases}. \tag{4.2.19}$$

For the discrete Kalman filter, Q_w and R_v can be set to the square of RMS values of system and measurement noise, respectively. For the aircraft, Q_w has been defined as a diagonal matrix

$$Q_w = \text{diag}[q_{w1}, q_{w2}, \ldots, q_{wn_x}] \tag{4.2.20}$$

where q_{wi} have been chosen as the $(\text{RMS})^2$ values of the response of the passive system. Since no measurement noise is present in the simulation model, the elements of R_v,

$$R_v = \text{diag}[r_{v1}, r_{v2}, \ldots, r_{vn_y}]\,, \tag{4.2.21}$$

have been set quite arbitrarily to $r_{vi}=10^{-3}$; it should be noted that the elements of R_v should not be selected to zero, but rather to a small value [54].

Note also that for a continuous system the Kalman filter is of equal order as the model, adding a corresponding number of differential equations. In the discrete implementation the filter can be calculated recursively [54].

Controller Design

The state controller can be obtained by a number of methods, pole placement and Riccati design (also called LQR = “linear quadratic regulator” control) being among the most used in active suspension design [21], [28]. In this work one type of controller was determined by means of Riccati design for the full state system. For an observable and controllable system of order n_x, arbitrary eigenvalues can be found using full-state feedback as described in equations (4.2.7) and (4.2.8). The fundamental idea of the quadratic synthesis is the determination of the least squares [54]

$$J = \int_0^\infty (x^T Q x + u^T R u)\,dt\,. \tag{4.2.22}$$

where Q and R are weighting matrices for the state and actuation effort, respectively. The gain matrix K of equation (4.2.8) is determined by the relation

$$K = R^{-1} B^T P \tag{4.2.23}$$

with $P = P^T > 0$ as the solution of the algebraic Riccati equation

$$0 = AP + PA^T + Q - PBR^{-1}B^T P\,. \tag{4.2.24}$$

For the solution of the Riccati equation, standard MATRIXx solvers are available and have been used for the determination of *K*. For the nose landing gear control, there is only one actuator, i.e. $n_u = 1$. Thus, the controller gain *K* is just a vector.

A central question of the Riccati design is the choice of the weighting matrices *Q* and *R*. Some special considerations about the application of the state feedback to suspension control help to find a strategy by linking the choice of *Q* and *R* to the desired system response.

For the optimization of the landing gear control algorithm, not the complete state vector *x* needs to be regarded for minimization (as done in the classical Riccati design) but only a selection according to measurements *y*:

$$y = H\,x. \tag{4.2.25}$$

Therefore, equation (4.2.22) for the integral of the least squares may be replaced by:

$$J = \int_0^\infty (y^T Q' y + u^T R u)\,dt, \tag{4.2.26}$$

$$\int_0^\infty (x^T H^T q H x + u^T R u)\,dt = \int_0^\infty (x^T H^T q H x + u^T R u)\,dt \quad , \tag{4.2.27}$$

with

$$Q' = H^T q H\,. \tag{4.2.28}$$

The matrix *Q* has now been replaced by a vector *q* with the same number of elements as measurements available in *y*. Those measurements can comprise those physical quantities that are to be reduced, e.g vertical accelerations at the cockpit and other locations of the fuselage. The selection of starting points for the elements in *q* for the state feedback controller follows the suggestions of Bryson and Ho [7], setting the elements of *q* according to the maximum values found for the corresponding outputs from the simulation of the passive system, i.e.

$$q_i = 1 / y_{i,\,max}^2\,. \tag{4.2.29}$$

Accordingly, the starting point for R as the weighting of the actuation effort is set to

$$R = 1 / F_{act,\,max}^2 \tag{4.2.30}$$

where $F_{act,max}$ is the maximum actuation force of the shock absorber.

It should be noted that this controller is no longer full-state feedback. For this type of controller stability cannot be theoretically guaranteed. However, since the underlying uncontrolled system is stable for semi-active control and good-natured for active control, stability can be postulated [6]

LQR Controller for Landing Gear Control

Whereas the optimization routine can change the control parameters of the skyhook and of the

fuzzy controller directly, this cannot be done for the LQR controller, as not the control gain vector K will be subject of optimization. A component-wise optimization of vector K would be cumbersome, especially for large systems. Instead, optimization changes the components of the vector q, which has as many components as criteria of interest, as well as R. Consequently, prior to each time simulation the algebraic Riccati equation ((4.2.23) and (4.2.24)) has to be solved once for q and R proposed by the optimization algorithm to calculate the gain vector K valid for that simulation run. This process has been automated by the author by calling the respective MATRIXx routines once per SIMPACK time integration run. MATRIXx reads q and R from the optimization routine and supplies the values of K in form of a SIMPACK control element. As for the skyhook controller, the control output, i.e. the commanded force, has to be modified for use with a semi-active damper according to (3.3.3).

4.2.4 Multi-Objective Optimization

The optimal values for the control parameters have been found using multi-objective parameter optimization. In this process, the optimization module supplies the multibody simulation with values of the parameters to be optimized, a time simulation is performed, criteria according to (3.5.1) and (3.5.2) are calculated and passed back to the optimization routine which, in turn, selects a new set of parameters to start a new time simulation. This process is depicted in Figure 46.

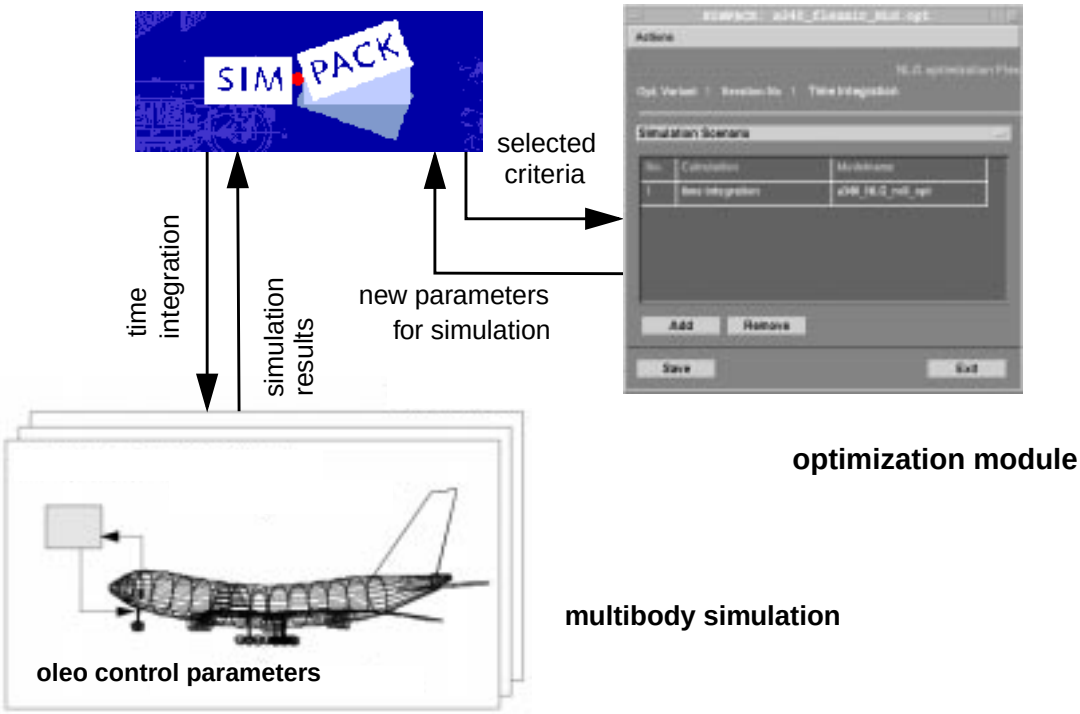

Figure 46: Multi-objective optimization strategy

The goal of multi-objective optimization is to find an optimal parameter set to improve a criterion without deteriorating another one, leading to a so-called PARETO-optimum [3]. All per-

formance criteria $c_i(\underline{p})$ are collected to form the criteria vector $\underline{c}(\underline{p})$ which dependends on the parameter set $\underline{p}$. The parameter set $\underline{p}_1$ is defined to be better than the parameter set $\underline{p}_2$ if the criteria vector $\underline{c}(\underline{p}_1)$ is smaller than the vector $\underline{c}(\underline{p}_2)$.
Since generally more than one parameter set $\underline{p}_{opt}$ satisfies condition (4.2.32), a final solution will always be a compromise which has to be accepted by the designer. A mathematical formulation of finding a solution for set $\underline{p}_{opt}$ may be defined as follows: $\underline{p}_{opt}$ has to be part of the multitude of compromise solutions and

$$\underline{c}(\underline{p}_{opt}) \leq \underline{d}^*, \tag{4.2.31}$$

$\underline{d}^*$ representing feasible design requirements. The vector $\underline{d}^*$ is called the design vector which has to be formulated by the design engineer. To find a PARETO-optimum, the problem is formulated as a variation of a min/max optimization problem. The performance criteria vector and the design vector form

$$\alpha(\underline{p}) = \max_i \left(\frac{c_i(\underline{p})}{d_i^*} \right), \quad c_i, d_i^* > 0 \tag{4.2.32}$$

Now, $\alpha^* = \alpha^*(\underline{p}_{opt})$ shall denote a minimum of α:

$$\alpha^* = \min_p \max_i \left(\frac{c_i(\underline{p})}{d_i^*} \right). \tag{4.2.33}$$

If $\alpha^* \leq 1$, then $\underline{p}_{opt}$ represents an acceptable compromise solution of the multi-objective optimization problem. With this strategy the multi-objective optimization has been reduced to a scalar min/max problem. The methodology is discussed in detail in [44].
The optimization algorithm which has been used for the optimization of control parameters is the so-called “Pattern Search”, a gradient-free method derived from the original pattern search algorithm by Hooke and Jeeves [38].

4.3 Design and Optimization Process for the Nose Landing Gear Controller

This section describes the design and optimization process for the nose landing gear controllers. The controller has been designed in a multi-step design process. Following the model set-up in the MBS environment as described in chapter 3.1, the first control design step has been to build up the control schemes and to test them on a linearized model inside MATRIXx/ SystemBuild. Second, the controller was exported to SIMPACK and the control parameters optimized in SIMPACK using the design model and multi-objective optimization methods. In a third step, an evaluation took place by multibody simulation on a complex evaluation model, see Figure 47.

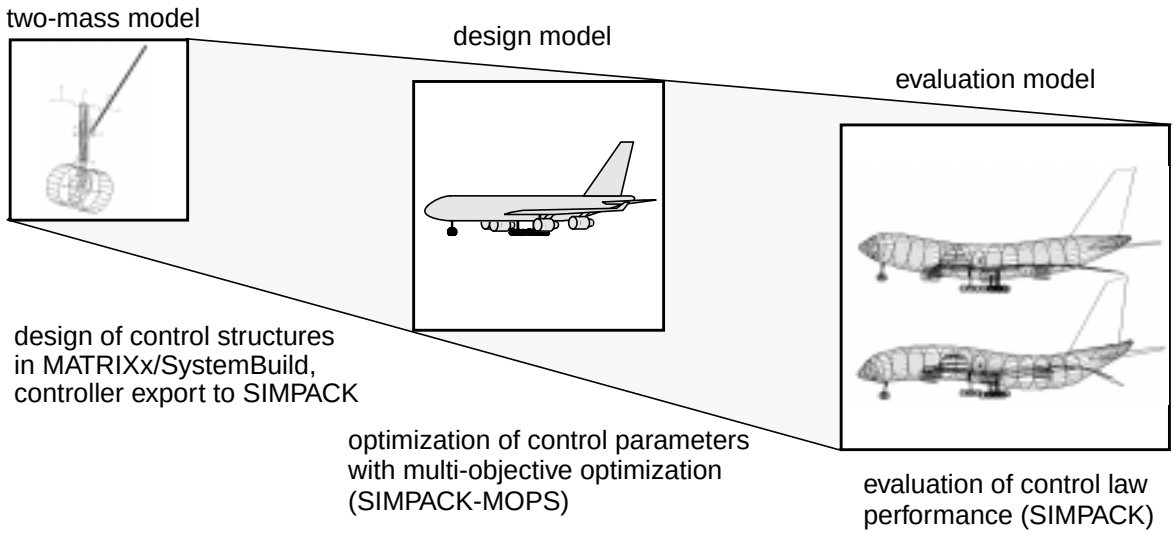

Figure 47: Control law design strategy

4.3.1 Design of a Controller using MATRIXx/SystemBuild

Control Design for a Two-Mass Model:

At the start of the design process a two-mass model of the nose landing gear (see chapter 3.2.3) has been set up in SIMPACK. This model has two degrees of freedom, “aircraft” heave and oleo stroke, and includes the air spring, tires and a force input vector in the place of the damping actuator. The equations of motion of this model have been linearized inside SIMPACK and exported to MATRIXx using the SIMAX Linear System Interface. Next, the control loop is set up in SystemBuild. This environment allows the simple modification of controller structure, control parameters and input and output variables. In addition, test simulations with the linearized plant and stochastic excitations can be performed inside SystemBuild to check the basic functionality of the control laws.

Figure 48 shows an example of such a design and simulation case for the state feedback controller. In comparison to the skyhook and the fuzzy controller, the loop consists of an additional estimator block to calculate the state vector from the measurements. For the state feedback controller, both system response and estimated state vector can be monitored to evaluate estimator and control quality. In parallel, a completely passive reference landing gear is simulated based on an identical mechanical model. This combination of a passive and an active or semi-active model in one block diagram simplifies the quick comparison of simulation results in the design stage.

The fuzzy controller has been realized by implementing the fuzzy control process in a User-Code block. For the state feedback controller, standard functions of the MATRIXx control toolbox for Kalman filter and state controller design, especially for calculation of a state estimator, the solution of the Riccati equation and the computation of a full-state feedback controller have been used according to the procedure given in chapter 4.2.3.

The landing gear controller is, in a first step, designed clipped optimal, assuming a fully active

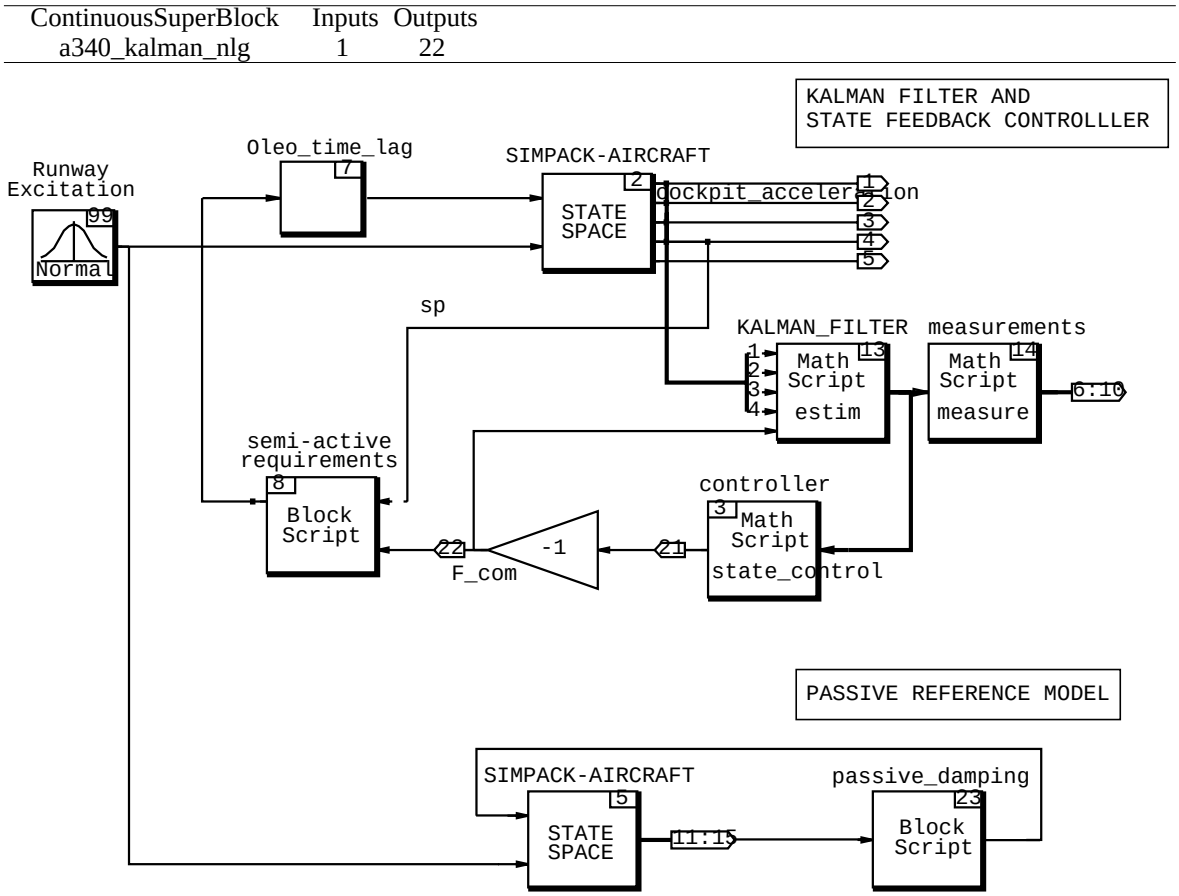

Figure 48: Control design loop using SystemBuild

approach. The fully active control signal is then converted into a semi-active control command according to equation (3.3.3).

Control Design for a Linearized Full Aircraft Model

For the design of the final control layout a linearized model of a full aircraft has been set up in SIMPACK, taking into account the vertical motion of nose landing gear, main landing gears and center landing gear as well as the three lowest symmetrical fuselage and wing eigenmodes. This model has also been linearized inside SIMPACK and transferred to SystemBuild via the SIMAX Linear System Interface. The controller is then re-designed for the full aircraft model. In the case of the skyhook-controller, only the feedback gains have been newly chosen; the same is true for the fuzzy-controller. In the case of the state feedback controller, both Kalman filter and controller have to be re-calculated according to chapter 4.2.3 because the order of the optimal observer changes as well as the size of the control matrix.

After the different control structures have been implemented and preliminary control parameter sets have been calculated inside SystemBuild, the controllers were exported to SIMPACK using two of the interfaces described in chapter 2.3.5. The skyhook controller has been exported as C-code by the MATRIXx AutoCode module and introduced as a SIMPACK user force element. The same way has been used for the fuzzy controller. In the case of the state feedback controller, a C-code export has not been possible, so the controller has been written from MATRIXx as a

file directly in the syntax of a standard SIMPACK force element using a custom-made MATRIXx script.
From this point on all control structures have remained fixed and have only been subject to parameter changes. The parameters of the fully active and the semi-active parameters will be determined independently from each other in the subsequent optimization in SIMPACK.

4.3.2 Controller Optimization in SIMPACK

The final phase of the controller design is the numerical optimization of the control law parameters with respect to pre-defined performance criteria. The criteria are selected to obtain improvement in comfort, i.e. a reduction of vertical accelerations. Thus, the criteria are the maximum vertical acceleration, the RMS of the vertical acceleration, and the frequency response in the region between 1 and 10 Hz (see chapter 3.5). Only the cockpit acceleration is used as input for the optimization criteria. However, it will also have to be shown in the evaluation simulations that an improvement in the cockpit region does not lead to a significant reduction of comfort at other points of the fuselage.
Optimization is a step-wise process. First, the upper and lower limits in between which a variation and optimization of the free parameters is physically sensible are determined. To find those boundaries a parameter study is performed in SIMPACK, varying those parameters open to optimization. The limits must be such that the model remains numerically and physically stable for all variations of parameters that might occur during an optimization run. Second, once the boundaries are defined, a parameter study inside SIMPACK-MOPS is used to identify the parameter region in which a global minimum is to be expected. Experience with this work and related activities [94] have shown that the selection of a good starting point is of utmost importance for the success of optimization of a semi-active landing gear. Third, an optimization run is performed from this starting point according to the strategy described in chapter 4.2.4.
The aircraft model used for optimization is a full aircraft of reduced complexity as described in chapter 3.1.1, with three elastic structural modes and the pitch motion of the main landing gear bogie neglected, but taking into consideration all nonlinearities of the landing gear oleos. The aircraft configuration for optimization was maximum landing weight (190 t). As excitation for the optimization simulations San Francisco Runway has been selected because this runway is a certification case for aircraft ground dynamics. Only one runway was used for optimization in order to keep the total computation time in tolerable limits. In all optimization simulations the aircraft has been rolling at a speed of 60 m/s for a simulation time of 10 seconds, thus covering 600 m of the runway. Optimization has been performed on a single aircraft configuration. However, the evaluation will be made for all three available loading cases, both on San Francisco and on the Rough Runway. Furthermore, the evaluation will assess the quality of the control laws for other speeds than the design speed.
The optimization parameters are controller type specific. For the skyhook controller the free parameters are the gains P and D of the PD controller, compare Figure 40. For the fuzzy con-

troller, the free parameters are those describing the linguistic variables of the input and output sets, vertical cockpit velocity ($pv_{1,2,4,5}$), vertical cockpit acceleration ($pa_{1,2}$), oleo closure velocity ($ps_{1,2,4,5}$), and damping coefficient ($pd_{1,2,4,5}$) (compare Figure 44). The free parameters for the LQR controller are the measurement-weighting constants q_i and the weighting constant R representing the control effort, see equations (4.2.26) and (4.2.28).

As mentioned above, a parameter study has to be performed to find the boundary conditions for the optimization parameters. For the skyhook controller a maximum gain of $P = 0.8$ has been found to be realistic, larger values lead to numerical problems for the integrator during the simulation. Evaluations of D yielded a maximum value of $D = 0.3$. The constant factor was chosen to be $K_c=10^7$. For the fuzzy controller, the parameters have direct physical meanings. Boundaries can be given by applying values taken from the simulation of the passive system. Furthermore, the constraint applies that the parameters of one set have to remain in ascending order, e.g. $pv_1 < pv_2 < ... < pv_5$.

The selection of starting points for the elements in q for the state feedback controller has followed the strategy suggested in chapter 4.2.3, setting the elements of q according to the values found for the corresponding outputs from the simulation of the passive system, $q_i = 1/y_{i,\,max}^2$, and from the available force level of the actuator, $R = 1/F_{act,\,max}^2$.

Table 4 gives an overview over the free parameters, as well as the boundary conditions.

skyhook controller	P	$0 < P < 0.8$	gain for cockpit velocity [-]
	D	$0 < D < 0.3$	gain for cockpit acceleration [-]
fuzzy controller	pv	$-10.0 < pv_1 < pv_2 < 0 < pv_4 < pv_5 < 10.0$	cockpit vertical velocity [m/s]
	pa	$0 < pa_1 < pa_2 < 10.0$	cockpit vertical acceleration [m/s^2]
	ps	$-10.0 < ps_1 < ps_2 < 0 < ps_4 < ps_5 < 10.0$	oleo stroke velocity [m/s]
	pd	$-5*10^7 < pd_1 < pd_2 < 0 < pd_4 < pd_5 < 5*10^7$	damping coefficient [$N/(m/s)^2$] (negative: oleo extension)
LQR controller	q_1	$20 < q_1 < 400$	weighting of measurements for cockpit vertical velocity [$1/(m/s)^2$]
	q_2	$0.06 < q_2 < 4.0$	weighting of measurements for cockpit vertical acceleration [$1/(m/s^2)^2$]
	q_3	$20 < q_3 < 400$	weighting of measurements for oleo stroke velocity [$1/(m/s)^2$]
	R	$10^{-10} < R < 10^{-8}$	weighting of control effort [$1/N^2$]

Table 4: List of optimization parameters and boundary condition

4.3.3 Control Parameters: Optimization Results

The optimization runs turned out to be a rather time consuming and complex process which can by no means be called straight-forward. As was to be expected, the RMS and the maximum-acceleration criteria were sometimes contradictory. In these cases it was a limit condition that the acceleration peak level should not exceed that of the passive reference suspension.

A second phenomenon posed another challenge. Since the excitation contains input over a wide frequency range but is not strictly stochastic (consisting of measured runway data), the optimization results depends on the length of the simulation as well as on the selected starting point on the runway. A singular event, e.g. a particular bad patch of runway, can influence the criteria considerably. Therefore, the simulation for the optimization was chosen to be a ten-second run to cover a wide section of runway. Still, the results had to be carefully evaluated to obtain globally valid predictions.

These phenomena lead to a low parameter sensitivity and thus to convergence problems of the optimization algorithm in the vicinity of the optima. The following plot of the variation of the skyhook control parameters exemplifies the difficulties. Figure 49 shows the progression of the RMS and maximum-acceleration criteria as a function of $P*K_c$ and $D*K_c$ for the semi-active landing gear. Clearly, the RMS criterion has a minimum in the region of $P*K_c=2*10^7$, but the sensitivity to the change of D is low. The maximum-acceleration criterion shows no clear pat-

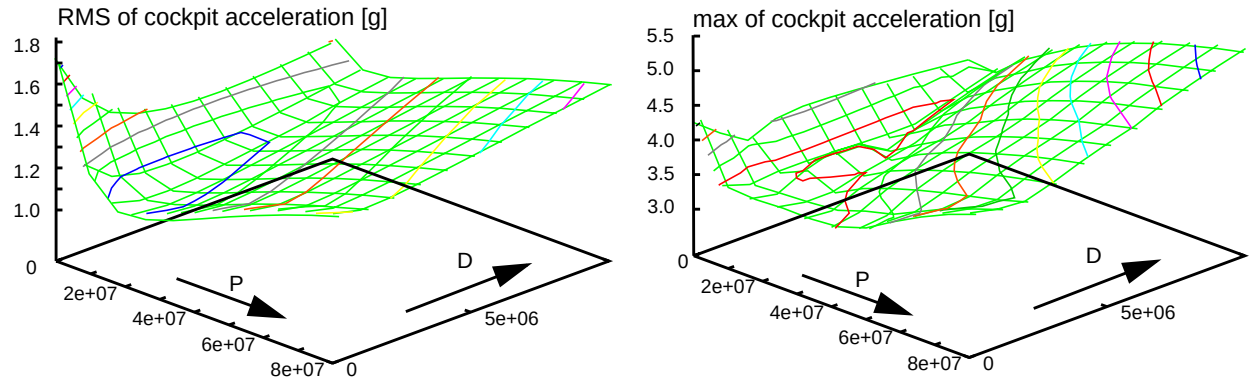

Figure 49: Criterion functions for semi-active skyhook control

tern in the region around the minimum, it depends strongly on singular events as mentioned above. For an optimization problem of this kind only the “Pattern Search” algorithm of MOPS could converge when started from a good starting point. For future optimization studies of aircraft ground response to runway input an optimization algorithm better suited for the handling of models with runway excitations should be implemented in the used optimization package.

Table 5 gives a list of all optimization results for semi-active and fully active systems. All solutions have been obtained by performing a parameter variation to localize the region of the global optimum and a following optimization run was started to find the exact location of the optimum.

Looking at the results one point comes to attention immediately - the optimal parameters deter-

controller type	parameters	semi-active	fully active
skyhook controller	P	$2.5*10^{7}$	$1.9*10^{6}$
	D	$1.2*10^{6}$	$2.1*10^{5}$
fuzzy controller	pv 1-5	-3.0, -2.0, 0, 1.0, 3.0	-3.0, -2.0, 0, 1.0, 3.0
	pa 1-3	0, 0.7, 1.0	0, 0.7, 1.0
	ps 1-5	-1.0, -0.1, 0, 0.1, 1.0	-1.0, -0.1, 0, 0.1, 1.0
	pd 1-5	$-1.0*10^{5}$, $-0.2*10^{5}$, 0, $0.2*10^{5}$, $1.0*10^{5}$	$-2.5*10^{4}$, $-0.1*10^{4}$, 0, $0.25*10^{4}$, $2.5*10^{4}$
LQR controller	q_1	110	100
	q_2	1.5	1.8
	q_3	150	130
	R	$7.5*10^{-8}$	$5.0*10^{-6}$

Table 5: List of optimized parameters for fully active and semi-active systems

mining the damping factor (i.e. the optimal gains for the skyhook controller, the values of the damping factor set for the fuzzy controller, the weighting of the control effort for the LQR controller) are higher for the semi-active cases than those for the passive cases. Evidently the loss of half of the control possibilities according to Figure 12 necessitates higher control gains to make up for the reduced actuation time. This effect leads to another interesting result - the stability limits found with the help of linear control theory for fully active actuators do not fully apply to the semi-active case. The optimized parameters for semi-active control have been found to be of a magnitude where a fully active system has already become unstable.

5 Evaluation of the Performance of Semi-Active Landing Gears

The controllers have been designed and their parameters optimized with a design model. To evaluate the control performance for a complex aircraft model and for operating points other than the design point simulation results obtained with the evaluation model on two different runways will be addressed in this chapter. The assessment is followed by a comparison between the performance of fully active and semi-active systems and a consideration whether a two-mass model is sufficient for control layout. Further simulations will investigate the robustness of the control design against changes in aircraft weight and aircraft speed. Finally, aspects of the dependence on realistic actuator limitations, i.e. force and flow limits as well as actuator time constants will be discussed. The chapter will close with a comparison of the benefits of a semi-active landing gear as compared with an optimized passive concept.

5.1 Comparison of Simulation Results for all Control Laws at the Design Point

The central performance evaluation is the comparison of aircraft models equipped with semi-active landing gears controlled by a skyhook-, a fuzzy-, and an LQR-controller designed according to the methodology presented above as well as a passive reference model. To assess the limitations of the semi-active control concept, the performance of a semi-active system is compared to an aircraft equipped with a potential fully active landing gear in section 5.1.3. Finally, the difference between a control design based on a two-mass model and one based on a full aircraft model is examined in section 5.1.4. All simulations in section 5.1.1 to section 5.1.4 have been performed at the control design point, i.e. an aircraft with a mass of 190 tons at a speed of 60 m/s.

5.1.1 San Francisco Runway, Semi-Active Landing Gear

In this section simulation results of the simulated aircraft equipped with semi-active landing gears controlled by a skyhook-, a fuzzy-, and an LQR-controller will be presented. As described above (chapter 4.3.3), no single global optimum exists for a set of control gains as an engineering decision is always necessary to evaluate the sometimes conflicting criteria “RMS” and “maximum” of vertical cockpit acceleration. To be able to compare the different control concepts, optimization has been performed such that the maximum acceleration is equal for all control concepts. Thus, the RMS values as well as the frequency response are available as a comparative scale.

The plots of the time response at the cockpit, Figure 50a, show that all control laws perform well at the design point with respect to the reduction of peak acceleration. The highest peak accelerations can be reduced by a factor of almost two with no evident differences in performance for the three controllers. The RMS values of the cockpit acceleration show no great difference, either. They are reduced by 37% (skyhook controller), 38% (fuzzy-controller) and 40%

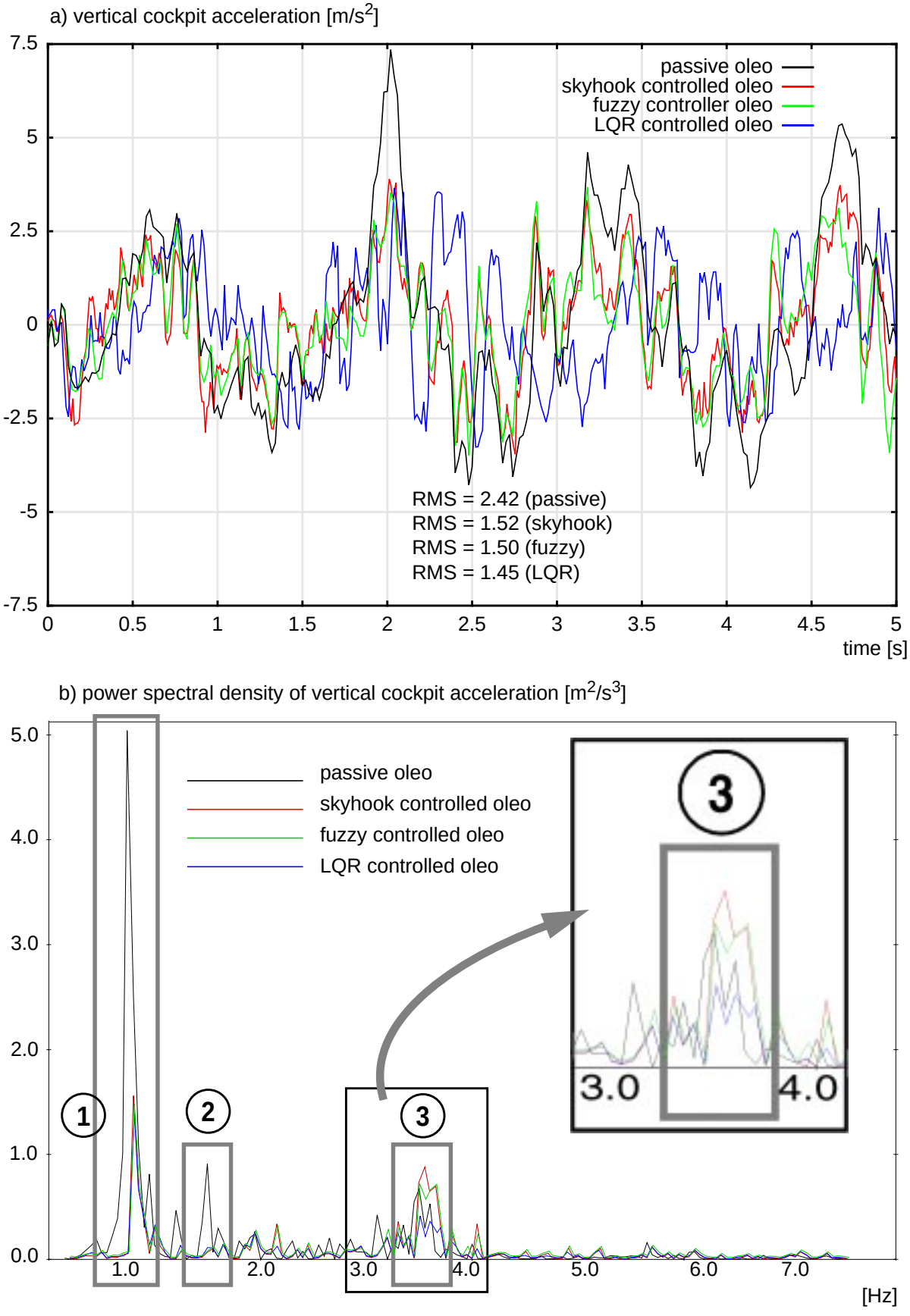

Figure 50: Time and frequency response of aircraft, comparison of control laws (SF Runway)

(LQR controller) when compared with the aircraft equipped with a conventional (single stage) passive landing gear.
The frequency response Figure 50b, however, shows a more differentiated picture. In this plot it can be seen from region 1 that for all control concepts the rigid body modes pitch and heave, at 0.66 Hz and 0.87 Hz, respectively, can be equally effectively damped. The performance, however, varies for elastic modes. Both skyhook and fuzzy controller achieve good damping for the first wing mode, see region 2. While the skyhook controller performance already deteriorates for frequencies greater than 2 Hz, the fuzzy controller does not perform as well as the passive suspension for frequencies greater than 4 Hz, see region 3. Only the LQR controller, where the design has included elastic airframe modes, is able to stay below, or approximately equal to the level achieved with the passive landing gear.
Looking at the results it can be stated that the fuzzy controller seems to have no great advantage over the skyhook controller for the San Francisco case. The LQR controller seems to be the best choice, not so much because of its marginal performance advantage on the maximum vertical accelerations but because of its ability to effectively suppress the rigid as well as also all low elastic natural frequencies of wings and fuselage.

5.1.2 Rough Runway, Semi-Active Landing Gear

The simulations on the Rough Runway have been performed with the same aircraft parameters (m_{AC} = 190 tons, v_x = 60 m/s) and control parameter settings as for the San Francisco case. The results differ in two respects - first, the aircraft response is about one quarter higher for the Rough Runway than for the San Francisco Runway (maximum acceleration well above 10 m/s^2, see Figure 51a, as compared to 7.5 m/s^2 in Figure 50a for the passive aircraft), mirroring the bad quality of the Rough Runway; second, the frequency response for passive and semi-active aircraft is of a different shape. While on the San Francisco Runway the rigid body eigenmodes dominate the aircraft response, the aircraft elastic modes are strongly excited by the Rough Runway, see Figure 51b, regions 2 and 3. These factors have an influence on the control performance. Again, all control concepts perform well and of comparable quality in the reduction of the maximum and the RMS of the vertical cockpit acceleration (see Figure 51a: 43% reduction of RMS for skyhook controller, 44% for fuzzy controller, 45% improvement for LQR controller), as they did in the San Francisco case. On the Rough Runway, the rigid body modes are damped well, however, for the frequency response, there is no deterioration of performance of the skyhook controller up to 4 Hz, see Figure 51b, regions 2 and 3, as it could be seen for San Francisco Runway. All three controllers remain below the maximum of excitation of the passive system up to that point.
From these results it can be concluded that the improvements of the control concepts do not deteriorate for excitations levels higher than that of the design. This conclusion is also supported by the results of the evaluation of the control performance as a function of runway roughness (section 5.2.3) where it can be seen that for a low aircraft response, i.e. low RMS of

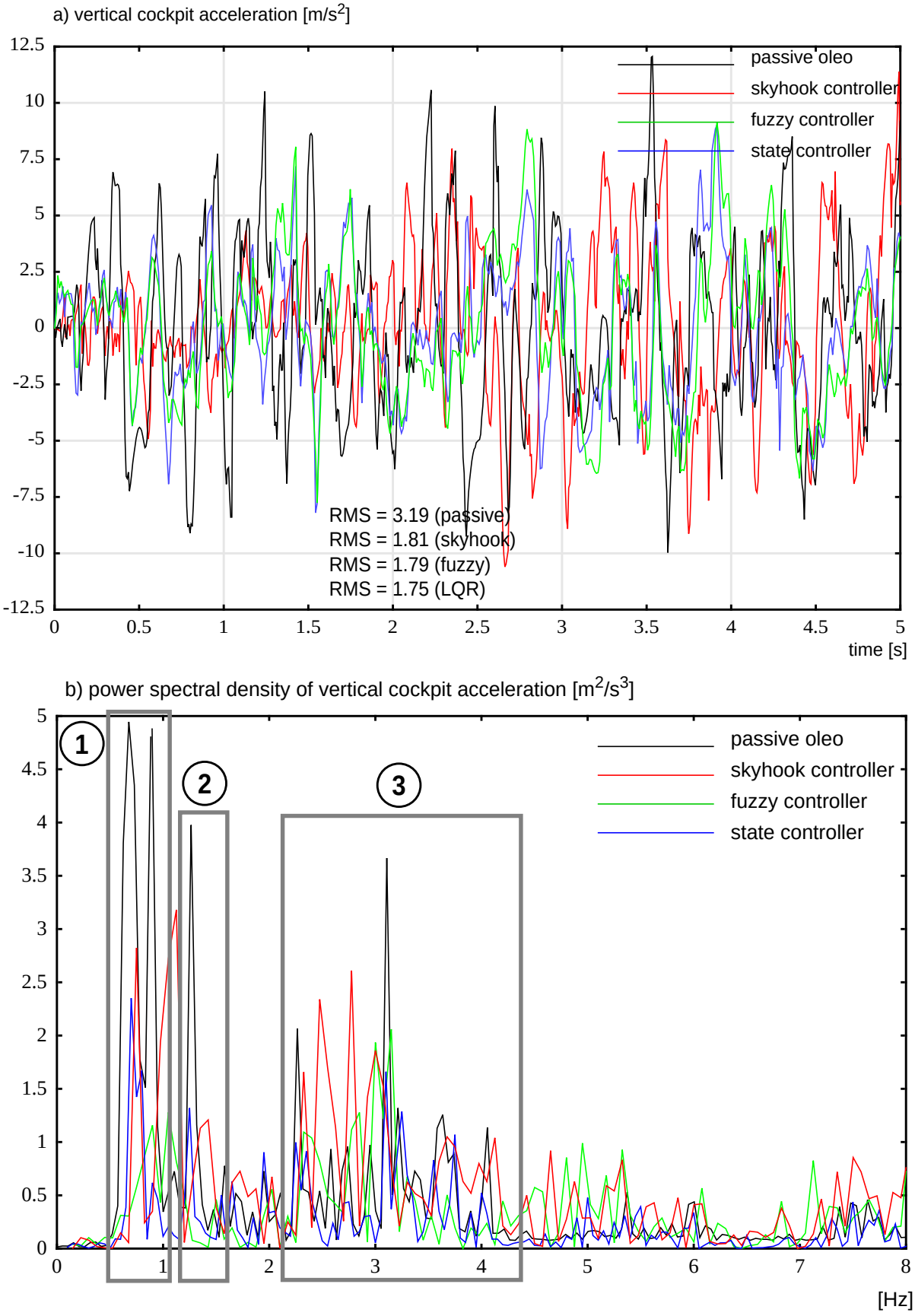

Figure 51: Time and frequency response of aircraft, comparison of control laws (Rough Runway)

vertical cockpit acceleration, the control performance deteriorates. It remains to be seen, however, if the predicted excitation of the higher modes by the skyhook controller in the San Francisco case will also result in mechanical vibrations on a real aircraft or if the rise is so small in its effective value that it will not show at all on a real structure. This topic is an important open question for a flight test.

5.1.3 Comparison of Passive System to Semi-Active and Fully Active Control

To assess the limitations of the semi-active control concept as compared to a fully active actuator, simulation results for an aircraft with a semi-active actuator are compared to results for an aircraft equipped with a fully active actuator. Both actuators are assumed to be able to provide unlimited force. Their transient behavior has been modeled by a first order low pass filter with time constants which are typical for active and semi-active components. In tests semi-active components have proven to be faster than their fully active counterparts. Consequently, the time constant for the semi-active actuator has been chosen to be 15 ms, for the fully active actuator a time constant of 50 ms. The investigation concentrates on the skyhook control approach; identical assumptions can be made for fuzzy controller and LQR controller. Again, the aircraft is of the 190 ton configuration, with a speed of 60 m/s, and the excitation is San Francisco Runway. In the simulation, the fully active oleo performs better than its semi-active counterpart. the reduction of RMS of vertical cockpit acceleration of 69% improvement against 33% for the semi-active case, see Figure 52. However, this performance improvement does not hold for the reduction of peak acceleration. Here, the slower fully active system only allows modest improvements against the semi-active suspension, additionally inducing oscillations of low amplitude but higher frequency. Thus, the influence of the actuator time constant is such that the difference between fully active and semi-active diminished for realistic actuators.
This result is in accordance with observation in the literature where a reduction of peak acceleration between 20% and 50%, depending on excitation and oil flow limits, is reported for a complex fully active test rig [26], which is better than the improvements predicted for the semi-active oleo in this study by a factor of 1.5 to 2. It is strongly questionable, however, if the difference is worth the highly increased system complexity necessary for the fully active system.

5.1.4 Two-Mass Model vs. Aircraft Design Model for Control Design

The use of reduced models in control design is customary, for one reason to keep the control design effort and the resulting controller structure as simple as possible. Furthermore a model will always be a reduced image of a real system. The questions is, to which point a model can be reduced without compromising the function and the performance of the controller.
It will be the task of this section to compare the performance of controllers developed on the two-mass model with those optimized on the full aircraft model to assess whether a full aircraft model is really necessary for suspension layout and to estimate loss of performance when using a reduced model. This comparison is executed for the evaluation model at the working point of

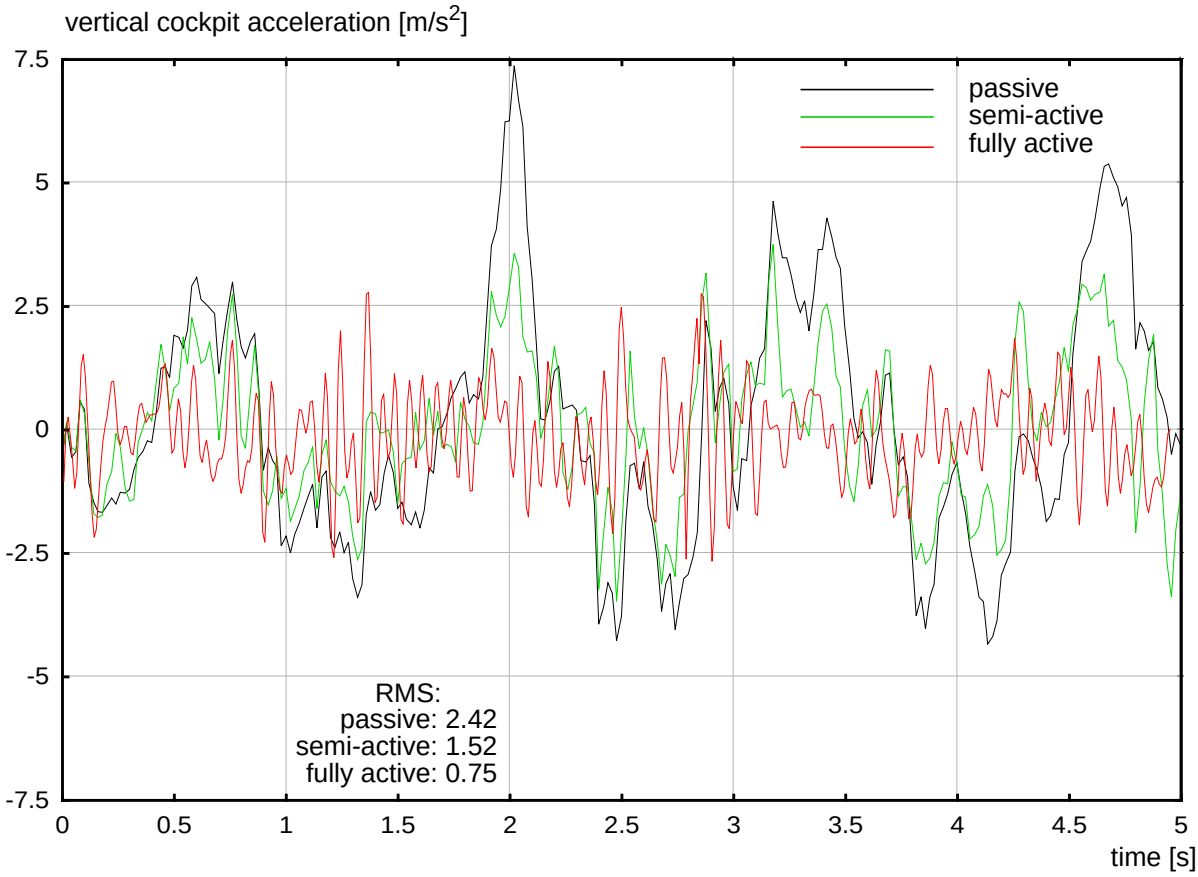

Figure 52: Comparison of passive, semi-active and fully active gear (skyhook controller)

60 m/s aircraft speed on the San Francisco Runway. The aircraft mass is 190 tons, the equivalent mass of the two-mass model representing the nose landing gear load is 16 tons. The vertical velocity and vertical acceleration for the two-mass model is measured at the substitutional mass ("top-of-landing-gear"), for the full aircraft model at the cockpit.

Seven sets of simulations will be performed:

1. the skyhook controller optimized on the two-mass model,
2. the skyhook controller optimized on the aircraft design model,
3. the fuzzy controller optimized on the two-mass model,
4. the fuzzy controller optimized on the aircraft design model,
5. the LQR controller designed for and optimized for the two-mass model,
6. the LQR controller designed and optimized on the aircraft design model,
7. the passive reference case.

For the cases 1 and 2, as well as 3 and 4, the control structures for two-mass model and full aircraft were identical, only the control parameters differed. For the LGR control approach, the structures of controller and observer designed for the full aircraft model cannot be the same as for the two-mass model due to the different number of degrees of freedom of the models. However, in case number 5 the controller which was designed and optimized for the two-mass model was implemented on the full aircraft. The analysis of the control performance has been done using the values of RMS of vertical cockpit accelerations for all control structures, Figure 53a.

In a second plot, the power spectral density of the vertical cockpit acceleration will be compared for the two LQR controller cases, Figure 53b.

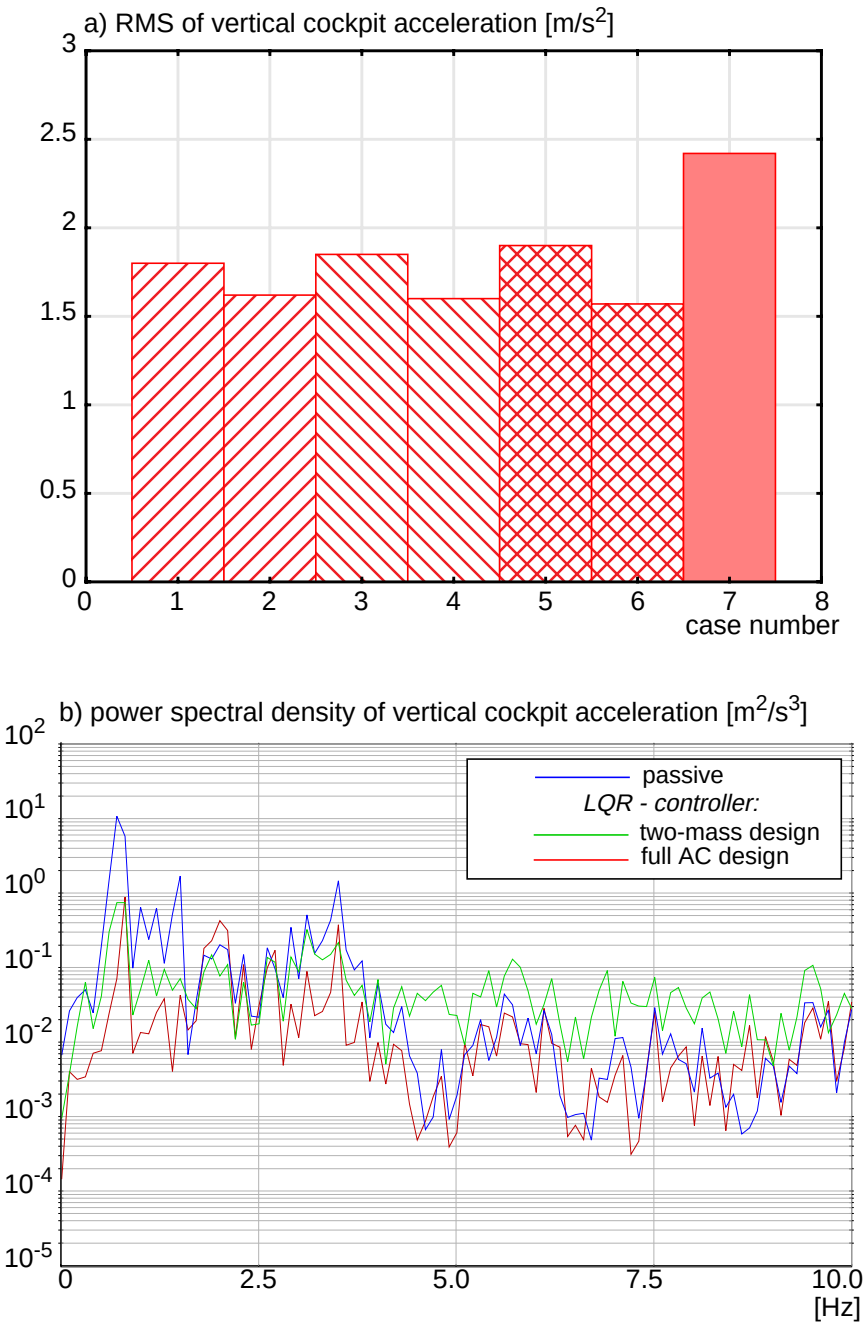

Figure 53: Comparison of control performance for controller optimized on two-mass model and on aircraft design model

Somewhat surprisingly, all controllers, also those designed with the two-mass model, are able to reduce the vertical cockpit acceleration well. Those controllers optimized on the full aircraft achieve a performance advantage of approximately 10% against their counterparts optimized on the two-mass model. The difference between the two design strategies is the smallest for the skyhook controller and the largest for the LQR controller. This result is not surprising because the skyhook controller, with only two parameters, is least tuned to a specific model whereas the

design process for the LQR controller is strongly connected to the structure of the model. The fuzzy controller lies in the middle of the two extremes.
The plot of the frequency response exemplifies the dependence between model and control design for the LQR controller. While the controller designed with the full aircraft model remains below the response of the passive system for the complete frequency range, the controller designed with the two-mass model achieves good damping of the rigid body modes only and shows a similar response as the skyhook controller discussed in section 5.1.1.
Summarizing it can be stated that the use of a two-mass model for control layout results in a significant decrease in performance. Yet, the system still performs considerably better than an aircraft with a passive suspension. If, however, structural vibration of higher modes becomes a problem, as it is the case for large transport aircraft, the use of a full aircraft model not only for evaluation but also for control system layout becomes a necessity.

5.2 Performance of Semi-Active Shock Absorber for Operational Cases

All the simulations of section 5.1 have been performed using the same aircraft model and aircraft speed as in the optimization process. In reality the aircraft operates in a weight envelope from almost empty to maximum take-off weight and in a speed range from slow taxi to take-off speed. In this chapter the control performance will be assessed if the operational parameters aircraft weight, aircraft speed, and runway roughness vary from the design point. The parameters of the semi-active control laws will be kept constant at the values of Table 5 for all cases.

5.2.1 Performance as a Function of Aircraft Weight

For the following investigation, the aircraft is simulated running over San Francisco Runway using three different weight configurations, 150 tons (OWE), 190 tons (MLW), and 250 tons (MTOW) with the aim to check the influence of the aircraft weight configuration on the control performance.
The design point (190 tons) has already been discussed in section 5.1.1, Figure 50. The performance improvement of the semi-active (skyhook controller) when compared to the passive landing gear for the design aircraft configuration is 37%, for the fuzzy controller 38%, for the LQR controller 40% (see Figure 54, center column). For aircraft configurations deviating from that point (OWE, MTOW) the improvement is still significant, although somewhat smaller than for MLW. The response for the semi-active suspension for MTOW is approximately 25% better than that for the passive suspension. This drop in performance can be explained by the fact that the aircraft operates at a steeper working point of the air spring, where a small change of stroke leads to large force changes, in other words, the air spring stiffens. Thus, excitation input cannot be effectively absorbed by the semi-active shock absorbers.
For OWE the vertical cockpit accelerations for the semi-active case are of approximately the same absolute value as those of the MLW configuration. The relative improvement for the OWE

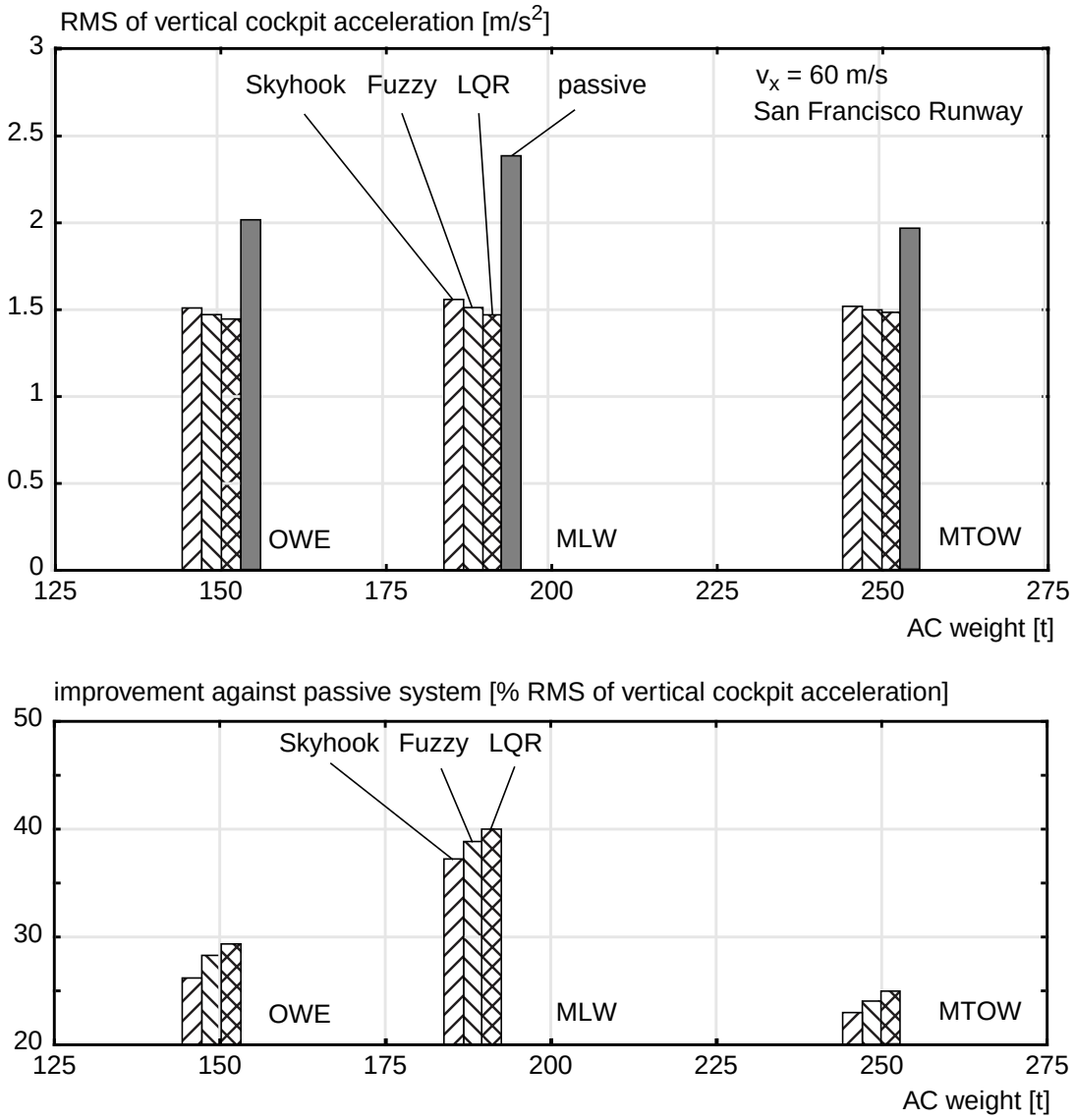

Figure 54: Performance of semi-active control as function of aircraft weight

case is less than that for the design point (26% ... 30% as compared to 37% ... 40%). Here, a different set of controller gains might improve the performance for OWE somewhat. For both OWE and MTOW the differences between the different control concepts remain small and do not increase for a deviation from the design.

5.2.2 Performance as a Function of Aircraft Speed

Another important question is whether the semi-active nose landing gear control is able to maintain its performance over the complete range of speeds during aircraft operation. Thus, the following investigation compares the performance of the skyhook control law for semi-active control at a constant forward speed for a 190-ton-aircraft; all effects of lift have been neglected for this comparison. The improvements for the fuzzy and the LQR controller do not deviate significantly from the values of the skyhook controller and have thus been left out of the figure for reasons of complexity.

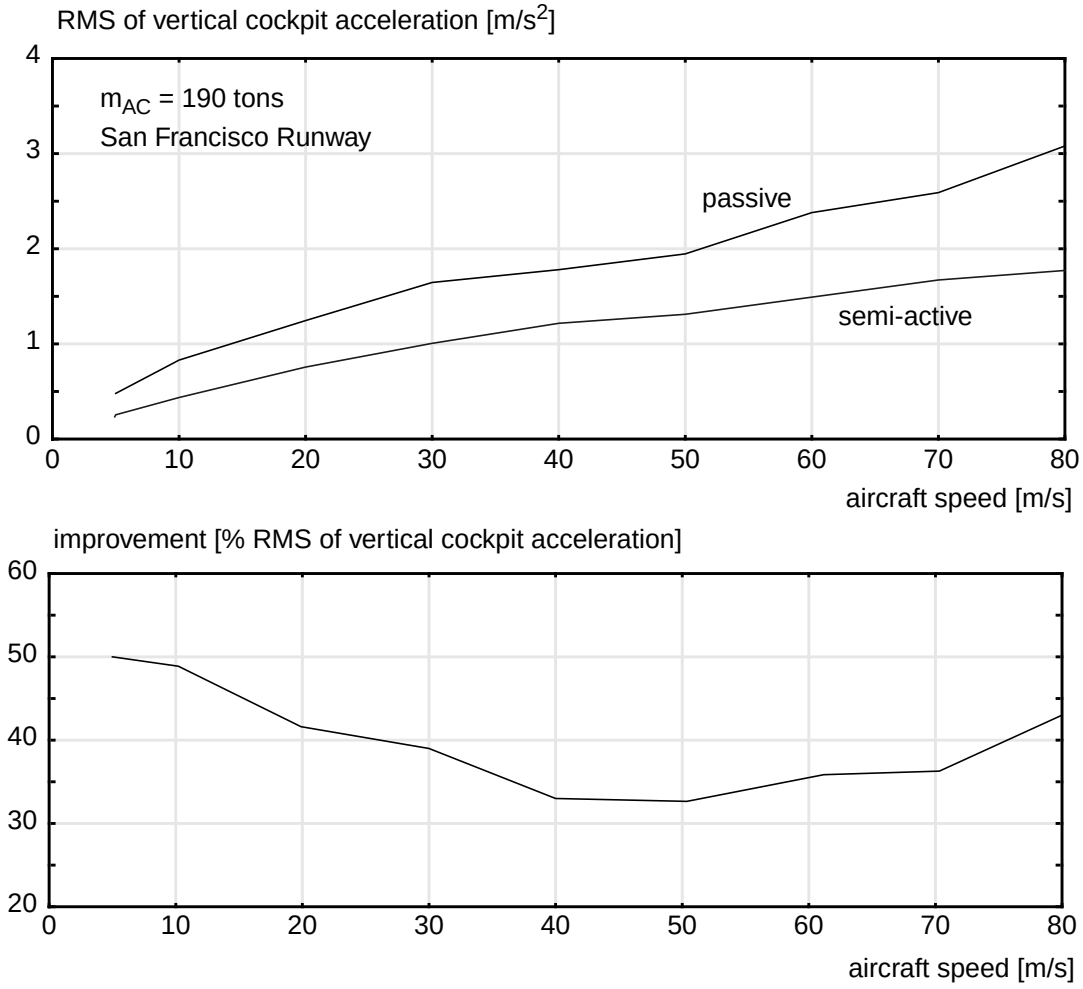

Figure 55: Performance of semi-active control as function of aircraft speed

The plots of Figure 55 show that the semi-active controller is able to reduce the vertical cockpit acceleration over the whole speed range, never sinking much below the performance achieved for the design speed of 60 m/s. The fact that the improvement seems to be *lowest* for the region around the design speed should not be misinterpreted, though. For low speeds, already small excitations are made even smaller by the controlled suspension; however, the absolute reduction of vibrations is not very significant. For high speeds, strong excitations can be damped very effectively, an effect which has already been discussed in section 5.1.2. It should be noted, though, that such speeds are usually reached shortly before take-off where the aerodynamic lift plays a role that cannot be neglected so that the improvements shown in Figure 55 should be extrapolated with care for aircraft at real operation.

5.2.3 Performance as a Function of Runway Roughness

The following investigation is an evaluation of the controller performance as a function of runway roughness. For this purpose, the aircraft model has been simulated travelling over runways of identical frequency content at a speed of 60 m/s. The runway profile is that of the Rough Runway (RR) multiplied by a factor of 0.05 to 2.0, as described in chapter 3.4. Figure 56 shows

the RMS of the vertical cockpit acceleration for both passive and semi-active nose landing gears. Since the results from section 5.2.1 and section 5.2.2 indicate no considerable deviation between the different control concepts this investigation will concentrate on the skyhook controller. The dependencies between runway roughness and controller performance found for the skyhook controller can be assumed to be similar for the fuzzy and the LGR controller.

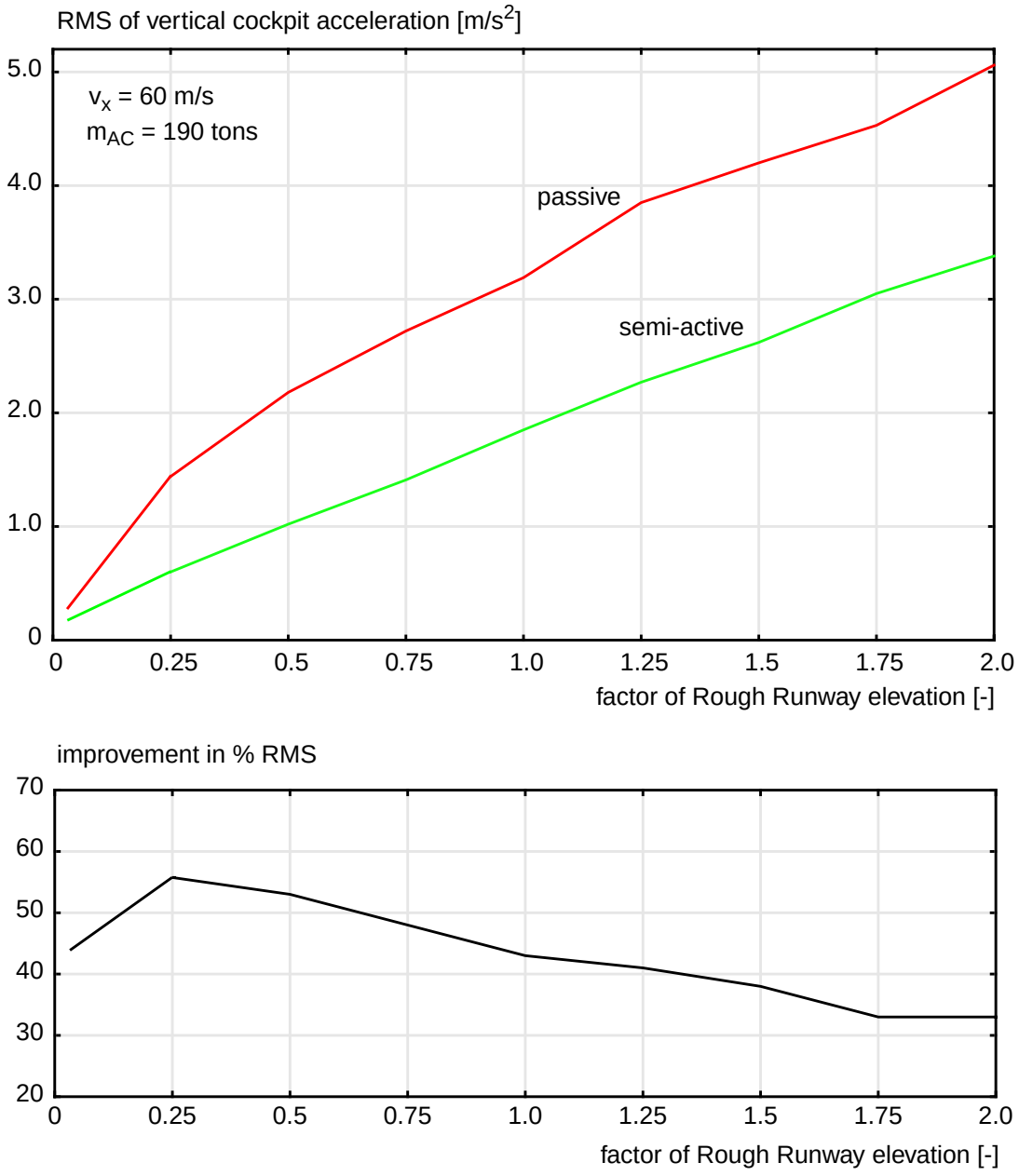

Figure 56: RMS of cockpit acceleration and improvements for different runway elevations

The semi-active system proofs to perform well over the whole range of runway elevations. The improvement above the passive system diminishes from 58% decrease of vertical cockpit acceleration for a relative smooth case (0.25 of RR elevation) to 33% improvement towards the rougher end (1.75 and 2.0 of RR elevation). For the original profile (factor 1.0) an improvement of 43% can be shown which is identical to the results from Figure 51.

The reason for the decreasing performance of the semi-active when compared to the passive gear is the nonlinear characteristic of the air spring. For a very rough runway the system operates more often in the stiff region of the air spring where small changes of stroke lead to large force changes. This effect is comparable to the reduction of performance for very heavy aircraft configurations, see section 5.2.1. As both responses for passive and semi-active suspension approach very small values towards small excitations the improvement likewise diminishes, i.e. for very small excitations the semi-active suspension behaves like a passive one.
It should be noted, however, that large civil transport aircraft will rarely, if ever, encounter a runway worse than the Rough Runway case. The effect shown here, though, is of interest for commuter and military transport aircraft which often have to operate from small and badly prepared runways.

5.2.4 Braking and Acceleration

All evaluation cases simulated above have assumed a constant aircraft velocity. In actual operation, this assumption is in good approximation only true for taxiing. However, the semi-active control concept also has to function at take-off, i.e. at maximum aircraft forward acceleration, and at the braking after a landing, i.e. at maximum aircraft deceleration.
These cases are important as the load on the nose landing gear can no longer be regarded as a static load as it has been for the cases above. At take-off the aircraft will rotate, taking load off the nose landing gear, at the same time lift will lessen the load on the main landing gears. After the landing the braking force on the main landing gears will induce a pitching moment, augmenting the load on the nose landing gear by a factor of up to 2.5.
Two simulations have been performed to account for these effects. First, a take-off run from zero velocity to take-off speed has been undertaken with the MLW model. Rotation starts at 15 s, the aircraft takes off at 25 s. The results for take-off are given in Figure 57. Second, a braked run from 80 m/s to standstill with a braking force of 0.8 of the aircraft weight has been simulated. The results for braking are given in Figure 58. Both runs use San Francisco runway. The semi-active control law used is the skyhook controller. Both Figure 57 and Figure 58 give time plots only. Since the runs are not of constant velocity a PSD representation is not valid and an RMS representation is of no great value for comparison purposes.
For the starting aircraft, see Figure 57, the vertical vibrations rise in amplitude with increasing aircraft speed, up to a time of 10 seconds. After the application of lift and the beginning of aircraft rotation, the vibrations become smaller again. For the whole acceleration phase the semi-active nose landing gear is able to reduce the vertical cockpit accelerations significantly, with the best performance during the phase shortly before rotation where the peak accelerations are highest.
For the case of the braking aircraft, see Figure 58, it can be seen that both the braking force, and therefore the resulting pitching moment, as well as the runway roughness excite strong cockpit accelerations. These vibrations can be reduced very effectively by a semi-active control of the

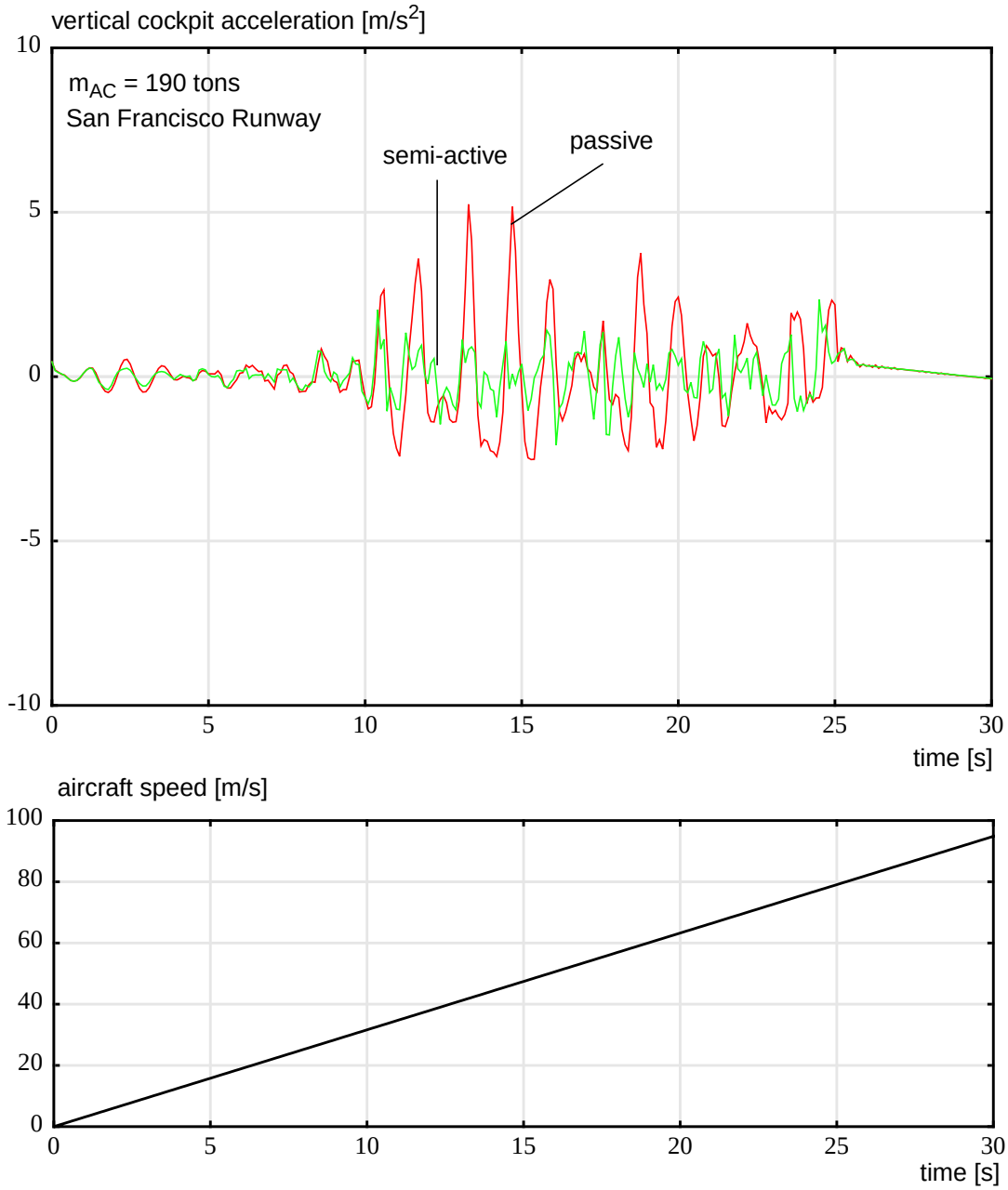

Figure 57: Comparison of passive and semi-active system for take-off run

nose landing gear. Most visibly, the pitching motion is reduced up to a factor of three in amplitude.

The simulations show that the semi-active controller works well not only for constant speed but also for braking and acceleration.

5.2.5 Influence of the Actuator Force Level

As described in chapter 3.3.3, semi-active controllers are often designed as “clipped optimal”, assuming an ideal actuator, i.e. an actuator which can provide zero minimum and unlimited maximum force. Actuators of that kind are, of course, rather rare, so the influence of the technical limits have to be assessed.

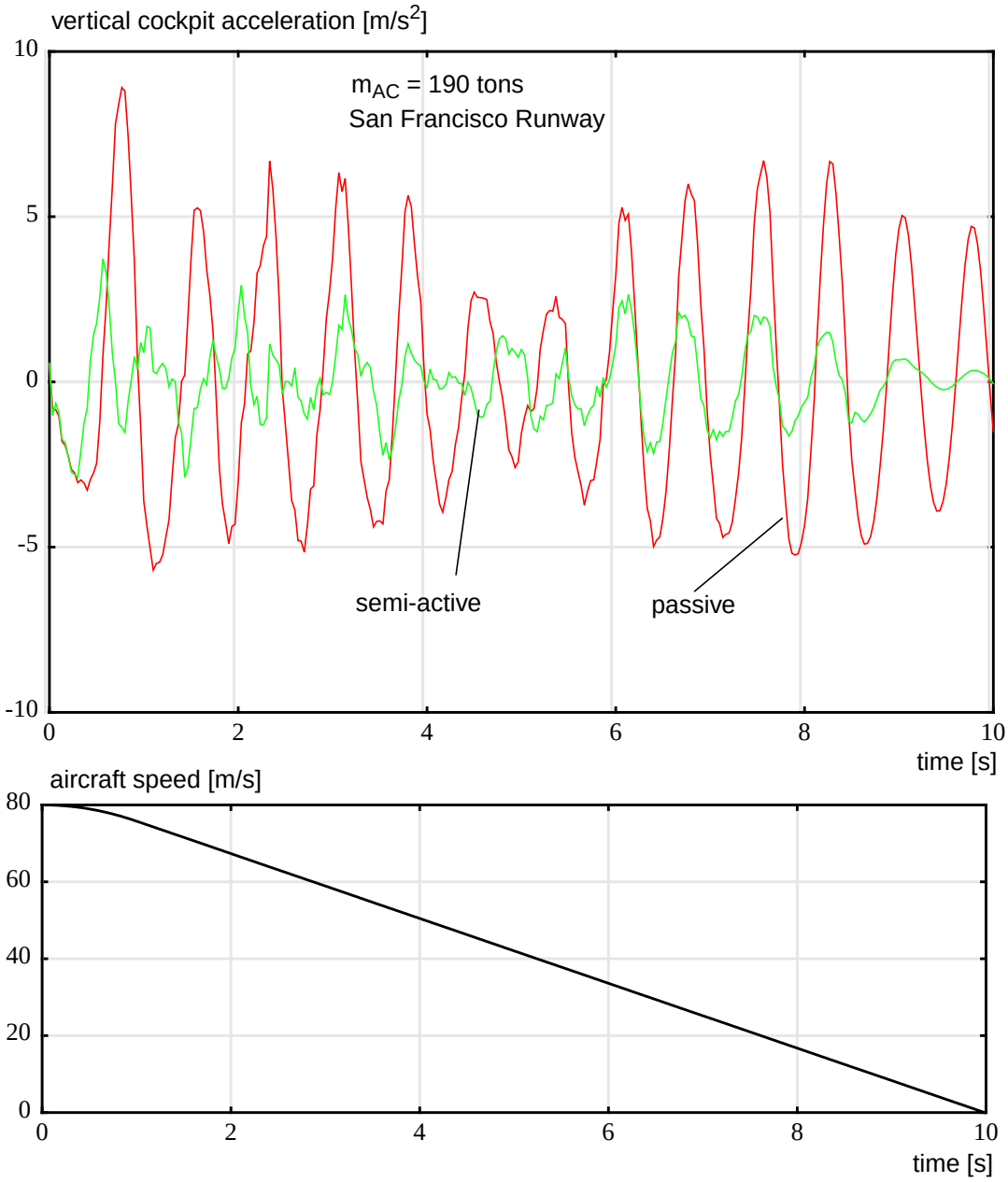

Figure 58: Comparison for semi-active and passive system for braking run

Regarding the upper force limit, the obtainable maximum damping coefficient of an oleo does not pose much of a technical problem since the valve can theoretically be closed completely so that only leakage oil travels between the oil chambers, providing a damping coefficient which is, for all practical purposes, almost infinitely high. In a real application, a small orifice cross section, i.e. a well defined maximum damping coefficient, would have to be maintained, however, to add security against system failure. Damping coefficients of up to $3.5*10^6$ N/(m/s)^2 are in use for passive shock absorbers of large aircraft [14].

Minimum damping for semi-active aircraft oleos, however, is more of a technical problem. Near zero damping coefficients require infinitely large oil flows, in effect demanding very large valve cross sections. Damping coefficients can go as low as 5000 N/(m/s)^2 in passive oleos for transport aircraft [14]. However, as experience with the ELGAR test rig [107] showed, no elec-

tromechanical valve is as yet on the market which can handle the oil flows necessaries for semi-active control at an acceptable actuation time.

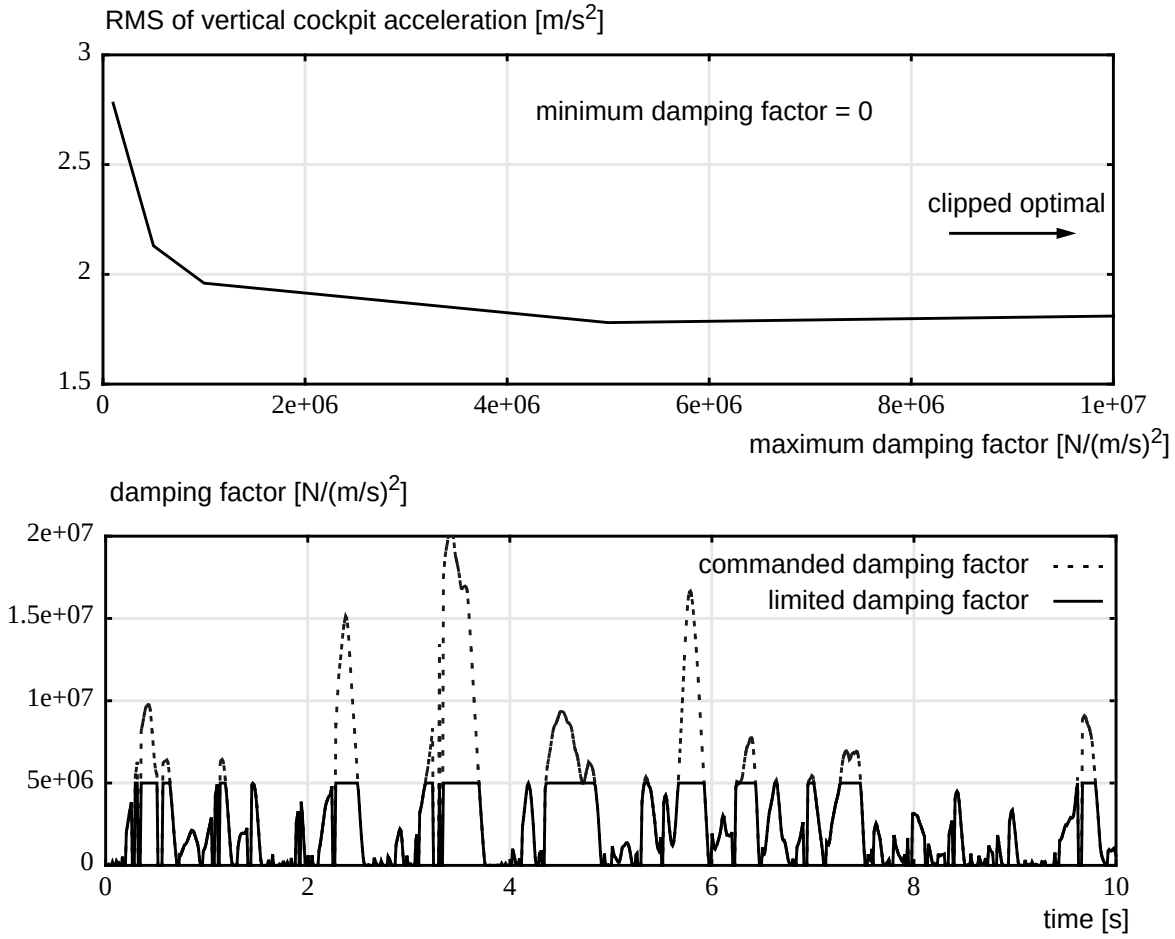

Figure 59: Influence of minimum and maximum damping factors

Figure 59 shows the influence of the maximum damping coefficient on the vertical cockpit acceleration for the aircraft configuration of 190 tons at a speed of 60 m/s. A maximum damping factor d_{max} of $2*10^7$ N/(m/s)^2 can be regarded as nearly infinite because it is rarely demanded by the controller. A maximum damping coefficient of $5*10^6$ N/(m/s)^2 would already be sufficient for a technical application.

Looking at the comparison of demanded vs. limited damping it can be seen that the control signal has highly varying history for values well below d_{max}. This is the reason why in state-of-the-art semi-active suspensions continuous valves are preferred over valves with just two working points (open/closed).

5.2.6 The Benefits of a Semi-Active vs. an Optimized Passive Landing Gear

As discussed in chapter 2.2.1, suspension requirements, especially the damping value, differ for touch-down and for taxiing. Since the damping force F_d is a function of damping factor d and oleo stroke velocity $\dot{s}$, i.e. $F_d = d \cdot \dot{s}^2$, and the oleo velocity at touch-down is relatively high,

a low damping factor is required allowing the oleo to make use of the full oleo stroke. At rolling, however, the stroke velocity is considerably lower, so the low damping value resulting from the landing requirements leads to low damping forces unable to reduce vertical aircraft dynamics like aircraft pitch and fuselage vibrations. It has been one of the main tasks of this thesis to show that a semi-active suspension is able to solve this conflict. However, another solution is to equip a landing gear with mechanical valves to achieve damping factors of a prescribed function of oleo stroke velocity (passive variable oleo, a so-called taxi-valve, see chapter 2.2.1, Figure 8).
The difference in performance for a two-stage passive damper and a semi-active damper (with skyhook controller) will be assessed in this chapter. A respective passive damper has been designed and optimized for the aircraft model also used in this thesis in the Flexible Aircraft Project [59]. Three damping coefficients were obtained for the passive oleo, two for oleo compression - d_2 = 80000 N/(m/s)^2 for the touch-down working point, d_1 = 1750000 N/(m/s)^2 for rolling - and one for expansion of the oleo, d_{exp} = 50000 N/(m/s)^2.
The effect of this “optimized passive“ design is displayed in Figure 60. A model of a large trans-

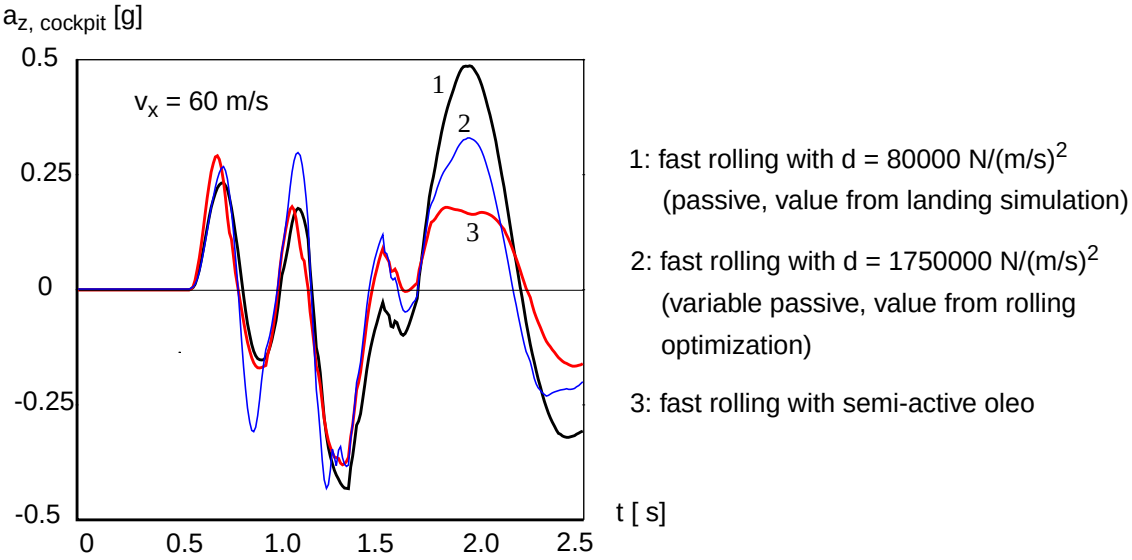

Figure 60: Comparison of optimized passive and semi-active oleo

port aircraft rolls over a double-cosine bump, see Figure 33. Curve number 1 is that of the aircraft equipped with a fixed-orifice oleo optimized for a hard landing. It can be clearly seen that this configuration leads to high vertical accelerations due to the low damping coefficient. A variable passive damping oleo, however, can effectively reduce the vertical oscillations, see curve number 2. The best result is shown by the semi-active oleo, see curve number 3. Contrary to the optimized passive oleo it will not only reduce aircraft pitch and heave but, as could be shown in this work, is also able to effectively damp elastic modes of the structure and thus reduce airframe oscillations up to a factor of 1.5 to 5, depending on the frequency spectrum of the excitation and the aircraft speed.
The advantages of semi-active damping over the “optimized passive” design and the dependency on aircraft velocity are demonstrated in Figure 61. The RMS value of cockpit accelera-

tion is plotted for simulation runs of variable aircraft velocity for two aircraft mass configurations. The improvements between the single-stage passive and the “optimized passive” suspension increases with aircraft velocity in about the same ratio as the ratio between the “optimized passive“ and the semi-active suspension, comparable to the results given in chapter 5.2.1 and chapter 5.2.2.

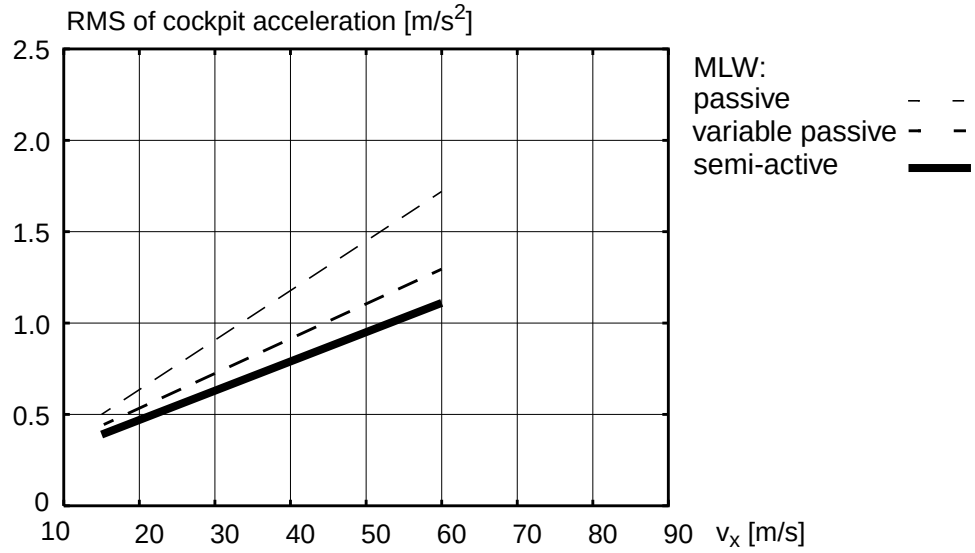

Figure 61: Performance of optimized passive and semi-active oleo

6 Summary and Outlook

6.1 Main Results

Aircraft landing gears have to absorb the energy of the landing impact and to provide a means for the aircraft to navigate on the ground; the latter aspect includes a smooth ground ride. The inherent design conflict between the requirements for rolling and touch-down, if it has been addressed at all, has conventionally been tackled by multi-stage passive shock absorbers. Additionally, some test-rigs have been operated with heavy and complex fully active devices.
The introduction of semi-active suspensions offers another solution to the design conflict. In such a suspension, the damping coefficient can be set to an arbitrary value inside technical limits by adjusting the orifice cross section between the oil chambers of the shock absorber. The damping coefficient is determined by a control law using measurements of aircraft and shock absorber motion as input.
In this thesis, the use of semi-active landing gears for rolling has been proposed and has been investigated taking into account aspects of system dynamics, control layout effort, and technical realization. It was the main task to investigate the design and performance of different control laws with respect to the reduction of ground-induced vibrations. Three control algorithms have been designed for use in a semi-active nose landing gear oleo, a skyhook controller, a fuzzy controller, and an LQR controller including an optimal estimator (a Kalman filter).
For this purpose, an aircraft model was established using techniques developed for the integrated design of aircraft and landing gears. The model of the airframe used for the control layout was derived from a finite element model supplied by the aircraft manufacturer and assembled in a multibody simulation (MBS) environment. The control layout was performed in a control design tool (CACE) using interfaces between the MBS and the CACE software. For this purpose a bi-directional interface between the MBS-tool SIMPACK and the CACE-tool MATRIXx has been developed. Finally, the controllers were transferred to the MBS package and the control parameters optimized by multi-objective optimization. While the parameters of the skyhook and of the fuzzy controller could be optimized directly, a methodology was developed to reduce the effort of optimizing the LQR controller by varying only selected weighting factors instead of the complete gain vector.
All three control algorithms, the skyhook controller, the fuzzy controller, and the LQR controller, perform well with respect to the reduction of vertical cockpit acceleration, obtaining a reduction in the RMS of vertical cockpit acceleration of 25% to 40% depending on aircraft configuration, speed, and runway roughness. A difference can be seen regarding the frequency response where the skyhook and the fuzzy controller are able to damp well the rigid body natural frequencies (aircraft pitch and aircraft heave) as well as the low frequency structural modes but appear to deteriorate in performance for modes of higher frequencies. This phenomenon, however, arose only on the San Francisco Runway and seems to depend on the excitation. The response of the landing gear equipped with an LQR controller remains below the values for

the passive system over the whole frequency range under consideration for all excitation cases. Generally, the improvement of semi-active over passive suspensions increases with the magnitude of the runway excitation, i.e. the worse the runway, the greater the improvement.
The advantages and disadvantages of the control algorithms concerning their use in a semi-active nose landing gear oleo can be summarized as follows:

skyhook controller	+	simple control structure independent of aircraft model, no knowledge of plant necessary
	+	design well supported by standard software, easy transfer of controller structure to simulation environment
	-	cannot adapt to special model properties
	-	performance might be frequency dependent
fuzzy controller	+	control structure independent of aircraft model, no knowledge of plant necessary
	+	easy to adapt to special model requirements
	-	large number of parameters to be adjusted
	-	performance might be frequency dependent
LQR	+	performs well over whole frequency range considered at design point because model information inherent in controller layout
	-	state feedback controller needs state observer or estimator (Kalman filter), requiring additional design effort and on-line calculation time for the observer/estimator

As a result of the evaluation, it can be stated that the differences in performance between the control concepts are not so significant that one concept can be given absolute priority over the others. The *skyhook controller* can be regarded as a good reference controller which works well over the whole operational envelope. It can also be used as a final control concept if simulations give rise to the assumption that no excitations of higher modes of technical relevance occur. The *fuzzy controller* has its advantages if the controller has to be adapted to model variations (weight, speed) and should be the choice in those cases. However, even a controller without those adaptations has worked well for the cases examined here. The *LQR controller* is the most complex controller to be designed and performs well over a broad frequency range. However, it requires the most effort for design and on-line calculation of the necessary state observer or estimator, an effort that is only justified if simulations and test runs show the risk of structural vibrations being induced by simpler control laws.
Due to the restrictions of the semi-active control scheme the performance of all semi-active control laws is below that of an ideal fully active suspension where arbitrary control commands can be executed. A comparison of the control parameters optimized for semi-active and for fully active control showed that semi-active controllers work best with considerably higher gains than their fully active counterparts, so a purely “clipped-optimal” approach will lead to a sub-optimal semi-active controller. It could be shown that the performance of fully active actuators decreases significantly for technical realistic actuator time constants. In addition, fully

active control schemes require heavy and complex actuation devices. Concluding, it can be stated that a semi-active solution offers the best compromise between performance and complexity.

Are Semi-Active Aircraft Suspensions Really Necessary? This question has been first posed in a similar form ("Are active suspensions really necessary", [45]) by Karnopp who tries to answer his own challenge with respect to ground vehicles. He is of the opinion that for some cases the best possible passive suspension performance is poor when compared to that which can be achieved when an active suspension is used. Also citing Karnopp's question, Goodall and Kortüm in [28] come to the conclusion that active systems should only be advocated in situations where one can demonstrate the limitations of passive realizations, or where a clear economic case can be made.

It is the conviction of the author that semi-active landing gears have a potential that might very well become important in the case of a new, large or stretched aircraft. Simulations have shown that the improvement can be significant, even if such a landing gear is not a feature that is considered to be essential for an existing aircraft. Semi-active landing gears can solve the inherent conflict between an optimization of a gear for minimum loads at landing and an optimization for a smooth ground ride. A semi-active oleo needs no external pressure reservoir. Therefore, it is expected that a semi-active landing gear will not be significantly heavier than a complex passive one - and it will be much lighter than the fully active gears that have been investigated in the 70s and 80s. A passive landing gear, on the other hand, can be modified to improve its performance by measures like double-stage air spring, metering pin, or taxi valve. Still, given that the complexity of such a passive shock absorber grows, and with it its price and maintenance costs, the cost gap between a passive and a semi-active device closes, or a semi-active oleo might even turn out to be less expensive. Thus, a semi-active suspension is a good compromise between a relatively light-weight, but inherently sub-optimal passive system, and a possibly highly effective, but heavy and complex fully active suspension.

A semi-active landing gear has the potential to reduce the accelerations and loads in the fuselage induced by rough runways and landings. One great advantage of a semi-active vs. an optimized passive design is that the semi-active oleo can be tuned to reduce structural response at specific frequencies. Since studies suggest that the benefits are greater for rolling than for touch-down, a landing gear might operate in passive mode during landing impact and be switched to active damping mode during taxiing. Semi-active actuators can be controlled using relatively simple control structures, feeding back aircraft and shock absorber motion which is easily accessible.

The technology is feasible. Semi-active shock absorbers are state-of-the-art in automotive, truck, and railway applications. For aircraft suspension, a demonstrator has been set up during the course of the ELGAR project, proving that the questions of hardware, software and signal processing can be successfully solved.

6.2 Open Problems

During the development of the thesis it has been realized that even though a number of problems have been addressed and solved some open questions remain to be studied in the future.
The influence of stick friction in landing gears is strong. The effect can be represented in the time simulation, however, it is difficult to obtain a mathematical model and reliable data to be used. It is clear that a landing gear in stick mode cannot be influenced by a semi-active oleo at all. No thorough examination on the question of stick friction on aircraft landing gears exists yet. No evaluation has been made, e.g., if the semi-active landing gear can be used to reduce the time a landing gear "sticks". The question of stick friction has to be examined before a potential control of all landing gears, including the main landing gears, can be investigated.
As seen in this work, the elastic response of the airframe can be significantly reduced in a certain frequency range of interest. However, there might be a shift of the response into a higher frequency range for some control laws. This has to be carefully studied for each case, and it has to be evaluated whether this shift affects the aircraft.
Some improvements regarding the aircraft simulation can be suggested. The aerodynamic effects have only been marginally addressed in this thesis. Take-off and touch-down simulations with the consideration of aeroelastic effects (e.g. distributed lift over the wings) remain to be performed. Concerning the control design, the optimization clearly showed the need to add optimization routines specialized on systems with stochastic excitation to the used multi-objective optimization package.
As to the technical realization, no valve is on the market yet (to the knowledge of the author) that is capable of handling the necessary oil flow for active damping. The development of such an integrated valve will be one of the main tasks at the development of an active damping oleo for a large transport aircraft. Details of application, e.g. the influence of temperature changes, aging, etc. on the control will have to be examined in practical tests.
The influence of active damping landing gears on fatigue is also an open question. The main effects to be investigated will probably be the reduced peak loads vs. a possible frequency shift mentioned above.
Last but not least much of the potential of the semi-active landing gear vs. the passive gear obtained in the studies using the transport aircraft nose landing gear comes from the fact that the conventional, passive gear has been optimized for the landing impact and is therefore subject to the design conflict mentioned in the first paragraph of this chapter. A modification and optimization of the passive landing gear for rolling conditions might improve the properties of the aircraft at ground ride - still, this also means a further increase in complexity and cost of the passive landing gear.
The scaled-down demonstrator built for the ELGAR project has shown that the technology is feasible; the test rig could be expanded to additionally simulate elastic aircraft modes by means of hardware-in-the-loop components. However, the next step should be the design of a demonstrator landing gear for field tests on a real test aircraft in order to prove that the open questions

of interest for aircraft manufacturers and operators, especially with regard to safety, cost effectiveness, reliability and maintainability, can be answered positively.

7 Bibliography

[1] E. Bakker, L. Nyborg, H.B. Pacejka: A New Tyre Model With an Application in Vehicle Dynamics Studies. SAE 890087, 1989.

[2] F.H. Besinger, D. Cebon, D.J. Cole: Force Control of a Semi-Active Damper. In: Vehicle System Dynamics, 24, 1995, pp. 695-723.

[3] D. Bestle: Analyse und Optimierung von Mehrkörpersystemen. Springer-Verlag, Berlin, 1994.

[4] H. Brandl, R. Johanny, M. Otter: An Algorithm for Simulation of Multibody Systems with Kinematic Loops. In: Proc. 7th World Congress, The Theory of Machines and Mechanisms, Sevilla, Spain, 1987, pp. 407-411.

[5] K.E. Brenan, S.L. Campbell, L.R. Petzold: Numerical Solution of Initial-Value Problems in Differential Algebraic Equations. Classics in Applied Mechanics, SIAM, North- Holland, New York, 1989 / 1996.

[6] R. Brockhaus: Flugregelung. Springer-Verlag, Berlin, 1994.

[7] A.E. Bryson, Y.C. Ho: Applied Optimal Control, Blaisdell, 1969.

[8] T. Catt, D. Cowling and A. Shepherd: Active Landing Gear Control for Improved Ride Quality during Ground Roll. Smart Structures for Aircraft and Spacecraft (AGARD CP 531), Stirling Dynamics Ltd, Bristol, 1993.

[9] P. Causemann, S. Irmscher: Neue semiaktive Fahrwerkssysteme für PKW und NKW. Aktive Fahrwerkstechnik, Haus der Technik, Essen, 1995.

[10] S.T. Chai, H.W. Mason: Landing Gear Interaction in Aircraft Conceptual Design, MAD 96-09-01, Virginia Polytechnics and State University, Blacksburg, VA, 1996.

[11] H.G. Conway: Landing Gear Design, Chapman & Hall, London, 1958.

[12] C.D. Corsetti, J. D. Dillow: A Study of the Practicability of Active Vibration Isolation Applied to Aircraft During the Taxi Condition, Technical Report AFFDL-TR-71-159, Air Force Flight Dynamics Laboratory, Wright-Patterson Air Force Base, Ohio, 1972.

[13] D.A. Crolla: Active Suspension Control: Review of Recent Applications. In: Pauwelussen, Pacejka (eds.): Smart Vehicles, Swets & Zeitlinger, Lisse, NL, 1995, pp. 183-202.

[14] N.S. Currey: Aircraft Landing Gear Design: Principles and Practices, AIAA Education Series, Washington, 1988.

[15] K. Deutrich: Drehzahlregelung eines Portalkrans mittels Fuzzy Logik. Konstruktiver Entwurf, IfRA 9523, Technische Universität Braunschweig, Institut für Regelungs- und Automatisierungstechnik, Braunschweig 1995.

[16] S. Dietz: Vibration and Fatigue Analysis of Vehicle Systems Using Component Modes, VDI Fortschrittsberichte Reihe 12, Nr. 401, VDI Verlag, Düsseldorf, 1999.

[17] G.A. Doyle: A Review of Computer Simulations for Aircraft-surface Dynamics. Journal of Aircraft, 23 (4), 1986.

[18] C. Drössler: Fuzzy Logic, Methodische Einführung in krauses Denken, Rowohlt Taschenbuch Verlag, Reinbek, 1994.

[19] W. Duffek: Active Shock Absorber Control During Landing Impact. Final Report BriteEuram Research Project 2014 (LAGER 1, Task 5), IB 515/95-19, DLR, Oberpfaffenhofen, 1995.

[20] R.V. Dukkipati, S.S. Vallurupalli, M.O.M. Osman: Adaptive Control of Active Suspension - A State of the Art Review. The Archives of Transport, Vol. IV, 1992.

[21] E.M. Elbeheiry, D.C. Karnopp, M.E.Elaraby, A.M. Abdelraaouf: Advanced Ground Vehicle Suspension Systems - A Classified Bibliography. In: Vehicle System Dynamics, 24, 1995, pp. 231-258.

[22] J. Etzkorn: ELGAR: European Landing Gear Advanced Research, Final Report, Subtask 1.1.2. IB 532-00-2, DLR Oberpfaffenhofen, 2000.

[23] R. Fletcher: Practical Methods of Optimization. Vol. 2. John Wiley and Sons, USA, 1981.

[24] O. Föllinger: Regelungstechnik (7. Auflage), Hüthig, Heidelberg, 1992.

[25] A. Fong: Shimmy Analysis of a Landing Gear System. ADAMS International User Conference, April 1995.

[26] R. Freymann: An Active Control Landing Gear for the Alleviation of Aircraft Taxi Ground Loads. Zeitschrift für Flugwissenschaft und Weltraumforschung, 1987.

[27] G.L. Ghiringhelli, M. Boschetto: Design Landing Loads Evaluation by Dynamic Simulation of Flexible Aircraft. In: Landing Gear Design Loads, AGARD-CP-848, 1991.

[28] R.M. Goodall, W. Kortüm: Active Controls in Ground Transportation - A Review of the State-of-the-Art and Future Potential. In: Vehicle System Dynamics, 12, 1983, pp. 225-257.

[29] J. Goroncy: Citroen Xantia Activa mit neuem Fahrwerk. In ATZ Automobiltechnische Zeitschrift 97, 1995, 7/8, pp. 416-417.

[30] G. Grübel, H.-D. Joos, M. Otter: The ANDECS Design Environment for Control Engineering. In IFAC World Congress, Sidney, 18-23 July 1993.

[31] M. Hanel, K.H. Well: Optimierte Sensorpositionierung zur Regelung elastischer Strukturen. DGLR-JT97-044, DGLR Jahrstagung, 1997.

[32] E.J. Haug: Concurrent Engineering: Tools and Technologies for Mechanical System Design, NATO Advanced Science Institute Series (ASI), Series F: Computer and System Sciences Vol. 108, Springer Verlag, Berlin, 1993.

[33] J.K. Hedrick: Railway Vehicle Active Suspensions. In Vehicle System Dynamics, 10, 1981, pp. 267-283.

[34] A. Heinrich, J. Kreft, F. Dörrscheidt, M. Boll: Fuzzy-Regelung eines semiaktiven PKW-Fahrwerks. atp - Automatisierungstechnische Praxis 36, 1994, pp. 23-30.

[35] H. Heumann, B.B. Hall, W. Weston: Fuzzy Logic Control of a Novel Suspension System. IMechE 1998 C553/032, 1998, pp. 323 ff.

[36] B. Hildreth: The Draft AIAA Flight Mechanics Modeling Standard: An Opportunity for Industry Feedback, Proceedings of the AIAA Modeling and Simulation Technologies Conference, Boston, 1998.

[37] H.P.Y. Hitch: Aircraft Ground Dynamics. Vehicle System Dynamics, 10, 1981, pp. 319-332.

[38] R. Hooke and T.A. Jeeves: “Direct Search” Solution of Numerical and Statistical Problems. Journal of the ACM, Vol.8, 1961, pp. 212-229.

[39] W.E. Howell, J.R. McGehee, R.H. Daugherty, W.A. Vogler: F-106 Airplane Active Control Landing Gear Drop Test Performance. In: Landing Gear Design Loads (CP 484), AGARD, 1990.

[40] R.G.M Huisman, F.E. Veldpaus, J.G.A.M. van Heck, J.J. Kok: Preview Estimation and Control for (Semi-) Active Suspensions. Vehicle System Dynamics, 22, 1993, pp. 335-346.

[41] D.A. Hullender, D.N. Wormley, H.H. Richardson: Active Control of Vehicle Air Cushion Systems. In ASME Journal of Dynamical Systems, Measurements and Control, Vol. 93, No. 1, 1972.

[42] P. Jackson (ed.): Jane's All the World's Aircraft, Edition 1996. Jane's Information Group Limited, 1996.

[43] S.F.N. Jenkins: Landing gear design and development. Proceedings of the Institution of Mechanical Engineers, Vol 203, 1989.

[44] H.-D. Joos: Informationstechnische Behandlung des mehrzieligen optimierungsgestützten regelungstechnischen Entwurfs, Ph.D. Thesis, Universität Stuttgart, Prof. R. Rühle, 1992.

[45] D. Karnopp: Are Active Suspension Really Necessary. ASME Paper No. 78, WA/DE-12, 1978.

[46] D. Karnopp: Active Damping in Road Vehicle Suspension Systems. Vehicle System Dynamics, 12(6), 1983.

[47] D. Karnopp and G. Heess: Electronically Controllable Vehicle Suspensions, Vehicle System Dynamics, 20, 1991, pp. 207-217.

[48] D. Karnopp, M. Crosby, R.A. Harwood: Vibration Control using Semi-active Force Generators. Journal of Engineering for Industry, No 96, 1974, pp. 619-626.

[49] Kapadoukas, A.W. Self, F. Marteau: The Simulation of Aircraft Landing Gear During Usual and Unusual Manoeuvres. Proceedings of the 20th Congress of the I.C.A.S., ICAS-96-4.11.3, Napoli, 1996.

[50] K. König: Die Lasten des Landestoßes, ZFW Band 3, Heft 6, 1979.

[51] W. Kortüm, R. S. Sharp (eds): Multibody Computer Codes in Vehicle System Dynamics. Vehicle System Dynamics, Supplement to Vol. 22, 1993.

[52] W. Kortüm, W. Rulka, M. Spieck: Simulation of Mechatronic Vehicles with SIMPACK. MOSIS 97, Ostrava, Czech Republic, 1997.

[53] W. Kortüm, W. Rulka, A. Eichberger: Recent Enhancements of SIMPACK and Vehicle Applications. European Mechanics Colloquium, EUROMECH 320, Prague, 1994.

[54] W. Kortüm, P. Lugner: Systemdynamik und Regelung von Fahrzeugen. Springer-Verlag, Berlin, 1994.

[55] D. Kraft: A Software Package for Sequential Quadratic Programming. DFVLR-FB 88-28, Oberpfaffenhofen, 1988.

[56] H. Kreuzer: Revue der Lufthansa - Flugzeuge, Air Gallery Verlag, Erding, 1996.

[57] W.R. Krüger et al: Aircraft Landing Gear Dynamics: Simulation and Control. Vehicle System Dynamics, 28, 1997, pp. 257-289.

[58] W.R. Krüger, W. Kortüm: Multibody Simulation in the Integrated Design of Semi-Active Landing Gears, Proceedings of the AIAA Modeling and Simulation Technologies Conference, Boston, 1998.

[59] W.R. Krüger, M. Spieck: Abschlußbericht "Flexible Aircraft", Abschließender Sachbericht des DLR zum nationalen Luftfahrtforschungsprogramm "Flexible Aircraft", AP6 "Integrierter Entwurf Fahrwerk / Flugzeug", DLR, Institut für Aeroelastik, Oberpfaffenhofen, Juni 1999.

[60] W.R. Krüger: SIMAX Manual, SIMPACK 8.0 Documentation, INTEC, Weßling, 1999.

[61] R. Kübler, W. Schiehlen: Vehicle Modular Simulation in System Dynamics. In: International Conference on Multi-Body Dynamics - New Techniques and Applications, IMechE Conference Transactions 1998-13.

[62] T.-W. Lee: Dynamic Response of Landing Gears on Rough Repaired Runways. In: J.A. Tanner et al (eds.): Emerging Technologies in Aircraft Landing Gear, SAE, PT-66, Warrendale, PA (USA), 1997.

[63] H. Li, R.M. Goodall: Linear and Non-linear Damping Control Laws for Active Railway Suspension. Control Engineering Practice 7, 1999, pp. 834-859.

[64] J.R. McGehee and D.L. Morris: Active Control Landing Gear for Ground Load Alleviation. Active Control Systems - Review, Evaluation and Projections (AGARD CP 384), NASA Langley R. C.,1981.

[65] M. Mecham: Getting Software Right Is Part of the New Airbus. In: Aviation Week & Space Technology, Nov. 16, 1998.

[66] H.E. Merritt: Hydraulic Control Systems. Wiley and Sons, New York, 1967.

[67] M. Mitschke: Dynamik der Kraftfahrzeuge, Band B: Schwingungen. Springer, Berlin, 1984

[68] W.J. Moreland: The Story of Shimmy, Journal of the Aeronautical Sciences, pp 793-808, December 1954.

[69] P.C. Müller, K. Popp, W.O. Schiehlen: Berechnungsverfahren für stochastische Fahrzeugschwingungen. In: Ingenieur-Archiv 49, 1980, pp. 235-254.

[70] B. Ohly: Landing Gear Design - Contemporary Philosophies and Future Trends. The International Journal of Aviation Safety Vol. 3, No.1, 1985.

[71] H.B. Pacejka: The Wheel Shimmy Phenomenon, a Theoretical and Experimental Investigation. Dissertation Technical University Delft, 1966.

[72] H.B. Pacejka (ed.): Tire Models for Vehicle Dynamics Analysis. In: 1st International Colloquium on Tyre Models for Vehicle Dynamics Analysis. Swets & Zeitlinger, 1991.

[73] L. Pazmany: Landing Gear Design for Light Aircraft. Vol 1. ISBN 0-9616777-0-8.

[74] J. Pink: Structural Integrity of Landing Gears. In: J.A. Tanner et al (eds.): Emerging Technologies in Aircraft Landing Gear, SAE, PT-66, Warrendale, PA (USA), 1997.

[75] K. Popp, W. Schiehlen: Fahrzeugdynamik. B.G. Teubner, Stuttgart 1993.

[76] G. Prokop, R.S. Sharp: Performance Enhancement of Limited Bandwidth Active Automotive Suspensions by Road Preview. In: CONTROL ’94 , University of Warwick, U.K., March 21-24, 1994 (IEE Publication No. 389), pp. 173-182.

[77] A. Pruckner: Virtuelles Prototyping zur Entwicklung von Fahrwerks-Regelungs-Systemen mit ADAMS und MATRIXx. 7. Aachener Kolloquium Fahrzeug- und Motorentechnik, Aachen 1998.

[78] D. v. Reith: Technology Assessment with Multi-Disciplinary Aircraft Design Tools on the Next Generation Supersonic Commercial Transport. ICAS-96-3.5.1, Naples, 1996.

[79] J. Renken: Vorhaben “Flexible Aircraft”. Statusseminar Leitkonzept MEGALINER, 9./10. Juni 1997, TU Hamburg-Harburg.

[80] M. Römer, H. Scheerer: Von Luft getragen - Das Federungs- und Dämpfungssystem. In: Die neue S-Klasse, ATZ Special Issue No 5, 1998.

[81] G. Roloff: Landing Gear Integration on a Supersonic Aircraft. ICAS-96-4.11.1, 1996, pp. 2659-2666.

[82] J. Roskam: Airplane Design, Part IV: Layout Design of Landing Gear and other Systems, 1986.

[83] W. Rulka: Effiziente Simulation der Dynamik mechatronischer Systeme für industrielle Anwendungen. Dissertation an der Technischen Universität Wien, 1998.

[84] B. v. Schlippe, R. Dietrich: Das Flattern der pneumatischen Rades. Lilienthal Gesellschaft für Luftfahrtforschung, 1941.

[85] R.S. Sharp: Preview Control of Active Suspensions. In: Pauwelussen, Pacejka (eds.): Smart Vehicles, Swets & Zeitlinger, Lisse, NL, 1995, pp. 166-182.

[86] A. Shepherd, T. Catt, D. Cowling: The Simulation of Aircraft Landing Gear Dynamics. Proceedings of the 18th Congress of the International Council of Aeronautical Sciences (ICAS 92), Beijing, 1992.

[87] R.F. Smiley, W.B. Horne: Mechanical Properties of Pneumatic Tires with Special Referece to Modern Aircraft Tires. National Advisory Committee for Aeronautics, Washington, 1958.

[88] P. T. Somm, H. H. Straub and J. R. Kilner: Adaptive Landing Gear for Improved Taxi Performance. Boeing Aerospace Company,1977, AFFDL-TR-77-119.

[89] J.A. Tanner: Langley ACLG Program. Presentation at the Workshop on Actively-Controlled Landing Gear (ACLG), July 10-11, 1995, NASA Langley Research Center, Hampton, VA.

[90] J.A. Tanner (ed.): Aircraft Landing Gear Systems, PT-37, Society of Automotive Engineers, 1990.

[91] J.A. Tanner, P.C. Ulrich, J.P. Medzorian, D.L. Morris (eds.): Emerging Technologies in Aircraft Landing Gear, SAE, PT-66, Warrendale, PA (USA), 1997.

[92] W. E. Thompson: Measurements and Power Spectra of Runway Roughness at Airports in Countries of the North Atlantic Treaty Organization. NACA Technical Note 4303, Washington, 1958.

[93] W. Trautenberg: Bidirektionale Kopplung zwischen CAD- und Mehrkörpersimulation, Dissertation, TU-München, Lehrstuhl für Feingerätebau und Mikrotechnik, 1999

[94] O. Vaculin, M. Valasek: COPERNICUS Semi-Active Damping of Truck Suspensions and their Influence on Driver and Road Loads, Final Technical Report. SADTS, CIPA-CT-94-0130, DLR (Project Coordinator), Weßling, 1998.

[95] P.J.Th. Venhovens, A.C.M. van der Knaap: Delft Active Suspension (DAS). In: Pauwelussen, Pacejka (eds.): Smart Vehicles, Swets & Zeitlinger, Lisse, NL, 1995, pp. 139-165.

[96] A. Vikas, S. Presser, A. Wöhler, H.-P. Willumeit: Optimierung und Auslegung von Fuzzy-Control-Strukturen mit Hilfe von Evolutionsstrategien - Ein Beitrag zu aktiven Fahrwerken. ATZ Automobiltechnische Zeitschrift 97 (1995).

[97] O. Wallrapp: Standardization of Flexible Body Modeling in Multibody System Codes, Part I: Definition of Standard Input Data. Mech. Struc. & Mach., 22(3), 1994, pp. 283-304.

[98] X. Wang: Semiaktive Fahrwerkssysteme mit Fuzzy-Regelung zur Strukturlastminderung. Proceedings of the “DGLR 2. Symposium Flugzeugsystemtechnik: Entwicklungstrends bei Basissystemen und ihre Wechselwirkung zum Flugzeugentwurf”, Technologiezentrum Hamburg-Finkenwerder, 16./17. September 1997.

[99] X. Wang, U. Carl: Fuzzy Control of Aircraft Semi-Active Landing System. 37th AIAA Aerospace Sciences Meeting and Exhibit, Reno, NV, 1999.

[100] H. Wegmann, D. Mohr: Fuzzy-Logik, erste Anwendung mit SIMATIC S5. atp - Automatisierungstechnische Praxis 3/93, 1993, pp. 169ff.

[101] H. Wentscher: Design and Analysis of Semi-Active Landing Gears for Transport Aircraft. DLR Forschungsbericht 96-11, Deutsches Zentrum für Luft- und Raumfahrt, Köln, 1995.

[102] H. Wentscher and W. Kortüm: Multibody Model-based Multi-Objective Parameter Optimization of Aircraft Landing Gears. Proceedings of IUTAM-Symposium on Optimization of Mechanical Systems, Stuttgart, 1995.

[103] R.R. Yager, D.P. Filev: Essentials of Fuzzy Modeling and Control. John Wiley and Sons, New York, 1994.

[104] D.W.S. Young: Aircraft Landing Gears: the Past, Present, and Future. Paper 864752 publ. by I.Mech.E (UK), 1986. In: J.A. Tanner (ed.): Aircraft Landing Gear Systems, Society of Automotive Engineers, 1990, pp. 179-196.

[105] International Organization for Standardization: Guide for the Evaluation of Human Exposure to Whole Body Vibration. ISO 2631-1974(E), July, 1974.

[106] A Concurrent Engineering Project for European Aeronautical Industry. Aerospatial ENHANCE homepage: http://www.avions.aerospatiale.fr/enhance, 2000.

[107] GEIE EUROGEAR (eds.): ELGAR - European Landing Gear Advanced Research, Publishable Summary. BriteEuram, Report Number EG-ELGAR-P10, 2000.

[108] AGARD Conference Proceedings - Landing Gear Design Loads (CP-484), AGARD, 1990.

[109] AGARD Report - The Design, Qualification and Maintenance of Vibration-Free Landing Gear (R-800), AGARD, 1996.

[110] Airplane Characteristics for Airport Planning, 747-400, Boeing Document D6-58326-1, Boeing Commercial Airplanes, Seattle, Washington, March 1990. Quoted according to [10].

[111] Federal Aviation Administration (FAA), Office of Airport Standards (publ.): Standardized Method of Reporting Airport Pavement Strength - PCN, FAA Advisory Circular 150/5335-5, 1983.

[112] Joint Aviation Authorities Committee (publ.): Joint Aviation Requirements JAR-25, Large Aeroplanes, Change 13, 1989.